UNIVERSIDADE FEDERAL DE PERNAMBUCO
CENTRO DE TECNOLOGIA E GEOCIÊNCIAS
DEPARTAMENTO DE ENGENHARIA CARTOGRÁFICA
PROGRAMA DE PÓS-GRADUAÇÃO EM CIÊNCIAS GEODÉSICAS E TECNOLOGIAS DA GEOINFORMAÇÃO

ISAAC RAMOS JUNIOR

ALIGNMENT STUDY OF AN ELECTRONIC DISTANCE MEASURING INSTRUMENTS CALIBRATION BASELINE USING GEODETIC TECHNIQUES

Recife
2024

ISAAC RAMOS JUNIOR

ALIGNMENT STUDY OF AN ELECTRONIC DISTANCE MEASURING INSTRUMENTS CALIBRATION BASELINE USING GEODETIC TECHNIQUES

Dissertation presented to the Postgraduate Program in Geodetic Sciences and Geoinformation Technologies, of the Federal University of Pernambuco, as part of the requirements for obtaining a Master's degree in Geodetic Sciences and Geoinformation Technologies.

Area of concentration: Geodetic Sciences and Geoinformation Technologies.

Advisor: Profª. Drª. Andréa de Seixas

Recife

2024

.Catalogação de Publicação na Fonte. UFPE - Biblioteca Central

Junior, Isaac Ramos.
   Alignment study of an electronic distance measuring instruments calibration baseline using geodetic techniques / Isaac Ramos Junior. - Recife, 2024.
   116f.: il.

   Dissertação (Mestrado) - Universidade Federal de Pernambuco, Centro de Tecnologia e Geociências, Programa de Pós-Graduação em Ciências Geodésicas e Tecnologias da Geoinformação, 2024.
   Orientação: Andrea de Seixas.

   1. Geodetic Engineering; 2. Metrology; 3. Precise Instrumentation. I. Seixas, Andrea de. II. Título.

UFPE-Biblioteca Central

ISAAC RAMOS JUNIOR

ALIGNMENT STUDY OF AN ELECTRONIC DISTANCE MEASURING INSTRUMENTS CALIBRATION BASELINE USING GEODETIC TECHNIQUES

Dissertation presented to the Postgraduate Program in Geodetic Sciences and Geoinformation Technologies, of the Federal University of Pernambuco, as part of the requirements for obtaining a Master's degree in Geodetic Sciences and Geoinformation Technologies.

Approved in: _____/_____/_____.

EXAMINATION COMMITTEE

_____

Profª. Drª. Andréa de Seixas (Advisor)
Federal University of Pernambuco

_____

Profº. Dr. Silvio Jacks dos Anjos Garnés (External Examiner to the Program)
Federal University of Pernambuco

_____

Profª. Drª. Juciela Cristina dos Santos (External Examiner to the Program)
Federal University of Alagoas

I dedicate this work to my father Isaac *(in memoriam*), to my mother Vera, and to my wife Maria Fernanda.

ACKNOWLEDGMENTS

To my advisor, Profª. Drª. Andréa de Seixas, for her exceptional performance and friendship.

To Profº. Dr. Sílvio Jacks dos Anjos Garnés, for all his collaboration throughout the work, and for granting a license to the AstGeoTop program.

To Profª. Drª. Juciela Cristina dos Santos, for accepting the invitation to be part of the dissertation committee.

To the Cartographic Engineering Department, in the person of the head, Profº. Dr. Cezário de Oliveira Lima Junior, who was very helpful every time he was asked.

To all professors and technicians of the Postgraduate Program in Geodetic Sciences and Geoinformation Technologies, especially Profº. Dr. Rodrigo Mikosz Gonçalves, Profª. Drª. Andréa Flávia Tenório Carneiro, Profª. Drª. Ligia Albuquerque de Alcântara Ferreira, Profº. Dr. Admilson da Penha Pacheco, Profº. Dr. Vagner Gonçalves Ferreira, and Profª. Drª. Ana Lúcia Bezerra Candeias, and the technicians Elizabeth Galdino do Nascimento and Ana Paula da Silva Vidal who were always very helpful and attentive at all times.

To my master's colleagues: Marina, Lucas, Thiago, Vinícius, Max, and Marcone, for their companionship and all their help.

To my brothers in life: Alex, Gustavo, Marcelo, Alexandre, Luiz Filipe, and Josué.

To the best teachers I had: Profº. Vicente Grus (*in memoriam*), Profº. Desidério Murcho, and Profº. Dr. Antônio Simões Silva.

To the Federal University of Pampa for granting leave to undertake this postgraduate course.

To the Coordination of Superior Level Staff Improvement (CAPES), for the opportunity given in relation to the authorization of this postgraduate course.

ABSTRACT

This dissertation studied the alignment of the calibration baseline of electronic distance measuring instruments, at Recife campus of the Federal University of Pernambuco. The seven pillars of the calibration baseline, which have a forced centering device, were labeled P1 through P7. Data collection was carried out in two stages. In the first of them, pillars P1 and P7 were used as ends of a presumed alignment, with the other pillars positioned between them, so that if they were all aligned, they would belong to this alignment. Thus, measurements were made using a Topcon GT-605 robotic total station, with P1 and P7 as stations, and through the radiation method, the other pillars were targeted. The field data was transferred to a computer and processed using an original program made in Python. Precision estimates were made for the results, revealing small alignment discrepancies between the pillars. However, pillars P2, P4, P5, and P6 presented values beyond the linear precision of the equipment, which is +/-(2mm +2ppm × D). Due to the geometry found, a closed traverse was perceived between the pillars, with the sequence P1, P3, P4, P7, P6, P5, P2, P1. For this reason, in the second stage, with the same equipment, measurements were taken of three different traverses, using three types of reflective surfaces (360° prism, circular prism, and reflective sheet). The field data were analyzed and subjected to two preliminary statistical tests (Shapiro-Wilk and t-test), followed by adjustment computations for the traverses using the Method of Least Squares, carried out with the AstGeoTop software. After adjustment, distances, angles and coordinates were compared using the 360° prism as reference, and no significant discrepancies were found. Finally, the reference adjusted coordinates of the pillars were used to calculate the distances between them, so they could be compared with previous work. The largest difference found was -2.2 mm, however, it is within the expected linear precision for the distances involved. For future work, it is recommended to carry out high-precision geometric leveling of the baseline to study the vertical component.

Keywords: *Geodetic Engineering. Metrology. Precise Instrumentation*. *Alignment of Structures.*

RESUMO

Esta dissertação estudou o alinhamento da base de calibração de instrumentos de medição eletrônica de distâncias, do campus Recife da Universidade Federal de Pernambuco. Os sete pilares da base de calibração, que possuem dispositivo de centragem forçada, foram nomeados de P1 a P7. A coleta de dados foi realizada em duas etapas. Na primeira delas, os pilares P1 e P7 foram utilizados como extremidades de um pressuposto alinhamento, com os demais pilares posicionados entre eles, de forma que se todos estivessem alinhados, pertenceriam a este alinhamento. Assim, as medições foram feitas usando uma estação total robótica Topcon GT-605, com P1 e P7 como estações e, através do método da irradiação, os outros pilares foram visados. Os dados de campo foram transferidos para um computador e processados usando um programa original feito em Python. Estimativas de precisão foram feitas para os resultados, revelando pequenas discrepâncias do alinhamento entre os pilares. Porém, os pilares P2, P4, P5 e P6 apresentaram valores além da precisão linear do equipamento, que é de +/-(2mm +2ppm). Em razão da geometria encontrada, foi percebida uma poligonal fechada entre os pilares, com a sequência P1, P3, P4, P7, P6, P5, P2, P1. Por esse motivo, na segunda etapa, com o mesmo equipamento, essa poligonal foi aferida três vezes, utilizando três tipos de superfícies refletivas como alvo (prisma 360°, prisma circular e folha refletiva). Os dados de campo foram analisados e submetidos a dois testes estatísticos preliminares (Shapiro-Wilk e teste-t), seguidos de um ajustamento utilizando o Método dos Mínimos Quadrados, feitos com o programa AstGeoTop. Depois do ajustamento, as distâncias, os ângulos e as coordenadas foram comparadas usando o prisma 360° como referência, e não foram encontradas discrepâncias significativas. Por fim, as coordenadas de referência ajustadas dos pilares foram utilizadas para calcular as distâncias entre eles, para que fossem comparadas com trabalho anterior. A maior diferença encontrada foi de -2,2 mm, porém está dentro da precisão linear esperada para as distâncias envolvidas. Para trabalhos futuros, recomenda-se realizar um nivelamento geométrico de alta precisão da base de calibração, para estudar a componente vertical.

Palavras-chave: *Engenharia Geodésica. Metrologia. Instrumentação de Precisão. Alinhamento de Estruturas.*

LIST OF FIGURES

ARTICLE 1 - ALIGNMENT STUDY OF AN ELECTRONIC DISTANCE MEASURING INSTRUMENTS CALIBRATION BASELINE USING TOTAL STATION

ARTICLE 2 - CLOSE TRAVERSE WITH TOTAL STATION IN A CALIBRATION BASELINE USING DIFFERENT REFLECTIVE SURFACES

LIST OF TABLES

ARTICLE 1 - ALIGNMENT STUDY OF AN ELECTRONIC DISTANCE MEASURING INSTRUMENTS CALIBRATION BASELINE USING TOTAL STATION

ARTICLE 2 - CLOSE TRAVERSE WITH TOTAL STATION IN A CALIBRATION BASELINE USING DIFFERENT REFLECTIVE SURFACES

LIST OF ABBREVIATIONS AND ACRONYMS

CTG	CENTER OF TECHNOLOGY AND GEOSCIENCES
DECART	DEPARTMENT OF CARTOGRAPHIC ENGINEERING
EDMI	ELECTRONIC DISTANCE MEASURING INSTRUMENT
GNSS	GLOBAL NAVIGATION SATELLITE SYSTEM
GPS	GLOBAL POSITIONING SYSTEM
ISO	INTERNATIONAL ORGANIZATION FOR STANDARDIZATION
LAMEPE	SPATIAL POSITIONING AND METROLOGY LABORATORY
LASER	LIGHT AMPLIFICATION BY THE STIMULATED EMISSION OF RADIATION
MLS	METHOD OF LEAST SQUARES
NGS	NATIONAL GEODETIC SURVEY
RTS	ROBOTIC TOTAL STATION
UFPR	FEDERAL UNIVERSITY OF PARANÁ
UFPE	FEDERAL UNIVERSITY OF PERNAMBUCO
USP	UNIVERSITY OF SÃO PAULO

SUMMARY

INTRODUCTION

Engineering geodesy is a science centered on measurement, crucial for its relevance to society and science. Its core expertise includes modeling measurement processes, understanding sensor models, and assessing environmental factors. The field work employs various instruments such as total stations, GNSS (Global Navigation Satellite System) receivers, levels, and terrestrial laser scanners (KUHLMANN et al., 2014, p. 331).

Space techniques as GNSS have truly revolutionized many technical and scientific areas (KAPLAN, HEGARTY, 2017, p. 924). However, this does not mean that terrestrial geodetic techniques have been completely discarded. Terrestrial geodetic measurements determine the relative positions of points on the Earth's surface, typically using electromagnetic waves to derive geometric quantities between them. Most observations are related to the local vertical, resulting in outcomes oriented within local gravity-related astronomic systems. By measuring horizontal and zenith angles and distances, relative three-dimensional positioning can be achieved. Nowadays, combined instruments known as total stations are commonly used, often integrated with absolute GNSS positioning. Additionally, laser tracking instruments are extensively employed in engineering geodesy (TORGE, MÜLLER, and PAIL, 2023, p. 269)

In an even more specific way, distance measurements are still relevant to engineering geodesy, since, according to Torge, Müller and Pail (2023, p. 272) “Terrestrial distance measurements have played and still play an important role for positioning. They provide geometric relations between neighboring control points, and they have also established the scale of classical geodetic networks”.

In this context, as seen above, the total station is an important instrument. According to Nadolinetz, Levin, Akhmedov (2017, p. 115) “A total station is a measuring instrument applied to measure distance, and vertical and horizontal angles. This is a tool that combines the functions of a theodolite and an electronic distance measurer, and has a microprocessor with software”.

Distances measured with a total station have the peculiarity of being collected with an electronic distance measurer, belonging to the instrument. According to Uren and Price (2010, p. 127) “When a distance is measured with a total station, an electromagnetic wave or pulse is used for the measurement, and this is propagated

through the atmosphere from instrument to reflector or target and back during a measurement".

From this point of view, consequently, engineering geodesists design measurement concepts, plan and execute data acquisition, and analyze data with quality control. They integrate multiple sensors into multi-sensor configurations, develop these systems, and ensure precise measurements, with calibration being a key task (KUHLMANN et al., 2014, p. 331).

Concerning calibration, component aging, temperature changes, and mechanical stress can gradually deteriorate equipment functions, making tests and measurements less reliable, which affects product design and quality. Calibration can avoid these problems by checking whether an instrument complies with applicable specifications or standards and establishing a relationship between the indicated value and the true value of the measured quantity (SOUZA, 2010, p. 73).

The calibration of an Electronic Distance Measuring Instrument (EDMI[1]), in which a total station can be considered as an example, in addition to being carried out in the laboratory, has been widely explored using field calibration baselines. These structures are used in determining of the zero error (or additive constant), which is the non-coincidence of the electronic center of the instrument with its mechanical center, materialized by its main axis; in determining of the scale factor, which is the variation of the frequency of the carrier wave, caused mainly by the aging of the crystal; and in determining of the cyclic error components, which consists of calculating its amplitude and phase angle (FAGGION, 2001, p. 01).

As an illustrative example of field calibration in practice, the United States of America can be cited, which has more than 400 calibration baselines in its territory, together with an online service to perform calculations related to EDMI calibration (NGS, 2024, p. 01).

In Brazil, there are also calibration baselines. Among them, one belongs to the Federal University of Paraná - UFPR (FAGGION and FREITAS, 2000, p. 21), another to the University of São Paulo - USP (NETTO and ERWES, 1998, p. 331), and another to the Federal University of Pernambuco - UFPE (BRANDÃO, 1996, p. 71).

---

[1] According to the National Geodetic Survey (NGS, 2017, p. 03), EDMI means Electronic Distance Measuring Instrumentation. However, in NGS (2024, p. 01) EDMI means Electronic Distance Measuring Instruments. In this dissertation we choose Electronic Distance Measuring Instrument, without changing the meaning given by the NGS.

The UFPE calibration baseline was implemented on the Recife Campus, in 1990, by the Spatial Positioning And Metrology Laboratory (LAMEPE), of the Department of Cartographic Engineering (DECART), however, it has a supposed slight misalignment between its pillars (GARNÉS, SEIXAS, and SILVA, 2014, p. 406).

Furthermore, the acquisition of new equipment by DECART, specifically a Topcon robotic total station (RTS), model GT-605, with a linear precision of ±(2mm + 2ppm × D), factory-calibrated, enabled new baseline measurements, facilitating further studies on its misalignment. It is worth noting that, currently, the UFPE calibration baseline has eight pillars, but originally had seven (BARBOSA, 2009, p. 74). In this work, the original configuration of the baseline was used, because the full test procedure for EDMI described by the international standard ISO 17123-4 has seven pillars (ISO, 2012, p. 04).

1.1 HYPOTHESIS

Based on what was discussed above, the following hypothesis can be made: The UFPE calibration baseline has a misalignment that can be treated as a traverse, that can be used to study the performance of different types of targets, thus enabling structural alignment analysis works.

1.2 GENERAL AND SPECIFIC OBJECTIVES

The general objective of this dissertation can be presented as follows:

- To use a robotic total station and geodetic techniques to study whether the UFPE calibration baseline has any misalignment and, if so, measure it as a traverse.

Regarding the specific objectives, the following were considered:

- To use the radiation method with a robotic total station to study the supposed misalignment in the UFPE calibration baseline;
- To perform new measurements, with the same equipment, but using the traverse method, so that three different traverses can be measured with three different types of targets (360° prism, circular prism, and reflective sheet), if the misalignment is confirmed;
- To use an original program in Python language to perform the computations of the radiation method;

- To use another original program in Python language to compute the horizontal angular measurements, made by traversing, by the Prussian (or directions) method;
- To use an scientific software, called AstGeoTop, to perform statistical analyses and to compute the traverses by the Method of Least Squares;
- To perform comparisons between the horizontal angles, horizontal distances and coordinates for the three traverses, and between the horizontal scale of the calibration baseline computed in this work in relation to a previous work.

1.3 JUSTIFICATIONS

As general justifications for this dissertation, two points can be highlighted:

- The first of these has to do with the evolution of equipment and measurement techniques, since recent years have brought dynamic developments in equipment and surveying techniques (GMITROWICZ et al., 2021, p. 01). This is why in this dissertation a new robotic total station was used. It is also worth noting that the use of a robotic total station with a 360° prism, which had not been used in the UFPE calibration baseline, especially using two different geodetic techniques, will benefit studies on automated data collection.
- The second point concerns the professional performance itself, since nowadays, engineers are entrusted to constantly deliver a higher level of increasingly sophisticated results in terms of mapping, positioning, control, monitoring, etc. (ROE, 2022, p. 03). This is why in this dissertation the same total station was used, but with three different types of targets (360° prism, circular prism, and reflective sheet), so that the respective measurements could be made and the respective errors could be studied and compared.

As justification for choosing the AstGeoTop software, it can be said that such a choice was made because it is a scientific software, developed in the academic environment, under rigorous perspectives, by the professor of the Department of Cartographic Engineering of the Federal University of Pernambuco, the Commander

Dr. Silvio Jacks dos Anjos Garnés. Such a choice brought consistency and security in relation to the proposal of this work.

1.4 CONTRIBUTIONS

This dissertation aims to contribute to the updating of studies on calibration baselines in Brazil, since, unlike countries such as the United States of America, in Brazilian territory, in addition to not having many calibration baselines, there is also few research on the subject; and opens up future perspectives for studies on structural alignment. Besides this, the use of a robotic total station with a 360° prism at the UFPE base was unprecedented, also opening up perspectives for future research.

1.5 DISSERTATION FORMAT

Regarding formatting, this dissertation followed the article format previously approved by the Postgraduate Program in Geodetic Sciences and Geoinformation Technologies (PPGCGTG, 2022, p. 41), whose template was made available by the library of the UFPE. Thus, after the Chapter 1 (Introduction), Chapter 2 (Results) contains the two already published articles, which make up the core of this dissertation; then, in Chapter 3 (Conclusions) there is a general conclusion; and, after the References, there are five Appendices, which provide a little more details on the development of the work.

2 RESULTS

2.1 ARTICLE 1 - ALIGNMENT STUDY OF AN ELECTRONIC DISTANCE MEASURING INSTRUMENTS CALIBRATION BASELINE USING TOTAL STATION

This article was published in the International Journal of Advances in Engineering and Technology, 2024, April. Brazilian Quallis (Geosciences): A3 rating in the 2017-2020 four-year period. Authors: Isaac Ramos Junior, Andrea de Seixas, and Sílvio Jacks dos Anjos Garnés.

Abstract

This article examines the alignment of an electronic distance measuring instrument calibration baseline at the Recife campus of the Federal University of Pernambuco, Brazil. The baseline consists of seven pillars equipped with a forced centering device labeled P1 to P7. Pillars P1 and P7 serve as the endpoints for the alignment, with the remaining pillars positioned in between. Data collection was performed using a Topcon GT-605 robotic total station, by the radiation method. Subsequently, the collected data was transferred to a computer and processed with a Python-based program. To delve into the results further, precision estimates were computed. The analysis revealed minor differences in alignment among the pillars, but P2, P4, P5, and P6 exhibited values exceeding the nominal precision of the equipment, that is +/- 2 mm +2ppm. Furthermore, the study indicated that the slight misalignment opens up the possibility of treating the base as a closed traverse in future surveys, such as that formed by pillars P1, P3, P4, P7, P6, P5, P2, P1, opening the way to numerous opportunities of future research.

Keywords: *Geodetic Engineering, Metrology, Precise Instrumentation.*

I. Introduction

The contemporary total station serves as a comprehensive surveying tool, integrating an electronic theodolite, an electronic distance measuring instrument (EDMI), and capabilities for data recording and computation. By combining these features into a singular device, the instrument facilitates the swift and precise 3D positioning of points. These advanced total stations, particularly those at the higher end, may include robotic capabilities [1,2], which incorporate several extra functionalities (such as motion control actuators, cameras, tracking software, etc.), allowing them to function autonomously by executing pre-loaded measurement programs or responding to remote commands [3].

Regarding application, robotic total stations are considered to be in the category of the single point measurement instruments, that is, that collect a single

point at a time. However, even though it takes longer, data collection has a value of just a few millimeters of precision, making it among the most accurate in engineering applications [4].

Alignment surveys are widely applicable in engineering, spanning various sectors such as tooling and deformation measurements of extensive engineering structures. Nevertheless, specific applications may demand distinct specialized tools. Practical methods can be categorized based on the approach to establishing the reference line. In this context, conventional surveying techniques, that include triangulation, trilateration, combined triangulation and trilateration, traversing, intersection, and resection where a reference line is defined by two coordinate points, are commonly employed [5].

One kind of structure that needs to be aligned is the EDMI calibration baselines. Comprising two or more stable geodetic monuments, a calibration baseline involves conducting measurements with precise instruments to determine the absolute value of the resultant measurement. The precise calibration of this baseline allows for the comparison of the precision performance of various types of geodetic instruments [6].

Works relating to the use of total stations precision surveying have been published in the most varied forms. Thus, [7] investigated the effect of battery capacity on the accuracy of Total Stations, as well as the effect of the angle of incidence on the reflecting surface for different colors and types, while [8] added the study of the influence of LASER beam size divergence. Furthermore, [9] studied the determination of a correction equation for the error in prismless distance measurements at a distance of 100 meters, due to the change in the angle of incidence; [10] investigated the accuracy of observations with a prismless Total Station during the process of monitoring and implementing engineering structures, while [11] studied the degree of reliability of prismless measurements applied to the construction of buildings; [12] and [13] incorporated into their studies the investigation of the divergence of LASER beam size from reflectorless Total Stations; [14] studied the monitoring of structures without using a prism, and [15] studied a method for measuring without a prism in tunnels.

Thus, for the current investigation, a EDMI calibration baseline was chosen. It consists of seven pillars (P1, P2, P3, P4, P5, P6 e P7) with a forced centering device, located on the campus of the Federal University of Pernambuco in Recife, Brazil. The

measurements were carried out with a Topcon GT-605 robotic total station, utilizing a 360° prism, and employing the radiation method from P1 and P7 pillars with the aim of studying the interpillar alignment.

II. Materials and Methods

The EDMI calibration baseline chosen to conduct this research was established by the Spatial Metrology Laboratory of the Department of Cartographic Engineering, of the Technology and Geosciences Center (CTG), of the Federal University of Pernambuco (UFPE), Brazil [16]. To enhance clarity, the seven pillars of the base were designated with the names P1, P2, P3, P4, P5, P6, and P7. Figure 1 depicts each pillar appropriately labeled for easy identification.

Figure 1. Each individual pillar of the EDMI calibration baseline, in February 2024.

A total station is utilized for measuring distances, as well as vertical angles and horizontal directions. An evolution of this instrument is the robotic total station, in which a single operator can conduct all necessary measurements through automatic aiming at a reflector and wireless communication between the device and its controller, that is stationed at a designated landmark with a reflector, grants complete control over the device when the operator is at a measured point [17].

To conduct the measurements of this paper, a Topcon robotic total station, model GT-605, and a 360° prism, both owned by UFPE, were utilized (refer to Figure 2 and Figure 3, respectively). The equipment has a linear accuracy of ±2mm + 2ppm (parts per million) and an angular accuracy of 5” [18].

The initial step involved selecting the coordinate system. In pursuit of this, the alignment between the first and last pillars (P1 and P7) was designated as the reference alignment. This alignment served as the basis for determining the positions of the remaining pillars if they were to be aligned. Consequently, the *y*-axis of the local coordinate system was established to coincide with the alignment between pillars P1 and P7.

Figure 2. The robotic total station used in the measurements, in February 2024.

Figure 3. The 360° prism used in the measurements, in February 2024.

The next step involved data collection using the radiation method [19], following this sequence: The equipment was set up at P1 with a backsight at P7, that was the last pillar of the sequence, and data were collected from the additional points (P2, P3, P4, P5, and P6). Then, the equipment was repositioned at P7 with a

backsight at P1, the first pillar of the sequence, and data were once again collected from the same set of points (P2, P3, P4, P5, and P6). This resulted in two sets of data that could be compared.

Subsequently, utilizing all the collected data, the radiation method was computed through a program developed in the Python language, because in its current state, this is an excellent language for developing engineering applications [20]. This program employed the equations (1) and (2) above [21]:

$$xp_i = xp_1 + D_{p1pi}sin(\alpha_{p1pi}) = xp_7 + D_{p7pi}sin(\alpha_{p7pi}) \quad (1)$$

$$yp_i = yp_1 + D_{p1pi}cos(\alpha_{p1pi}) = yp_7 + D_{p7pi}cos(\alpha_{p7pi}) \quad (2)$$

In which:

xp_i is the unknown *x* coordinate of pillar *i*;

yp_i is the unknown *y* coordinate of pillar *i*;

xp_1 is the know *x* coordinate of pillar P1;

yp_1 is the know *y* coordinate of pillar P1;

xp_7 is the know coordinate of pillar P7

yp_7 is the know coordinate of pillar P7;

D_{p1pi} is the horizontal distance between P1 and Pi;

D_{p7pi} is the horizontal distance between P7 and Pi;

α_{p1pi} is the angle centered at P1, backsight at P7 and foresight at Pi;

α_{p7pi} is the angle centered at P7, backsight at P1 and foresight at Pi.

The final step involved estimating uncertainties, utilizing the special law of propagation of variances [22,23]. The general expressions for this law for the equations (1) and (2) are equations (3) and (4):

$$\sigma_{xp_i} = \sqrt{(\frac{\partial xp_i}{\partial xp1}\sigma_{xp1})^2 + (\frac{\partial xp_i}{\partial \bar{D}_{p1pi}}\sigma_{\bar{D}_{p1pi}})^2 + (\frac{\partial xp_i}{\partial \alpha_{p1pi}}\sigma_{\alpha_{p1pi}})^2} \quad (3)$$

$$\sigma_{yp_i} = \sqrt{(\frac{\partial yp_i}{\partial yp1}\sigma_{yp1})^2 + (\frac{\partial yp_i}{\partial \bar{D}_{p1pi}}\sigma_{\bar{D}_{p1pi}})^2 + (\frac{\partial yp_i}{\partial \alpha_{p1pi}}\sigma_{\alpha_{p1pi}})^2} \quad (4)$$

In addition to all the calculations, all the tables that present the results were also generated by the same program mentioned above, in the Python language.

III. Results and Discussions

When retrieving data from the equipment, the program specifically chose pertinent information for this study, focusing exclusively on horizontal directions and overall horizontal distances. The relevant data can be found in table 1, where (D) means reading in the direct position of the telescope, and (I) means reading in the reverse position of the telescope.

Table 1. Raw data collected for P1 and P7 stations.

Station	Point	Horizontal Direction	Horizontal Distance (m)
P1	P2	00°00’03” (D)	8.3009
P1	P2	179°59’56” (I)	8.3009
P1	P3	359°58’53” (D)	12.7380
P1	P3	179°58’54” (I)	12.7380
P1	P4	359°58’38” (D)	45.8650
P1	P4	179°58’36” (I)	45.8650
P1	P5	00°00’23” (D)	95.7540
P1	P5	180°00’20” (I)	95.7540
P1	P6	359°59’41” (D)	135.2359
P1	P6	179°59’40” (I)	135.2359
P1	P7	359°59’27” (D)	167.4939
P1	P7	179°59’26” (I)	167.4939
P7	P1	00°00’02” (D)	167.4940
P7	P1	179°59’57” (I)	167.4940
P7	P2	359°59’56” (D)	159.1939
P7	P2	179°59’57” (I)	159.1939
P7	P3	00°00’04” (D)	154.7549
P7	P3	180°00’00” (I)	154.7549
P7	P4	00°00’18” (D)	121.6288
P7	P4	180°00’13” (I)	121.6286
P7	P5	359°58’47” (D)	71.7380
P7	P5	179°58’45” (I)	71.7380
P7	P6	359°58’50” (D)	32.2569
P7	P6	179°58’47” (I)	32.2569

Subsequently, the program conducted the initial processing of the raw data independently for stations P1 and P7. This process involved the calculation and reduction of angles, yielding the outcomes showcased in tables 2 and 3.

Table 2. Horizontal Angles and Horizontal distances for P1 station.

Backsight	Station	Foresight	Angle	Horizontal Distance (m)
P7	P1	P7	00°00’00.0”	167.4939
P7	P1	P2	00°00’34.0”	8.3009
P7	P1	P3	359°59’27.0”	12.7380
P7	P1	P4	359°59’10.5”	45.8650
P7	P1	P5	00°00’55.0”	95.7540
P7	P1	P6	00°00’14.0”	135.2358

Table 3. Horizontal Angles and Horizontal distances for P7 station.

Backsight	Station	Foresight	Angle	Horizontal Distance (m)
P1	P7	P1	00°00’00.0”	167.4940
P1	P7	P2	359°59’56.0”	159.1939
P1	P7	P3	00°00’01.5”	154.7549
P1	P7	P4	00°00’15.0”	121.6287
P1	P7	P5	359°58’45.5”	71.7380
P1	P7	P6	359°58’48.0”	32.2569

Subsequently, using equation (1), the distances of pillars P2, P3, P4, P5, and P6 from the alignment formed by points P1 and P7 were calculated for each station. This process yielded two outcomes representing the misalignment of the pillars, facilitating a comparative analysis. The comparison involved subtracting the respective values, calculating their average, and estimating the standard deviation. All these details are presented in table 4.

Table 4. Result of misalignment.

Point	∆xP1 (m)	∆xP7 (m)	dif (m)	media (m)	sd (m)
P2	0.00137	0.00309	-0.00172	0.00223	±0.0002
P3	-0.00204	-0.00113	-0.00091	-0.00159	±0.0007
P4	-0.01101	-0.00885	-0.00216	-0.00993	±0.0017

P5	0.02553	0.02591	-0.00037	0.02572	±0.0027
P6	0.00918	0.01126	-0.00207	0.01022	±0.0036

Derived from the disparities in alignment among the pillars, as indicated in table 4, figure 4 was generated. This illustration geometrically represents the values obtained for the pillar positions, with an exaggerated scale on the *y*-axis compared to the *x*-axis. Take note of the formation of a closed clockwise traverse, following the sequence: P1, P3, P4, P7, P6, P5, P2, P1.

The scale of the X axis is in tenths of a millimeter, so that the traverse could appear. If scales were used only in meters, the misalignments of the points in relation to the ordinate axis would not be visible, due to their smallness in relation to the distances between the pillars. This change in scale was made only so that the formation of the traverse could be clearly seen, and does not represent its real geometry, given that there is this difference in scale.

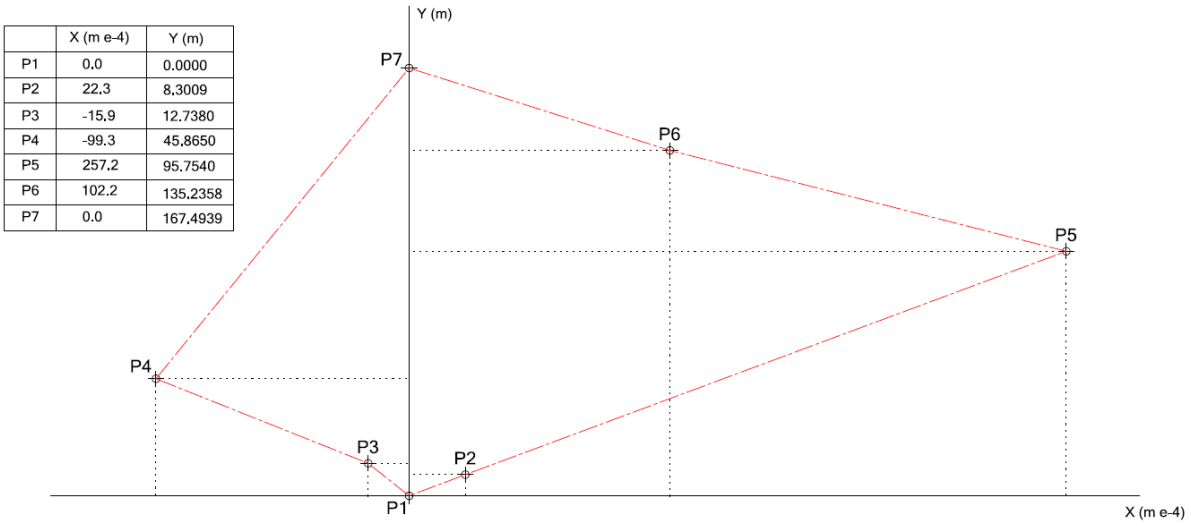

	X (m e-4)	Y (m)
P1	0.0	0.0000
P2	22.3	8.3009
P3	-15.9	12.7380
P4	-99.3	45.8650
P5	257.2	95.7540
P6	102.2	135.2358
P7	0.0	167.4939

Figure 4. Misalignment of the pillars in relation to the alignment P1 P7.

IV. Conclusions

A study on the alignment of the EDMI calibration baseline at The Federal University of Pernambuco was carried out. The results showed that, in relation to the alignment formed by pillars P1 and P7, all other pillars have some misalignment, however, four of them were found values greater than that relative to the nominal precision of the robotic total station used, which is ±2mm + 2ppm. Although the measurements reflected small misalignments between the pillars, due to its

geometric configuration, the calibration base was presented in a way that can be treated as a traverse one, formed by the pillars P1, P3, P4, P7, P6, P5, P2, P1. This means that this traverse can be used as a reference for future monitoring of the pillars, because, if it is measured from time to time, and if new discrepancies are found, it means that there is a settlement that can be monitored through a time series, for example. Therefore, as future work, in addition to measuring the traverse, it is suggested that measurements be made using other equipment, such as precision GNSS receiver, and also the precision leveling of the pillars can be proposed, with a high precision level, so that the vertical misalignment can also be studied.

Acknowledgements

The authors would like to thank the Department of Cartographic Engineering of the Federal University of Pernambuco, for providing the equipment and the technical infrastructure used for the acquisition of field data.

References

[1]. J. Uren, B. Price: Surveying for Engineers. Fifth edition. New York: Palgrave Macmillan, 2010.

[2]. N. W. J. Hazelton: Levelling and Total Stations. In: Surveying and Geomatics Engineering: principles, technologies, and applications, edited by D. T. Gillins, M. L. Dennis, A. Y. Reston: 2022. American Society of Civil Engineers, ASCE.

[3]. H. Simas, R. Di Gregorio, R. Simoni, M. Gatti: Parallel Pointing Systems Suitable for Robotic Total Stations: Selection, Dimensional Synthesis, and Accuracy Analysis. Machines 2024, 12, 54. https://doi.org/10.3390/machines12010054.

[4]. I. da Silva: Geomatics Applied to Civil Engineering, State of the Art. In: J. K. Ghosh and I. da Silva (eds.): Applications of Geomatics in Civil Engineering, Lecture Notes in Civil Engineering 33. Springer Nature Singapore, 2020.

[5]. J. O. Ogundare: Precision Surveying: the principles and geomatics practice. Hoboken: John Wiley & Sons, 2016.

[6]. G. E. V. Becerra, R. A. Bennett, M. C. Chávez, M. E. T Soto, J. R. Camacho: Short Baseline Calibration using GPS and EDM Observations. Geofísica International 54-3: 255-266, 2015.

[7]. K. Daliga, Z. Kurałowicz: Examination method of the effect of the incidence angle of laser beam on distance measurement accuracy to surfaces with different color and roughness. Bol. Ciênc. Geod. Curitiba, v. 22, n°3, p.420-436, jul-set, 2016.

[8]. A. Geethalankara, A. Rupasinghe, N. C. Niriella: Studying the factors affect for the accuracy of reflectorless Total Station observations. Proceedings in

Engineering, Built Environment and Spatial Sciences, 9th International Research Conference-KDU. Suriyawewa, p.325-330, 2016.

[9]. E. Lambrou: Modeling the Deviations of the Reflectorless Distance Measurement due to the Laser Beam's Incident Angle. International Journal of Applied Science and Technology. Online, v. 8, n. 1, p. 11-23, março, 2018.

[10]. Z. M. Zeidan, A. A. Beshr,; S. M. Sameh: Precision Comparison and Analysis of Reflectorless Total Station Observations. Mansoura Engineering Journal, (MEJ). Mansoura, v. 40, n°4, dez, 2015.

[11]. P. Holley, T. Perrine, T. Gamble: Is Reflectorless EDM Technology Reliable for Building Construction Layout Tolerances? Proceedings of 47th ASC Annual International Conference, Omaha, 6-9 April 2011.

[12]. H. S. Ali: An investigation into the Accuracy of Distance Measurements to an object with the Pulse (Non-Prism) Total Station. Sulaimani Journal for Engineering Sciences. Sulaimaniya, v. 03, n°03, p. 51-63, April, 2016.

[13]. S. I. Mohammed: Important methods measurements to examine the accuracy and reliability of reflectorless total station measurements. 2nd International Conference for Civil Engineering Science (ICCES 2021). Journal of Physics: Conference Series 1895 (2021). IOP Publishing.

[14]. C. J. Hope, S. W. Dawe: Precision survey monitoring with a reflectorless total station. FMGM 2015 – PM Dight (ed.). Australian Centre for Geomechanics. Perth, 2015.

[15]. S. Zakeri, S. Farzaneh: Measurement Methods for Cross-Sections of Tunnels Using Reflectorless Total Stations. Journal of the Earth and Space Physics, Vol. 46, n°4, p.93-101, winter 2021.

[16]. S. J. A. Garnés, A. Seixas, T. F. Silva: Análise do alinhamento da base de calibração multi pilar do LAMEP/UFPE com proposição de modelo de correção. V Simpósio Brasileiro de Ciências Geodésicas e Tecnologias da Geoinformação Recife - PE, 12- 14 de Novembro de 2014.

[17]. L. Nadolinetz, E. Levin, D. Akhmedov: Surveying Instruments and Technology. CRC Press. Boca Raton: 2017.

[18]. TOPCON: Instruction Manual - Geodetic Total Station GT series, 2022.

[19]. J. C. McCormack, W. A. Sarusa, W. J. Davis: Surveying, 6th Edition, 2012.

[20]. J. Kiusalaas: Numerical Methods in Engineering With Python 3. Cambridge University Press, Year: 2013.

[21]. H. Kahmen, W. Faig: Surveying. Berlin: de Gruyter, 1988.

[22]. C. D. Ghilani: Adjustment Computations: Spatial Data Analysis. Sixth edition. Hoboken: John Wiley & Sons, 2017.

[23]. J. O. Ogundare: Understanding least squares estimation and geomatics data analysis. Hoboken: John Wiley & Sons, 2019.

2.2 ARTICLE 2 - CLOSE TRAVERSE WITH TOTAL STATION IN A CALIBRATION BASELINE USING DIFFERENT REFLECTIVE SURFACES

This article was published in the International Journal of Advances in Engineering and Technology, in 2024, August. Brazilian Quallis (Geosciences): A3 rating in the 2017-2020 four-year period. Authors: Isaac Ramos Junior, Andrea de Seixas, and Sílvio Jacks dos Anjos Garnés.

Abstract

This article examines three different traverses, measured with three different types of reflective surfaces, of an calibration baseline at the Recife campus of the Federal University of Pernambuco, Brazil. The baseline, which has seven pillars, labeled with P1 to P7, with forced centering devices, has a slight misalignment that made the traverse analysis possible. Due to this, it was used a close traverse formed by the pillar sequence P1, P3, P4, P7, P6, P5, P2, P1, opening up the possibility for various types of comparisons. Field data were first subjected to preliminary statistical analysis, and after that, the traverses calculations were made using the least square method. After that, three comparisons were made using one of the targets as reference, referring to angles, distances and coordinates. No cases were found in which differences between quantities exceeded significantly those predicted by least squares estimates. The next step was to use the adjusted coordinates of the reference target to calculate the distances between the pillars, in pairs, so that they could be compared with previous work. This comparison was made, and the largest difference between the distances was -2.2 mm, which is not beyond the estimated linear precision for any of the distances involved. Furthermore, among future works, it is recommended that high-precision geometric leveling of the base be carried out, so that the vertical component can be studied.

Keywords: *Geodetic Engineering, Metrology, Precise Instrumentation.*

I. Introduction

The total station integrates an electronic theodolite, an electronic distance measuring device, and a microprocessor with a memory unit. This instrument is designed for measuring horizontal and slope distances, horizontal and vertical angles, and elevations in topographic surveys, in geodetic works, as well as for other survey applications [1,2]. Total stations advanced into robotic total stations (RTS), incorporating various extra features such as motion-controlling actuators, cameras, and tracking software. These enhancements allow them to operate independently, either by adhering to a preloaded measurement program or by being directed via remote control [3].

A common approach for integrating RTS measurements is by using a traverse. A traverse is a method for establishing horizontal control by determining the rectangular coordinates of a series of control points situated around a site, using a combination of angle and distance measurements [4].

Before taking further measurements at the instrument point, it is essential to complete traverse observations. This allows future measurements to be linked to the traverse, even if the instrument is moved. Traverses can be closed to detect any errors, enabling the calculation of the vector sum. Discrepancies can be checked for errors, and adjustments can be made if needed [5].

A baseline is a spatial line defined by a set of permanent aligned points with a precise distance. These points, known as baseline points, typically consist of elevated pillars above ground. Often, the term "length baseline" refers to multiple outdoor baseline points and is primarily used to calibrate the additive and other constants of distance-measuring instruments like total stations [6], but other synonymous can be found for length baseline, such as geodetic calibration baseline [7], baseline [8], electronic distance measuring instrument (EDMI) calibration baseline [9] or calibration baseline [10].

However, from the point of view of technical and scientific research, calibration baselines, even after they are deployed to perform calibrations, have been used to investigate different variables, beyond investigations into the instrumental constants of EDMI’s. Thus, for example, [11] studied variations in the length of a calibration baseline in relation to changes in air temperature over time; in [12] there is a research that used a calibration baseline to compare observations made with a total station and a Global Positioning System (GPS) receiver; and in [13] there is a study on the stability of the pillars of a calibration baseline, carried out for different periods.

Besides these, in [14], a slight misalignment of a calibration baseline in Federal University of Pernambuco - Brazil was identified, which can be treated as a closed traverse, composed of pillars P1, P3, P4, P7, P6, P5, P2 and P1. From this specific result, several research hypotheses can be raised. In this context, the hypothesis tested in this work was that, based on three closed traverses, measurements made with a RTS, with three different types of targets (a 360° prism, a circular prism, and a reflective sheet) there are no significant differences between the angles, distances and coordinates of the pillars, when using as a reference the 360° prism, because it is the original target that accompanies the equipment.

II. Materials and Methods

The calibration baseline at the Federal University of Pernambuco was implemented in 1990 by the Spatial Metrology Laboratory of the Department of Cartographic Engineering. The pillars were built to allow intervisibility between them, and all of them have a forced centering device [15]. In this study, seven pillars of these calibration baseline were designated with the names P1, P2, P3, P4, P5, P6, and P7, however, because the misalignment, the close traverse sequence used were P1, P3, P4, P7, P6, P5, P2 and P1, as mentioned in item I. Figure 1 depicts the baseline from P7 to P1.

Figure 1. The calibration baseline is composed of seven pillars with forced centering, in June 2024.

The fieldwork was carried out using a Topcon RTS, model GT-605, in fine measurement mode, factory calibrated, configured to collect only horizontal directions and horizontal distances. The equipment has a linear accuracy of ±2mm + 2ppm (parts per million) and an angular accuracy of 5” [16]. Figure 2 shows the equipment installed on one of the baseline pillars.

Figure 2. The Topcon GT-605 RTS used in the measurements, in June 2024.

Three accessories were used as targets: a Topcon 360° prism ATP1, a Geodetic 04S Circular Prism, and a Xpex reflective sheet. As they have different reflective surfaces, each of them was used independently in the baseline, enabling the measurement of three closed traverses that can be compared. Figure 3 shows the three targets used.

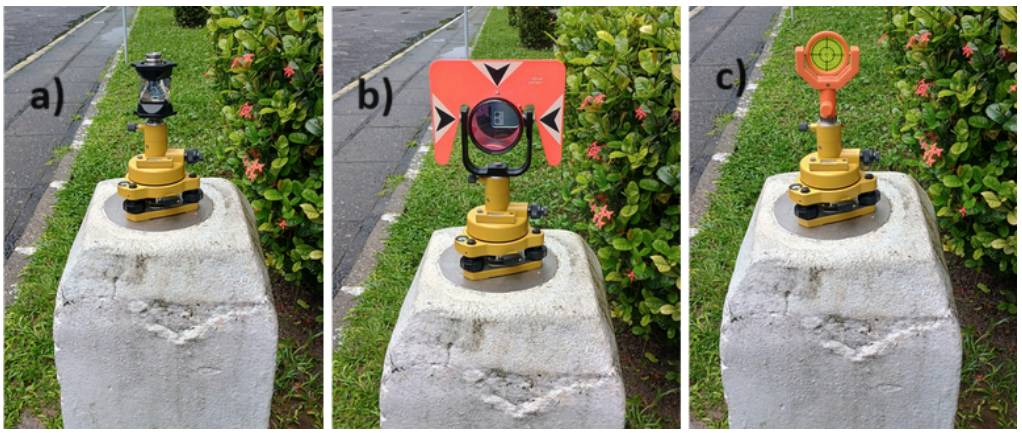

Figure 3. Three different reflective surfaces used as target, in June 2024: a) 360° prism; b) circular prism; and c) reflective sheet.

The first phase of the work consisted of measuring the angles and horizontal distances of the traverse, for each of the targets, accounting for three traverses. For each pillar, the angular measurements and computations were made using the Direction Measurement in Sets [17], as follows: Initially with the telescope in direct position and the circle close to 0°, the targets (backsight and foresight) were observed clockwise in sequence. Next, the telescope was flipped, and all targets were observed in the reverse telescope position and order. This series of measurements is called a set. Then, the circle was shifted by close to 60° and the process was repeated. And then, the circle was shifted again by close to 120° and the process was repeated.

The measurements were carried out starting and ending at pillar 1, traveling along the traverse in a clockwise direction, reading external angles. For each angular reading, a horizontal distance was also collected.

After collecting data in the field, the observations were transferred from the equipment to a computer using a Python program made specifically for this purpose. At this time, from the raw data, the mean angular directions are then adjusted to the starting direction (that is, the zero direction) by subtracting the initial value from all others, and the final directions are obtained by averaging the reduced means of the

individual sets. The calculations of means and reduced means were verified with sum checks. These calculations were made using another original Python program, made specifically for this work.

As the angular observations were made for three different types of targets, in different days, after the calculations described above, the results were subjected to the two statistical tests. The first test was the Shapiro-Wilk normality test [18], to check whether observations of each point of the traverse, for each target, belong to a normal distribution; and the statistical t-test to determine if there is a significant difference between the means of the observations sets [18], in pairs, for each pillar.

To carry out these statistical tests, the statistical module of a scientific program called AstGeoTop [19] was used. In relation to horizontal distances, arithmetic averages were calculated for each target, for each pillar.

Once the average of horizontal angles and distances were calculated, and statistical tests were carried out for angles, the data was submitted again to the scientific program AstGeoTop, however, this time to the module planimetric surveying [20], so that the three traverses could be calculated using the least squares method, using the specific program module. The least squares method was chosen because this is the most rigorous adjustment procedure available [21].

After adjustment using the least squares method, the results could be compared. Thus, for each traverse, the horizontal angles, horizontal distances, and the coordinates (X, Y), with their respective precision estimates, were selected and compared, using the traverse with the 360° prism as a reference, as this is the accessory that originally accompanies the equipment.

III. Results and Discussions

The first results were those referring to the Shapiro-Wilk normality test for horizontal angles. All sets of observations, selected for each target and for each pillar were tested, and, after the test, all of them were statistically considered to come from a normal distribution at the 1% significance level, which means that the set of observations for each target and for each pillar were found to be normally distributed with a confidence of 99%. According to [18] results significant at the 1% level are more persuasive and offer stronger evidence against the null hypothesis than those significant at the, for example, 5% level.

The second results referred to the t-test, which analyzed the samples in pairs, for the three types of targets, for each pillar. The results of the t-test are found in tables 1 to 7, below. To carry it out in all cases, a significance level of 1% was used, and a degree of freedom equal to 5, since, for each sample of observations, six angular readings were taken, three in the direct position of the telescope, and three in the inverted position. From the results of the t-test, it can be concluded with a 99% confidence level that in none of the cases do the means have statistically relevant differences, as all t-statistics values are below the t-critical values.

Table 1. T-test results for Pillar 1.

Backsight	Station	Foresight	set	sample	mean	variance	t statistics	t critical	conclusion
P2	P1	P3	1st	360° prism	359°58`57,7"	0°00`00,06441"	0,4342	4,032	do not differ
				circular prism	359°59`01,3"	0°00`00,01007"			
			2nd	360° prism	359°58`57,7"	0°00`00,06441"	0,6525	4,032	do not differ
				reflective sheet	359°58`59,8"	0°00`00,06027"			
			3rd	circular prism	359°59`01,3"	0°00`00,01007"	0,1984	4,032	do not differ
				reflective sheet	359°58`59,8"	0°00`00,06027"			

Table 2. T-test results for Pillar 2.

Backsight	Station	Foresight	set	sample	mean	variance	t statistics	t critical	conclusion
P5	P2	P1	1st	360° prism	179°59`26,3"	0°00`00,01741"	2,2203	4,032	do not differ
				circular prism	179°59`35,2"	0°00`00,00305"			
			2nd	360° prism	179°59`26,3"	0°00`00,01741"	1,3587	4,032	do not differ
				reflective sheet	179°59`33,2"	0°00`00,02638"			
			3rd	circular prism	179°59`35,2"	0°00`00,00305"	0,5806	4,032	do not differ
				reflective sheet	179°59`33,2"	0°00`00,02638"			

Table 3. T-test results for Pillar 3.

Backsight	Station	Foresight	set	sample	mean	variance	t statistics	t critical	conclusion
P1	P3	P4	1st	360° prism	179°59`36,5"	0°00`00,07997"	0,024	4,032	do not differ
				circular prism	179°59`36,7"	0°00`00,00019"			
			2nd	360° prism	179°59`36,5"	0°00`00,07997"	1,0077	4,032	do not differ
				reflective sheet	179°59`31,8"	0°00`00,01082"			
			3rd	circular prism	179°59`36,7"	0°00`00,00019"	1,8681	4,032	do not differ

				reflective sheet	179°59`31,8"	0°00`00,01082"			

Table 4. T-test results for Pillar 4.

Backsight	Station	Foresight	set	sample	mean	variance	t statistics	t critical	conclusion
P3	P4	P7	1st	360° prism	180°01`11,3"	0°00`00,00874"	0,3555	4,032	do not differ
				circular prism	180°01`12,2"	0°00`00,00071"			
			2nd	360° prism	180°01`11,3"	0°00`00,00874"	1,5492	4,032	do not differ
				reflective sheet	180°01`09,3"	0°00`00,01207"			
			3rd	circular prism	180°01`12,2"	0°00`00,00071"	1,1415	4,032	do not differ
				reflective sheet	180°01`09,3"	0°00`00,01207"			

Table 5. T-test results for Pillar 5.

Backsight	Station	Foresight	set	sample	mean	variance	t statistics	t critical	conclusion
P6	P5	P2	1st	360° prism	180°02`13,0"	0°00`00,01711"	2,2328	4,032	do not differ
				circular prism	180°02`19,2"	0°00`00,00427"			
			2nd	360° prism	180°02`13,0"	0°00`00,01711"	0,9682	4,032	do not differ
				reflective sheet	180°02`12,0"	0°00`00,01822"			
			3rd	circular prism	180°02`19,2"	0°00`00,00427"	2,5507	4,032	do not differ
				reflective sheet	180°02`12,0"	0°00`00,01822"			

Table 6. T-test results for Pillar 6.

Backsight	Station	Foresight	set	sample	mean	variance	t statistics	t critical	conclusion
P7	P6	P5	1st	360° prism	179°59`46,2"	0°00`00,00260"	3,4616	4,032	do not differ
				circular prism	179°59`56,5"	0°00`00,00775"			
			2nd	360° prism	179°59`46,2"	0°00`00,00260"	1,0518	4,032	do not differ
				reflective sheet	179°59`47,8"	0°00`00,00494"			
			3rd	circular prism	179°59`56,5"	0°00`00,00775"	2,9942	4,032	do not differ
				reflective sheet	179°59`47,8"	0°00`00,00494"			

Table 7. T-test results for Pillar 7.

Backsight	Station	Foresight	set	sample	mean	variance	t statistics	t critical	conclusion
P4	P7	P6	1st	360° prism	359°58`36,0"	0°00`00,00433"	1,6308	4,032	do not differ
				circular prism	359°58`32,7"	0°00`00,00152"			
			2nd	360° prism	359°58`36,0"	0°00`00,00433"	1,5524	4,032	do not differ

				reflective sheet	359°58`32,8"	0°00`00,00582"			
			3rd	circular prism	359°58`32,7"	0°00`00,00152"	0,0617	4,032	do not differ
				reflective sheet	359°58`32,8"	0°00`00,00582"			

After being accepted in initial statistical tests, the data were subjected to traverse calculations using the least squares method, for each type of target, generating three traverses. In this way, results were obtained for the adjusted observations (angles and horizontal distances), and for the adjusted parameters (plane coordinates), as well as the precision estimate (standard deviation, or s.d) for each of them. For all traverses, coordinates X=1000,000 meters and Y=1000,000 meters for pillar 1, and the azimuth from pillar 1 to pillar 3 was arbitrated in 0°0`00,0" for all traverses, because in this way the coordinates could be compared. The results of the observations adjustment computations are in tables 8 and 9.

Table 8. Results for the adjusted horizontal angles.

Backsight	Station	Foresight	360° Prism		Circular Prism		Reflective Sheet	
			Angle	s.d angle (")	Angle	s.d angle (")	Angle	s.d angle (")
P2	P1	P3	359°59`02,8"	3,0219	359°58`57,9"	3,6870	359°59`02,9"	3,6797
P1	P3	P4	179°59`40,7"	3,2431	179°59`33,8"	3,9570	179°59`34,5"	3,9492
P3	P4	P7	180°01`11,0"	0,5588	180°01`12,1"	0,6819	180°01`09,5"	0,6806
P4	P7	P6	359°58`36,3"	1,1249	359°58`31,8"	1,3725	359°58`33,9"	1,3697
P7	P6	P5	179°59`48,6"	1,7525	179°59`51,0"	2,1382	179°59`52,6"	2,134
P6	P5	P2	180°02`13,9"	1,7926	180°02`18,0"	2,1872	180°02`13,6"	2,1828
P5	P2	P1	179°59`26,6"	2,3448	179°59`35,3"	2,8610	179°59`33,2"	2,8553

Table 9. Results for the adjusted horizontal distances.

Station	Foresight	360° Prism		Circular Prism		Reflective Sheet	
		H. dist (m)	s.d H. dist (m)	H. dist (m)	s.d H. dist (m)	H. dist (m)	s.d H. dist (m)
P1	P3	12,739	0,0025	12,739	0,0029	12,740	0,0030
P3	P4	33,125	0,0025	33,126	0,0029	33,127	0,0030
P4	P7	121,629	0,0026	121,630	0,0029	121,630	0,0030
P7	P6	32,258	0,0025	32,259	0,0029	32,261	0,0030
P6	P5	39,480	0,0025	39,480	0,0029	39,478	0,0030
P5	P2	87,453	0,0026	87,454	0,0029	87,455	0,0030
P2	P1	8,301	0,0025	8,301	0,0029	8,303	0,0030

The results for the parameters adjustment (i.e, for the pillars coordinates) were separated in table 10 for the 360° prism and in table 11 for the other two targets, because the 360° prism was the reference target, as already mentioned. After

adjustment, the three polygonals were subjected to a quality control analysis, in which the chi-square test was used to test whether the adjusted observations belong to a normal distribution, at a significance level of 5%. All three were approved.

Table 10. Results for the adjusted coordinates for 360° prism, that was used as reference.

Station	360° Prism			
	X (m)	s.d X (m)	Y (m)	s.d Y (m)
P1	1000,0000	0,0000	1000,0000	0,0000
P3	1000,0000	0,0000	1012,7388	0,0025
P4	999,9969	0,0005	1045,8636	0,0033
P7	1000,0274	0,0024	1167,4924	0,0036
P6	1000,0324	0,0019	1135,2342	0,0036
P5	1000,0407	0,0014	1095,7540	0,0033
P2	1000,0023	0,0001	1008,3008	0,0025

Table 11. Results for the adjusted coordinates for circular prism and reflective sheet.

Station	Circular Prism				Reflective Sheet			
	X (m)	s.d X (m)	Y (m)	s.d Y (m)	X (m)	s.d X (m)	Y (m)	s.d Y (m)
P1	1000,0000	0,0000	1000,0000	0,0000	1000,0000	0,0000	1000,0000	0,0000
P3	1000,0000	0,0000	1012,7389	0,0029	1000,0000	0,0000	1012,7395	0,0030
P4	999,9958	0,0006	1045,8648	0,0038	999,9959	0,0006	1045,8660	0,0039
P7	1000,0229	0,0030	1167,4947	0,0041	1000,0218	0,0030	1167,4955	0,0043
P6	1000,0295	0,0024	1135,2356	0,0041	1000,0284	0,0024	1135,2350	0,0043
P5	1000,0393	0,0017	1095,7555	0,0038	1000,0379	0,0017	1095,7575	0,0039
P2	1000,0025	0,0001	1008,3014	0,0029	1000,0023	0,0001	1008,3030	0,0030

The results above allow for several comparisons. For this work, comparisons were made between horizontal angles, horizontal distances and coordinates, always using the 360° prism as a reference. In this way, tables 12 to 14 were created, which show the results for the differences obtained for angles, distances and coordinates, respectively.

Table 12. Results for comparing adjusted horizontal angles.

Backsight	Station	Foresight	360° Prism -Circular Prism	360° Prism - Reflective Sheet
P2	P1	P3	4,9"	-0,1"
P1	P3	P4	6,9"	6,2"
P3	P4	P7	-1,1"	1,5"
P4	P7	P6	4,5"	2,4"
P7	P6	P5	-2,4"	-4,0"
P6	P5	P2	-4,1"	0,3"
P5	P2	P1	-8,7"	-6,6"

Table 13. Results for comparing adjusted horizontal distances.

Station	Foresight	360° Prism - Circular Prism (mm)	360° Prism - Reflective Sheet (mm)
P1	P3	0	-1
P3	P4	-1	-2
P4	P7	-1	-1
P7	P6	-1	-3
P6	P5	0	2
P5	P2	-1	-2
P2	P1	0	-2

Table 14. Results for comparing adjusted coordinates.

Station	360° Prism and Circular Prism		360° Prism and Reflective Sheet	
	delta X (m)	delta Y (m)	delta X (m)	delta Y (m)
P1	0,0000	0,0000	0,0000	0,0000
P3	0,0000	-0,0001	0,0000	-0,0007
P4	0,0011	-0,0012	0,001	-0,0024
P7	0,0045	-0,0023	0,0056	-0,0031
P6	0,0029	-0,0014	0,0040	-0,0008
P5	0,0014	-0,0015	0,0028	-0,0035
P2	-0,0002	-0,0006	0,0000	-0,0022

In relation to the information provided by the RTS manufacturer, with regard to angles, no estimative of precision was found greater than the value of 5" reported by the manufacturer, as can be seen in table 8.

Regarding the distances, for the 360° prism, no significant differences were found in relation to those specified by the RTS manufacturer, as the highest precision estimates were ±2,6mm for the P4-P7 and P5-P2 alignments, which are those with the longest traverse lengths, with 121,629m and 87,453m respectively. For the circular prism, the precision estimates for all distances after adjustment were ±2,9mm, which does not mean a discrepant value, however, as this prism is not an original accessory from the same RTS manufacturer, the difference between the estimates of precision, even if very small, may originate from this fact. The same reasoning applies to the reflective sheet, however, we add the fact that, in this case, the RTS was used manually, as the reflective sheet was not automatically detected by the equipment in the same way that the two prisms were. It is probably for these reasons that the precision estimates for the reflective sheet for all distances were ±3mm.

Another result that can be obtained is in relation to the scale of the base, that is, in relation to the measurements of the horizontal distances between the pillars, in

pairs, according to the order in which they are found in the field. Namely, the distances are as follows: P1-P2, P2-P3, P3-P4, P4-P5, P5-P6, and P6-P7. Therefore, based on the adjusted coordinates, these distances were calculated and are found in Table 15, for the three targets, and the comparisons between the distances for the 360° prism and the other two targets are in table 16.

Table 15. Results for baseline horizontal distances from the adjusted coordinates.

Alignment		Distances (m)		
		360° Prism	Circular Prism	Reflective Sheet
P1	P2	8,3008	8,3014	8,3030
P2	P3	4,4380	4,4375	4,4365
P3	P4	33,1248	33,1259	33,1265
P4	P5	49,8904	49,8907	49,8915
P5	P6	39,4802	39,4801	39,4775
P6	P7	32,2582	32,2591	32,2605

Table 16. Results for comparing baseline horizontal distances.

Alignment		Distances differences	
		360° Prism - Circular Prism (mm)	360° Prism - Reflective Sheet (mm)
P1	P2	-0,6	-2,2
P2	P3	0,5	1,5
P3	P4	-1,1	-1,7
P4	P5	-0,3	-1,1
P5	P6	0,1	2,7
P6	P7	-0,9	-2,3

The biggest difference found for the comparison between the distances for the 360° prism and the circular prism was -1.1 mm for the alignment between pillars P3 and P4. This difference does not exceed the precision estimates for the distances involved, as shown in table 9. The same applies to the comparison between the 360° prism and the reflective sheet, as the largest difference found was 2.7 mm, which also does not exceed the precision estimates of the distances involved, provided in table 9.

A suitable analysis, based on the calculated distances between the pillars, can be made through a comparison with the same measurements that were presented in [22], that is, in Garnés, Seixas e Silva (2014). In this way, table 17 was created, which shows the distances found in this work and in [22], with the respective differences.

Table 17. Comparison of horizontal distances to the 360° prism in relation to Garnés, Seixas e Silva (2014).

Alignment		Distances (m)		Difference (mm)
		360° Prism	Garnés, Seixas e Silva (2014)	
P1	P2	8,3008	8,3000	0,8
P2	P3	4,4380	4,4390	-1
P3	P4	33,1248	33,1270	-2,2
P4	P5	49,8904	49,8900	0,4
P5	P6	39,4802	39,4810	-0,8
P6	P7	32,2582	32,2580	0,2

According to table 17, the biggest difference found was -2.2mm, for the alignment between pillars P3 and P4. Considering that the work carried out previously used a Topcon total station, model GPT3200, which has a linear precision of ±5 mm +5 ppm (parts per million) [22], the results of the comparisons are compatible.

IV. Conclusions

A study on closed traverses, measured with a Topcon GT-605 RTS, for three different types of reflective surfaces (360° prism, circular prism, and reflective sheet), at the calibration baseline of the Federal University of Pernambuco was carried out. After the positive results of the statistical analyzes for horizontal angles, referring to the Shapiro-Wilk normality test and the t-test, the field data were subjected to traverse calculations using the least squares method. Once, for each of three traverses, with the results for the adjusted observations and parameters, with respective precision estimates, it was possible to carry out some analyzes and comparisons.

In this way, the adjusted horizontal angles, the adjusted horizontal distances and the adjusted coordinates were compared, always using the 360° prism as a reference, as this accessory originally accompanies the RTS used. For horizontal angles, in comparisons, the most significant differences were observed at pillars P2 and P3, that was -8,7” and 6,9” respectively, for the 360° prism and circular prism; this could be due mainly to the relatively short distances measured from these stations to both the backsight and foresight, as can be seen in table 9.

In terms of distances, in comparisons, only one measurement exceeded the equipment's linear precision. This was at station P7 for the reflective sheet, in

comparison with the 360° prism, with a value of 3 mm. Nonetheless, this difference did not surpass the precision estimation for the reflective sheet, which was also 3 mm, as can be seen in table 9.

With the adjusted coordinates in table 11, it was possible to estimate the distances between the pillars, in pairs. Such calculations were made, and the results were compared with the results of a previous study, revealing that the differences found are within the precisions of the equipment used in the two studies, as can be seen in table 17.

As future work on the same baseline, a precision geometric leveling can be carried out so that the heights of the pillars can be analyzed and/or compared with those arising from a trigonometric leveling with a total station, for example.

Furthermore, another application in which the methodology proposed in this work can be used refers to the study of alignments of engineering structures. This statement is justified because these surveys are essential across a wide range of engineering applications, from the tooling industry to measuring deformations in long engineering structures, and the conventional surveying techniques that use total stations in an adequate coordinate system, among the other methods, can be employed [23].

Acknowledgements

The authors would like to thank the Department of Cartographic Engineering of the Federal University of Pernambuco, for providing the equipment and the technical infrastructure used for the acquisition of field data.

References

[1]. S. Gopi, R. Sathikumar, N. Madhu: Advanced Surveying. Second Edition. Uttar Pradesh: Pearson India Education Services Pvt. Ltd, 2018.

[2]. L. Nadolinetz, E. Levin, D. Akhmedov: Surveying Instruments and Technology. CRC Press. Boca Raton: 2017.

[3]. H. Simas, R. Di Gregorio, R. Simoni, M. Gatti: Parallel Pointing Systems Suitable for Robotic Total Stations: Selection, Dimensional Synthesis, and Accuracy Analysis. Machines 2024, 12, 54.

[4]. J. Uren, B. Price: Surveying for Engineers. Fifth edition. New York: Palgrave Macmillan, 2010.

[5]. N. W. J. Hazelton: Levelling and Total Stations. In: Surveying and Geomatics Engineering: principles, technologies, and applications, edited by D. T. Gillins, M. L. Dennis, A. Y. Reston: 2022. American Society of Civil Engineers, ASCE.

[6]. G. Youyi, J. Lixing, W. Ancheng, W. Li, O. Yangwen: Error Analysis of Calibration Length Baseline based on μ-base Distance Meter. IOP Conf. Series: Earth and Environmental Science 237 (2019) 032022.

[7]. S. Saadati, M. Abbasi, S. Abbasy, A. Amiri-Simkooei: Geodetic calibration network for total stations and GNSS receivers in sub-kilometer distances with sub-millimeter precision. Measurement 141 (2019), 258–266.

[8]. D. M. Zakari, A. Aliyu: Establishment of Baseline using Electronic Distance Measurement. IOSR Journal Of Environmental Science, Toxicology And Food Technology (IOSR-JESTFT), e-ISSN: 2319-2402, p- ISSN: 2319-2399. Volume 8, Issue 1 Ver. IV (Feb. 2014), pp 79-85.

[9]. NGS: Electronic Distance Measuring Instrumentation Calibration Baseline Program Policy. NOAA's National Geodetic Survey - NGS, 2017.

[10]. A. Buga, R. Birvydiene, R. Kolosovskis, B. Krikstaponis, R. Obuchovski, E. Parseliunas, R. Putrimas, D. Slikas: Analysis of the calibration quality of the Kyviskes Calibration Baseline. Acta Geod Geophys (2016) 51:505–514.

[11]. A. Buga, R. Putrimas, D. Slikas, J. Jokela: Kyviskes Calibration Baseline: measurements and improvements analysis. The 9th Conference Environmental Engineering. Selected Papers, 22–23 May 2014, Vilnius, Lithuania Article number: enviro.2014.195.

[12]. G. E. V. Becerra, R. A. Bennett, M. C. Chávez, M. E. T Soto, J. R. Camacho: Short Baseline Calibration using GPS and EDM Observations. Geofísica International 54-3: 255-266, 2015.

[13]. B. Bozic, H. Fan, Z. Milosavljevic: Establishment of the MGI EDM calibration baseline. Survey Review, 2013, Vol 45, n° 331.

[14]. I. R. Junior, A. Seixas, S. J. A. Garnés: Alignment Study of an Electronic Distance Measuring Instruments Calibration Baseline Using Total Station.

International Journal of Advances in Engineering & Technology, April, 2024, Vol. 17, Issue 2, pp. 90-97.

[15]. F. S. Barbosa: A Escala do Basímetro Linear. Aplicação: Base Multipilar da UFPE. Dissertação de Mestrado apresentada ao programa de pós graduação em Ciências Geodésicas e Tecnologias da Geoinformação da Universidade Federal de Pernambuco. Recife, 2009.

[16]. TOPCON: Instruction Manual - Geodetic Total Station GT series, 2022.

[17]. H. Kahmen, W. Faig: Surveying. Berlin: de Gruyter, 1988.

[18]. M. F. Triola: Elementary Statistics. 14th edition. Hoboken: Pearson, 2022.

[19]. S. J. A. Garnés: AstGeoTop. Software. Módulo Análise Estatística. Recife-PE: Departamento de Engenharia Cartográfica. Universidade Federal de Pernambuco, 2024.

[20]. S. J. A. Garnés: AstGeoTop. Software. Módulo Levantamento Planimétrico Recife-PE: Departamento de Engenharia Cartográfica. Universidade Federal de Pernambuco, 2024.

[21]. C. D. Ghilani: Adjustment Computations: Spatial Data Analysis. Sixth edition. Hoboken: John Wiley & Sons, 2017.

[22]. S. J. A. Garnés, A. Seixas, T. F. Silva: Análise do alinhamento da base de calibração multi pilar do LAMEP/UFPE com proposição de modelo de correção. V Simpósio Brasileiro de Ciências Geodésicas e Tecnologias da Geoinformação Recife - PE, 12- 14 de Novembro de 2014.

[23]. J. O. Ogundare: Precision Surveying: the principles and geomatics practice. Hoboken: John Wiley & Sons, 2016.

3 CONCLUSIONS

A study was conducted on the alignment of the Electronic Distance Measuring Instruments calibration baseline at Federal University of Pernambuco (UFPE), in Recife, Brazil. The results indicated that, in relation to the alignment between pillars P1 and P7, all other pillars showed a slight misalignment. However, four pillars (P2, P4, P5 and P6 as shown in table 4 of article 1) exhibited values exceeding the nominal precision of the Topcon GT-605 robotic total station (RTS) used, which is ±(2mm + 2ppm × D). Despite these misalignment, the geometric configuration of the calibration baseline allowed it to be considered as a traverse, formed by pillars P1, P3, P4, P7, P6, P5, P2, and P1.

The identification of a traverse enabled a new geodetic surveying, namely a traversing, which was conducted for three different types of targets: a 360° prism, a circular prism, and a reflective sheet.

The field data of the three traverses were downloaded to a computer and the horizontal angles were calculated using the direction method (or Prussian method) using an original program written in Python, which can be found in Appendix E. Next, a preliminary statistical analysis for horizontal angles was performed by the statistical module of the AstGeoTop software (GARNÉS, 2024a), using the Shapiro-Wilk normality test and the t-test, and, after that, the data underwent traverse computations using the Method of Least Squares, with another module of the same software (GARNÉS, 2024b). This process was repeated for the three traverses, and with the results for the adjusted observations and parameters, along with their respective precision estimates, various analyses and comparisons were made.

The adjusted horizontal angles, distances, and coordinates were compared, with the 360° prism as the reference as it originally accompanies the robotic total station used. The most significant differences in horizontal angles were observed at pillars P2 and P3, with -8.7” and 6.9” respectively, when comparing the 360° prism and circular prism (table 12 of article 2). This was likely due to the relatively short distances measured from these stations to both the backsight and foresight, as shown in table 9 of article 2.

In terms of horizontal distances, only one difference slightly exceeded the equipment's linear precision. This happened at station P7 for the reflective sheet, compared to the 360° prism, with a value of -3 mm (table 13 of article 2). However,

this difference did not surpass the precision estimation for the reflective sheet, also 3 mm, as seen in table 9 of article 2.

Using the adjusted coordinates for 360° prism, in table 10 of article 2, distances between pillar pairs were estimated and compared with results from a previous study (table 17 of article 2). The differences found were within the linear precision of the equipment used.

As described above, it can be seen that the hypothesis formulated in item 1.1 of this dissertation was accepted, and both the general objective and the specific objectives presented in item 1.2 of this dissertation were achieved.

Future work on the same baseline could involve precision geometric leveling to analyze and/or compare the heights of the pillars with those obtained from trigonometric leveling using a total station. Additionally, the methodology proposed in this study could be applied to the alignment studies of engineering structures, that are crucial in various applications, from the tooling industry to measuring deformations in long structures, utilizing conventional surveying techniques with total stations in an appropriate coordinate system.

If new discrepancies are detected over time, it would indicate settlement that can be monitored through a time series analysis. Future work also should include measuring the traverse with other equipment, such as a precision GNSS receiver, and can consider a RTS surveying in conjunction with other variables such as temperature, atmospheric pressure and air humidity, for example.

As a complement, after References, there are five Appendices, which contain: all horizontal angles and horizontal distances collected in the field for the three traverses (Appendix A); all results of the original program developed in Python for the angular computations, made by the method of directions (or Prussian method) for the three traverses (Appendix B); all reports of the AstGeoTop software (GARNÉS, 2024a) for the preliminary statistical analyses, made for horizontal angles of the three traverses (Appendix C); all reports of the AstGeoTop software (GARNÉS, 2024b) for the computations made by the Least Squares Method for the three traverses (Appendix D); and the scripts of the original programs written in Python for the two articles (Appendix E).

Regarding Appendix D, as a final consideration, it is worth noting that it contains a table for each traverse, which compares the coordinates of the vertices calculated by the traditional method (with linear adjustment proportional to the sides,

and with angular adjustment by the adjacent sides) in relation to those calculated by the Least Squares Method. The differences found were of a sub millimetric order.

REFERENCES

ALI, H. S. An investigation into the Accuracy of Distance Measurements to an object with the Pulse (Non-Prism) Total Station. **Sulaimani Journal for Engineering Sciences**. Sulaimaniya, v. 03, n°03, p. 51-63, April, 2016.

BARBOSA, F. S. **A Escala do Basímetro Linear. Aplicação: Base Multipilar da UFPE**. Dissertação de Mestrado apresentada ao programa de pós graduação em Ciências Geodésicas e Tecnologias da Geoinformação da Universidade Federal de Pernambuco. Recife, 2009.

BECERRA, G. E. V.; BENNETT, R. A.; CHÁVEZ, M. C.; SOTO, M. E. T.; CAMACHO, J. R. Short Baseline Calibration using GPS and EDM Observations. **Geofísica International** 54-3: 255-266, 2015.

BOZIC, B.; FAN, H.; MILOSAVLJEVIC, Z. Establishment of the MGI EDM calibration baseline. **Survey Review**, 2013, Vol 45, n° 331.

BUGA, A.; PUTRIMAS, R.; SLIKAS, D.; JOKELA, J. Kyviskes Calibration Baseline: measurements and improvements analysis. **The 9th Conference Environmental Engineering**. Selected Papers, 22–23 May 2014, Vilnius, Lithuania Article number: enviro.2014.195.

BUGA, A.; BIRVYDIENE, R.; KOLOSOVSKIS, R.; KRIKSTAPONIS, B.; OBUCHOVSKI, R.; PARSELIUNAS, E.; PUTRIMAS, R.; SLIKAS, D. Analysis of the calibration quality of the Kyviskes Calibration Baseline. **Acta Geod Geophys** (2016) 51:505–514.

BRANDÃO, A. C. **Possibilidades de Emprego de um Campo de Pontos Planimétrico como Definidor de um Comparador de Distâncias Colineares**. Dissertação de Mestrado apresentada ao programa de pós-graduação em Ciências Geodésicas da Universidade Federal do Paraná. Curitiba, 1996.

DALIGA, K.; KURAŁOWICZ, Z. Examination method of the effect of the incidence angle of laser beam on distance measurement accuracy to surfaces with different color and roughness. **Bol. Ciênc. Geod.** Curitiba, v. 22, n°3, p.420-436, jul-set, 2016.

FAGGION, P. L. **Obtenção dos Elementos de Calibração e Certificação de Medidores Eletrônicos de Distância em Campo e Laboratório**. Tese de doutorado

apresentada ao programa de pós-graduação em Ciências Geodésicas da Universidade Federal do Paraná. Curitiba, 2001.

FAGGION, P. L.; DE FREITAS, S. R. C. Determinação do Fator de Escala em Estações Totais e MED Utilizando Observações de Campo e Laboratório. **Revista Brasileira de Cartografia**, *[S. l.]*, v. 52, p. 20–28, 2000.

GARNÉS, S. J. A. **AstGeoTop**. Software. Módulo Análise Estatística. Versão 2014.09.08. Recife-PE: Departamento de Engenharia Cartográfica/CTG/UFPE. Universidade Federal de Pernambuco, 2024a.

GARNÉS, S. J. A. **AstGeoTop**. Software. Módulo Levantamento Planimétrico. Versão 2013.08.25. Recife-PE: Departamento de Engenharia Cartográfica/CTG/UFPE. Universidade Federal de Pernambuco, 2024b.

GARNÉS, S. J. A.; SEIXAS, A.; SILVA, T. F. Análise do alinhamento da base de calibração multi pilar do LAMEP/UFPE com proposição de modelo de correção. **V Simpósio Brasileiro de Ciências Geodésicas e Tecnologias da Geoinformação.** Recife - PE, 12- 14 de Novembro de 2014.

GEETHALANKARA, A.; RUPASINGHE, A.; NIRIELLA, N. C. Studying the factors affect for the accuracy of reflectorless Total Station observations. Proceedings in Engineering, Built Environment and Spatial Sciences, **9th International Research Conference-KDU**. Suriyawewa, p.325-330, 2016.

GHILANI, C. D. **Adjustment Computations: Spatial Data Analysis**. Sixth edition. Hoboken: John Wiley & Sons, 2017.

GMITROWICZ-IWAN, J.; MYSZURA, M; OLENDEREK, T.; LIGĘZA, S.; OLENDEREK, H. **The Influence of Target Properties on the Accuracy of Reflectorless Distance Measurements**. Sensors, 21, 6421, september, 2021.

GOPI, S.; SATHIKUMAR, R.; MADHU, N. **Advanced Surveying**. Second Edition. Uttar Pradesh: Pearson India Education Services Pvt. Ltd, 2018.

HAZELTON, N. W. J. Leveling and Total Stations. In: **Surveying and Geomatics Engineering: principles, technologies, and applications**, edited by Gillins, D.T; Dennis, M.L; Reston, A,Y: 2022. American Society of Civil Engineers, ASCE.

HOLLEY, P.; PERRINE, T.; GAMBLE, T. Is Reflectorless EDM Technology Reliable for Building Construction Layout Tolerances? Proceedings of **47th ASC Annual International Conference**, Omaha, 6-9 April 2011.

HOPE, C. J.; DAWE, S. W. Precision survey monitoring with a reflectorless total station. **FMGM 2015** – PM Dight (ed.). Australian Centre for Geomechanics. Perth, 2015.

INTERNATIONAL ORGANIZATION FOR STANDARDIZATION. **ISO 17123-4**: Optics and optical instruments — Field procedures for testing geodetic and surveying instruments — Part 4: Electro-optical distance meters (EDM measurements to reflectors). Geneva: ISO, 2012.

KAHMEN, H.; FAIG, W. **Surveying**. Berlin: de Gruyter, 1988.

KAPLAN, E. D.; HEGARTY, C.J. **Understanding GPS/GNSS Principles and Applications**. Third Edition. Artech House: Boston, 2017.

KIUSALAAS, J. **Numerical Methods in Engineering With Python 3**. Cambridge University Press, Year: 2013.

KUHLMANN, H.; SCHWIEGER, V.; WIESER, A.; NIEMEIER, W. Engineering Geodesy - Definition and Core Competences. **Journal of Applied Geodesy,** 2014; 8(4): 327–333. DOI 10.1515/jag-2014-0020.

LAMBROU, E. Modeling the Deviations of the Reflectorless Distance Measurement due to the Laser Beam's Incident Angle. **International Journal of Applied Science and Technology**. Online, v. 8, n. 1, p. 11-23, março, 2018.

MCCORMACK, J. C.; SARUSA, W. A.; DAVIS, W. J. **Surveying**, 6th Edition, 2012.

MOHAMMED, S. I. Important measurements methods to examine the accuracy and reliability of reflectorless total station measurements. **2nd International Conference for Civil Engineering Science** (ICCES 2021). Journal of Physics: Conference Series 1895 (2021). IOP Publishing.

NADOLINETZ, L.; LEVIN, E.; AKHMEDOV, D. **Surveying Instruments and Technology**. CRC Press. Boca Raton: 2017.

NATIONAL GEODETIC SURVEY. **Electronic Distance Measuring Instrumentation Calibration Baseline Program Policy**. NOAA's National Geodetic Survey - NGS, 2017.

NATIONAL GEODETIC SURVEY. **EDMI Calibration Baseline Program.** Available at https://geodesy.noaa.gov/CBLINES/. Accessed on 26/07/2024.

NETTO, N. P.; ERWES, H. Test Range for Calibration and Classification of Geodetic Instruments, **Survey Review**, 34:267, 331-342, 1998.

OGUNDARE, J. O. **Precision Surveying: the principles and geomatics practice**. Hoboken: John Wiley & Sons, 2016.

OGUNDARE, J. O. **Understanding least squares estimation and geomatics data analysis**. Hoboken: John Wiley & Sons, 2019.

PROGRAMA DE PÓS-GRADUAÇÃO EM CIÊNCIAS GEODÉSICAS E TECNOLOGIAS DA GEOINFORMAÇÃO - PPGCGTG. **Regimento Interno**. B.O. UFPE, Recife, 57 (60 Boletim de Serviço): 1 - 67, 04 de Abril de 2022. Avaliable at https://www.ufpe.br/documents/39694/4029294/BO_60-2022-28-50_Regimento+interno.pdf/3668de84-8b8c-4fa5-9ccd-f29f6d8c9892. Accessed on 01/08/2024.

RAMOS JUNIOR, I.; SEIXAS, A.; GARNÉS, S. J. A. Alignment Study of an Electronic Distance Measuring Instruments Calibration Baseline Using Total Station. **International Journal of Advances in Engineering & Technology**, April, 2024, Vol. 17, Issue 2, pp. 90-97.

RAMOS JUNIOR, I.; SEIXAS, A.; GARNÉS, S. J. A. Close Traverse With Total Station in a Calibration Baseline Using Different Reflective Surfaces. **International Journal of Advances in Engineering & Technology**, August, 2024, Vol. 17, Issue 4, pp. 376-387.

ROE, G. V. Engineering Surveying With ASCE. In: **Surveying and Geomatics Engineering Principles, Technologies, and Applications,** edited by Gillins, D.T; Dennis, M.L; Reston, A,Y: 2022. American Society of Civil Engineers, ASCE.

SAADATI, S.; ABBASI, M.; ABBASY, S.; A. AMIRI-SIMKOOEI, A. Geodetic calibration network for total stations and GNSS receivers in sub-kilometer distances with sub-millimeter precision. **Measurement** 141 (2019), 258–266.

SILVA, I. Geomatics Applied to Civil Engineering, State of the Art. In: J. K. Ghosh and I. da Silva (eds.): **Applications of Geomatics in Civil Engineering**, Lecture Notes in Civil Engineering 33. Springer Nature Singapore, 2020.

SIMAS, H.; DI GREGORIO, R.;SIMONI, R.; GATTI, M. Parallel Pointing Systems Suitable for Robotic Total Stations: Selection, Dimensional Synthesis, and Accuracy Analysis. **Machines** 2024, 12, 54. https:// doi.org/10.3390/machines12010054.

SOUZA, I. A. M. **A Calibração de Instrumentos de Medições Topográficas e Geodésicas: A Busca Pela Acreditação Laboratorial**. Dissertação de Mestrado apresentada ao programa de pós graduação em Engenharia de Transportes da Universidade de São Paulo. São Carlos, 2010.

TOPCON. **Instruction Manual - Geodetic Total Station GT series**, 2022.

TORGE, W.; MÜLLER, J.; PAIL, R. **Geodesy**. 5th edition. Walter de Gruyter: Berlin, 2023.

TRIOLA, M. F. **Elementary Statistics**. 14th edition. Hoboken: Pearson, 2022.

UREN, J.; PRICE, B. **Surveying for Engineers.** Fifth edition. New York: Palgrave Macmillan, 2010.

YOUYI, G.; LIXING, J.; ANCHENG, W.; LI, W.; YANGWEN, O. Error Analysis of Calibration Length Baseline based on μ-base Distance Meter. **IOP Conf. Series: Earth and Environmental Science** 237 (2019) 032022.

ZAKARI, D. M.; ALIYU, A. Establishment of Baseline using Electronic Distance Measurement. **IOSR Journal Of Environmental Science, Toxicology And Food Technology** (IOSR-JESTFT), e-ISSN: 2319-2402, p- ISSN: 2319-2399. Volume 8, Issue 1 Ver. IV (Feb. 2014), pp 79-85.

ZAKERI, S.; FARZANEH, S. Measurement Methods for Cross-Sections of Tunnels Using Reflectorless Total Stations. **Journal of the Earth and Space Physics**, Vol. 46, n°4, p.93-101, winter 2021.

ZEIDAN, Z. M.; BESHR, A. A.; SAMEH, S. M. Precision Comparison and Analysis of Reflectorless Total Station Observations. **Mansoura Engineering Journal**, (MEJ). Mansoura, v. 40, n°4, dez, 2015.

APPENDIX A - FIELD NOTES

Field notes for 360° prism (Article 2)

Station	Target	H Dist (m)	H Direction DMS
P1	P2	8,3007	0,0002
P1	P2	8,3007	179,5959
P1	P3	12,7389	359,5859
P1	P3	12,7389	179,5901
P1	P2	8,3007	60,0000
P1	P2	8,3007	239,5952
P1	P3	12,7389	59,5911
P1	P3	12,7389	239,5908
P1	P2	8,3007	120,0002
P1	P2	8,3007	300,0001
P1	P3	12,7389	119,5841
P1	P3	12,7389	299,5842
P3	P1	12,7381	0,0001
P3	P1	12,7381	179,5958
P3	P4	33,1249	179,5955
P3	P4	33,1254	0,0000
P3	P1	12,7381	59,5957
P3	P1	12,7381	239,5959
P3	P4	33,1249	239,5925
P3	P4	33,1259	59,5926
P3	P1	12,7381	119,5959
P3	P1	12,7381	300,0000
P3	P4	33,1249	299,5925
P3	P4	33,1259	119,5922
P4	P3	33,125	0,0001

P4	P3	33,125	179,5956
P4	P7	121,6289	180,0112
P4	P7	121,6289	0,0111
P4	P3	33,125	60,0004
P4	P3	33,125	240,0001
P4	P7	121,6289	240,0106
P4	P7	121,6289	60,0109
P4	P3	33,126	119,5959
P4	P3	33,126	299,5957
P4	P7	121,6279	300,0114
P4	P7	121,6289	120,0114
P7	P4	121,629	359,5959
P7	P4	121,63	179,5956
P7	P6	32,259	359,5837
P7	P6	32,2585	179,5835
P7	P4	121,629	60,0002
P7	P4	121,629	240,0000
P7	P6	32,2589	59,5841
P7	P6	32,2589	239,5838
P7	P4	121,63	120,0003
P7	P4	121,63	300,0000
P7	P6	32,258	119,5833
P7	P6	32,258	299,5832
P6	P7	32,259	359,5959
P6	P7	32,258	179,5958
P6	P5	39,48	179,5943
P6	P5	39,48	359,5942

P6	P7	32,258	60,0005
P6	P7	32,258	239,5958
P6	P5	39,48	239,5952
P6	P5	39,48	59,5949
P6	P7	32,258	119,5959
P6	P7	32,258	300,0000
P6	P5	39,479	299,5947
P6	P5	39,48	119,5943
P5	P6	39,4787	0,0000
P5	P6	39,4787	180,0001
P5	P2	87,453	180,0216
P5	P2	87,453	0,0217
P5	P6	39,4797	60,0001
P5	P6	39,4797	239,5956
P5	P2	87,453	240,0201
P5	P2	87,453	60,0203
P5	P6	39,4792	120,0001
P5	P6	39,4797	299,5958
P5	P2	87,453	300,0220
P5	P2	87,453	120,0218
P2	P5	87,4519	359,5958
P2	P5	87,4529	179,5957
P2	P1	8,3006	179,5916
P2	P1	8,3006	359,5918
P2	P5	87,4519	59,5959
P2	P5	87,4524	239,5957
P2	P1	8,3001	239,5931

P2	P1	8,2996	59,5935
P2	P5	87,4519	120,0001
P2	P5	87,4519	299,5956
P2	P1	8,3006	299,5921
P2	P1	8,3006	119,5925

Field notes for reflective sheet (Article 2)

Station	Target	H Dist (m)	H Direction DMS
P1	P2	8,3032	0,0000
P1	P2	8,3042	180,0004
P1	P3	12,7435	359,5854
P1	P3	12,7355	179,5856
P1	P2	8,3032	60,0005
P1	P2	8,3042	239,5954
P1	P3	12,7435	59,5919
P1	P3	12,7355	239,5916
P1	P2	8,3032	120,0000
P1	P2	8,3042	300,0005
P1	P3	12,7435	119,5853
P1	P3	12,7355	299,5849
P3	P1	12,7371	359,5959
P3	P1	12,7376	179,5956
P3	P4	33,125	179,5940
P3	P4	33,1255	359,5934
P3	P1	12,7371	59,5956
P3	P1	12,7376	239,5958
P3	P4	33,125	239,5924

P3	P4	33,1255	59,5927
P3	P1	12,7371	119,5957
P3	P1	12,7376	300,0000
P3	P4	33,125	299,5927
P3	P4	33,1255	119,5925
P4	P3	33,1294	0,0002
P4	P3	33,1259	180,0004
P4	P7	121,6279	180,0109
P4	P7	121,6284	0,0112
P4	P3	33,1294	60,0005
P4	P3	33,1259	240,0002
P4	P7	121,6279	240,0105
P4	P7	121,6284	60,0109
P4	P3	33,1294	119,5959
P4	P3	33,1259	299,5956
P4	P7	121,6279	300,0116
P4	P7	121,6284	120,0113
P7	P4	121,6289	359,5958
P7	P4	121,6299	180,0000
P7	P6	32,2625	359,5828
P7	P6	32,263	179,5828
P7	P4	121,6289	60,0002
P7	P4	121,6299	240,0000
P7	P6	32,2625	59,5841
P7	P6	32,263	239,5838
P7	P4	121,6289	120,0003
P7	P4	121,6299	300,0000

P7	P6	32,2625	119,5833
P7	P6	32,263	299,5832
P6	P7	32,259	359,5959
P6	P7	32,259	179,5957
P6	P5	39,4789	179,5952
P6	P5	39,4789	359,5942
P6	P7	32,259	60,0000
P6	P7	32,259	239,5955
P6	P5	39,4789	239,5949
P6	P5	39,4789	59,5945
P6	P7	32,259	119,5959
P6	P7	32,259	300,0000
P6	P5	39,4789	299,5948
P6	P5	39,4789	119,5941
P5	P5	39,4769	0,0000
P5	P5	39,4769	179,5956
P5	P2	87,455	180,0211
P5	P2	87,455	0,0213
P5	P5	39,4769	60,0001
P5	P5	39,4769	239,5958
P5	P2	87,455	240,0202
P5	P2	87,455	60,0202
P5	P5	39,4769	120,0001
P5	P5	39,4769	299,5956
P5	P2	87,455	300,0219
P5	P2	87,455	120,0217
P2	P5	87,4549	0,0001

P2	P5	87,4549	180,0000
P2	P1	8,3058	179,5943
P2	P1	8,3003	359,5942
P2	P5	87,4549	59,5959
P2	P5	87,4549	239,5955
P2	P1	8,3058	239,5930
P2	P1	8,3003	59,5935
P2	P5	87,4549	120,0001
P2	P5	87,4549	299,5956
P2	P1	8,3058	299,5920
P2	P1	8,3003	119,5921

Field notes for circular prism (Article 2)

Station	Target	H Dist (m)	H Direction DMS
P1	P2	8,3012	0,0000
P1	P2	8,3012	180,0000
P1	P3	12,7386	359,5858
P1	P3	12,7386	179,5856
P1	P2	8,3012	60,0001
P1	P2	8,3012	240,0001
P1	P3	12,7386	59,5859
P1	P3	12,7386	239,5859
P1	P2	8,3012	120,0000
P1	P2	8,3012	300,0001
P1	P3	12,7386	119,5910
P1	P3	12,7386	299,5909
P3	P1	12,7386	0,0002

P3	P1	12,7386	180,0002
P3	P4	33,126	179,5938
P3	P4	33,126	359,5939
P3	P1	12,7386	59,5959
P3	P1	12,7386	239,5958
P3	P4	33,126	239,5936
P3	P4	33,126	59,5934
P3	P1	12,7381	119,5959
P3	P1	12,7386	299,5959
P3	P4	33,126	299,5937
P3	P4	33,126	119,5935
P4	P3	33,1259	0,0001
P4	P3	33,126	180,0002
P4	P7	121,6299	180,0113
P4	P7	121,6299	0,0112
P4	P3	33,1259	60,0000
P4	P3	33,126	240,0000
P4	P7	121,6299	240,0111
P4	P7	121,6299	60,0114
P4	P3	33,1259	119,5959
P4	P3	33,126	300,0000
P4	P7	121,6299	300,0113
P4	P7	121,6299	120,0112
P7	P4	121,6299	0,0001
P7	P4	121,6299	180,0002
P7	P6	32,259	359,5836
P7	P6	32,259	179,5836

P7	P4	121,6299	60,0000
P7	P4	121,6299	240,0001
P7	P6	32,259	59,5830
P7	P6	32,259	239,5831
P7	P4	121,6299	120,0001
P7	P4	121,6299	300,0000
P7	P6	32,259	119,5833
P7	P6	32,259	299,5835
P6	P7	32,2585	0,0001
P6	P7	32,2585	180,0000
P6	P5	39,4799	180,0002
P6	P5	39,4799	0,0003
P6	P7	32,258	60,0002
P6	P7	32,258	240,0000
P6	P5	39,4799	239,5954
P6	P5	39,4799	59,5957
P6	P7	32,2585	120,0002
P6	P7	32,2585	299,5958
P6	P5	39,4799	299,5951
P6	P5	39,4799	119,5955
P5	P6	39,4799	0,0002
P5	P6	39,4799	180,0002
P5	P2	87,4529	180,0219
P5	P2	87,4539	0,0217
P5	P6	39,4799	60,0000
P5	P6	39,4799	240,0000
P5	P2	87,4529	240,0217

P5	P2	87,4534	60,0218
P5	P6	39,4799	119,5958
P5	P6	39,4799	300,0000
P5	P2	87,4529	300,0223
P5	P2	87,4539	120,0223
P2	P5	87,4539	359,5956
P2	P5	87,4539	179,5956
P2	P1	8,3008	179,5932
P2	P1	8,3013	359,5937
P2	P5	87,4539	59,5959
P2	P5	87,4544	240,0002
P2	P1	8,3003	239,5932
P2	P1	8,3003	59,5935
P2	P5	87,4539	120,0001
P2	P5	87,4539	300,0000
P2	P1	8,3003	299,5933
P2	P1	8,3003	119,5936

APPENDIX B - RESULTS FOR ANGULAR COMPUTATIONS

Results for Angular Computations (Directions or Prussian Method – 360° prism), Article 2

Station	Target	Direct_(dec)	Reverse_(dec)	Mean_(dec)	Reduced_Mean _(dec)	Final_Directions _(DMS)
P1	P2	0,00055556	179,99972222	0,00013889	0,00000000	359,585767
P1	P3	359,98305556	179,98361111	359,98333333	359,98319444	0,000000
P1	P2	60,00000000	239,99777778	59,99888889	0,00000000	0,000000
P1	P3	59,98638889	239,98555556	59,98597222	359,98708333	0,000000
P1	P2	120,00055556	300,00027778	120,00041667	0,00000000	0,000000
P1	P3	119,97805556	299,97833333	119,97819444	359,97777778	0,000000
P3	P1	0,00027778	179,99944444	-0,00013889	0,00000000	179,593650
P3	P4	179,99861111	0,00000000	179,99930556	179,99944444	0,000000
P3	P1	59,99916667	239,99972222	59,99944444	0,00000000	0,000000
P3	P4	239,99027778	59,99055556	239,99041667	179,99097222	0,000000
P3	P1	119,99972222	300,00000000	119,99986111	0,00000000	0,000000
P3	P4	299,99027778	119,98944444	299,98986111	179,99000000	0,000000
P4	P3	0,00027778	179,99888889	-0,00041667	0,00000000	180,011133
P4	P7	180,02000000	0,01972222	180,01986111	180,02027778	0,000000
P4	P3	60,00111111	240,00027778	60,00069444	0,00000000	0,000000
P4	P7	240,01833333	60,01916667	240,01875000	180,01805556	0,000000
P4	P3	119,99972222	299,99916667	119,99944444	0,00000000	0,000000
P4	P7	300,02055556	120,02055556	300,02055556	180,02111111	0,000000
P7	P4	359,99972222	179,99888889	359,99930556	0,00000000	359,583600
P7	P6	359,97694444	179,97638889	359,97666667	359,97736111	0,000000
P7	P4	60,00055556	240,00000000	60,00027778	0,00000000	0,000000
P7	P6	59,97805556	239,97722222	59,97763889	359,97736111	0,000000
P7	P4	120,00083333	300,00000000	120,00041667	0,00000000	0,000000
P7	P6	119,97583333	299,97555556	119,97569444	359,97527778	0,000000
P6	P7	359,99972222	179,99944444	359,99958333	0,00000000	179,594617
P6	P5	179,99527778	359995,00000	179,99513889	179,99555556	0,000000
P6	P7	60,00138889	239,99944444	60,00041667	0,00000000	0,000000
P6	P5	239,99777778	59,99694444	239,99736111	179,99694444	0,000000
P6	P7	119,99972222	300,00000000	119,99986111	0,00000000	0,000000

P6	P5	299,99638889	119,99527778	299,99583333	179,99597222	0,000000
P5	P6	0,00000000	180,00027778	0,00013889	0,00000000	180,021300
P5	P2	180,03777778	0,03805556	180,03791667	180,03777778	0,000000
P5	P6	60,00027778	239,99888889	59,99958333	0,00000000	0,000000
P5	P2	240,03361111	60,03416667	240,03388889	180,03430556	0,000000
P5	P6	120,00027778	299,99944444	119,99986111	0,00000000	0,000000
P5	P2	300,03888889	120,03833333	300,03861111	180,03875000	0,000000
P2	P5	359,99944444	179,99916667	359,99930556	0,00000000	179,592633
P2	P1	179,98777778	359,98833333	179,98805556	179,98875000	0,000000
P2	P5	59,99972222	239,99916667	59,99944444	0,00000000	0,000000
P2	P1	239,99194444	59,99305556	239,99250000	179,99305556	0,000000
P2	P5	120,00027778	299,99888889	119,99958333	0,00000000	0,000000
P2	P1	299,98916667	119,99027778	299,98972222	179,99013889	0,000000

Results for Angular Computations (Directions or Prussian Method – Circular prism), Article 2

Station	Target	Direct_(dec)	Reverse_(dec)	Mean_(dec)	Reduced_Mean _(dec)	Final_Directions _(DMS)
P1	P2	0,000000000	180,000000000	0,000000000	0,000000000	359,590133
P1	P3	359,982777778	179,982222222	359,982500000	359,982500000	0,000000
P1	P2	60,000277778	240,000277778	60,000277778	0,000000000	0,000000
P1	P3	59,983055556	239,983055556	59,983055556	359,982777778	0,000000
P1	P2	120,000000000	300,000277778	120,000138889	0,000000000	0,000000
P1	P3	119,986111111	299,985833333	119,985972222	359,985833333	0,000000
P3	P1	0,000555556	180,000555556	0,000555556	0,000000000	179,593667
P3	P4	179,993888889	359,994166667	179,994027778	179,993472222	0,000000
P3	P1	59,999722222	239,999444444	59,999583333	0,000000000	0,000000
P3	P4	239,993333333	59,992777778	239,993055556	179,993472222	0,000000
P3	P1	119,999722222	299,999722222	119,999722222	0,000000000	0,000000
P3	P4	299,993611111	119,993055556	299,993333333	179,993611111	0,000000
P4	P3	0,000277778	180,000555556	0,000416667	0,000000000	180,011217
P4	P7	180,020277778	0,020000000	180,020138889	180,019722222	0,000000
P4	P3	60,000000000	240,000000000	60,000000000	0,000000000	0,000000
P4	P7	240,019722222	60,020555556	240,020138889	180,020138889	0,000000

P4	P3	119,999722222	300,000000000	119,999861111	0,000000000	0,000000
P4	P7	300,020277778	120,020000000	300,020138889	180,020277778	0,000000
P7	P4	0,000277778	180,000555556	0,000416667	0,000000000	359,583267
P7	P6	359,976666667	179,976666667	359,976666667	359,976250000	0,000000
P7	P4	60,000000000	240,000277778	60,000138889	0,000000000	0,000000
P7	P6	59,975000000	239,975277778	59,975138889	359975,000000000	0,000000
P7	P4	120,000277778	300,000000000	120,000138889	0,000000000	0,000000
P7	P6	119,975833333	299,976388889	119,976111111	359,975972222	0,000000
P6	P7	0,000277778	180,000000000	0,000138889	0,000000000	179,595650
P6	P5	180,000555556	0,000833333	180,000694444	180,000555556	0,000000
P6	P7	60,000555556	240,000000000	60,000277778	0,000000000	0,000000
P6	P5	239,998333333	59,999166667	239,998750000	179,998472222	0,000000
P6	P7	120,000555556	299,999444444	120,000000000	0,000000000	0,000000
P6	P5	299,997500000	119,998611111	299,998055556	179,998055556	0,000000
P5	P6	0,000555556	180,000555556	0,000555556	0,000000000	180,021917
P5	P2	180,038611111	0,038055556	180,038333333	180,037777778	0,000000
P5	P6	60,000000000	240,000000000	60,000000000	0,000000000	0,000000
P5	P2	240,038055556	60,038333333	240,038194444	180,038194444	0,000000
P5	P6	119,999444444	300,000000000	119,999722222	0,000000000	0,000000
P5	P2	300,039722222	120,039722222	300,039722222	180,040000000	0,000000
P2	P5	359,998888889	179,998888889	359,998888889	0,000000000	179,593583
P2	P1	179,992222222	359,993611111	179,992916667	179,994027778	0,000000
P2	P5	59,999722222	240,000555556	59,999583333	0,000000000	0,000000
P2	P1	239,992222222	59,993055556	239,992638889	179,993055556	0,000000
P2	P5	120,000277778	300,000000000	120,000138889	0,000000000	0,000000
P2	P1	299,992500000	119,993333333	299,992916667	179,992777778	0,000000

Results for Angular Computations (Directions or Prussian Method – reflective sheet), Article 2

Station	Target	Direct_(dec)	Reverse_(dec)	Mean_(dec)	Reduced_Mean _(dec)	Final_Directions _(DMS)
P1	P2	0,000000000	180,001111111	0,000555556	0,000000000	359,585983
P1	P3	359,981666667	179,982222222	359,981944444	359,981388889	0,000000
P1	P2	60,001388889	239,998333333	59,999861111	0,000000000	0,000000
P1	P3	59,988611111	239,987777778	59,988194444	359,988333333	0,000000
P1	P2	120,000000000	300,001388889	120,000694444	0,000000000	0,000000
P1	P3	119,981388889	299,980277778	119,980833333	359,980138889	0,000000
P3	P1	359,999722222	179,998888889	359,999305556	0,000000000	179,593183
P3	P4	179,994444444	359,992777778	179,993611111	179,994305556	0,000000
P3	P1	59,998888889	239,999444444	59,999166667	0,000000000	0,000000
P3	P4	239,990000000	59,990833333	239,990416667	179,991250000	0,000000
P3	P1	119,999166667	300,000000000	119,999583333	0,000000000	0,000000
P3	P4	299,990833333	119,990277778	299,990555556	179,990972222	0,000000
P4	P3	0,000555556	180,001111111	0,000833333	0,000000000	180,010933
P4	P7	180,019166667	0,020000000	180,019583333	180,018750000	0,000000
P4	P3	60,001388889	240,000555556	60,000972222	0,000000000	0,000000
P4	P7	240,018055556	60,019166667	240,018611111	180,017638889	0,000000
P4	P3	119,999722222	299,998888889	119,999305556	0,000000000	0,000000
P4	P7	300,021111111	120,020277778	300,020694444	180,021388889	0,000000
P7	P4	359,999444444	180,000000000	359,999722222	0,000000000	359,583283
P7	P6	359,974444444	179,974444444	359,974444444	359,974722222	0,000000
P7	P4	60,000555556	240,000000000	60,000277778	0,000000000	0,000000
P7	P6	59,978055556	239,977222222	59,977638889	359,977361111	0,000000
P7	P4	120,000833333	300,000000000	120,000416667	0,000000000	0,000000
P7	P6	119,975833333	299,975555556	119,975694444	359,975277778	0,000000
P6	P7	359,999722222	179,999166667	359,999444444	0,000000000	179,594783
P6	P5	179,997777778	359,995000000	179,996388889	179,996944444	0,000000
P6	P7	60,000000000	239,998611111	59,999305556	0,000000000	0,000000
P6	P5	239,996944444	59,995833333	239,996388889	179,997083333	0,000000
P6	P7	119,999722222	300,000000000	119,999861111	0,000000000	0,000000

P6	P5	299,996666667	119,994722222	299,995694444	179,995833333	0,000000
P5	P5	0,000000000	179,998888889	0,000555556	0,000000000	180,021200
P5	P2	180,036388889	0,036944444	180,036666667	180,037222222	0,000000
P5	P5	60,000277778	239,999444444	59,999861111	0,000000000	0,000000
P5	P2	240,033888889	60,033888889	240,033888889	180,034027778	0,000000
P5	P5	120,000277778	299,998888889	119,999583333	0,000000000	0,000000
P5	P2	300,038611111	120,038055556	300,038333333	180,038750000	0,000000
P2	P5	0,000277778	180,000000000	0,000138889	0,000000000	179,593317
P2	P1	179,995277778	359,995000000	179,995138889	179,9950000000	0,000000
P2	P5	59,999722222	239,998611111	59,999166667	0,000000000	0,000000
P2	P1	239,991666667	59,993055556	239,992361111	179,993194444	0,000000
P2	P5	120,000277778	299,998888889	119,999583333	0,000000000	0,000000
P2	P1	299,988888889	119,989166667	299,989027778	179,989444444	0,000000

APPENDIX C - AstGeoTop STATISTICAL TESTS REPORTS

PILAR 1 (Article 2)

Amostra1 = prisma 360°
Amostra2 = prisma circular
Amostra3 = folha refletiva

ESTATíSTICA DESCRITIVA
Amostra1
Número de elementos =6
Média aritmética = 359°58`57,7"
Variância amostral = 0°00`00,06441" unid.^2
Desvio padrão amostral = 0°00`15,22717"
Coef. de variação = 1,17499236986383E-5
Momento de assimetria = -0,118978475750321 (distribuição negativamente assimétrica - alongada à esquerda)

Estatística com distribuição de Frequências
Número de classe = 4
Valor inferior = 359°58`39,00000"
Valor superior = 359°59`16,00000"
Amplitude total = 0°00`37,00000"
Amplitude de classe = 0°00`09,25000"

Amostra2
Número de elementos =6
Média aritmética = 359°59`01,3"
Variância amostral = 0°00`00,01007" unid.^2
Desvio padrão amostral = 0°00`06,02218"
Coef. de variação = 4,64695512589133E-6
Momento de assimetria = 0,522306572906874 (distribuição positivamente assimétrica - alongada à direita)

Estatística com distribuição de Frequências
Número de classe = 4
Valor inferior = 359°58`56,00000"
Valor superior = 359°59`10,00000"
Amplitude total = 0°00`14,00000"
Amplitude de classe = 0°00`03,50000"

Amostra3
Número de elementos =6
Média aritmética = 359°58`59,8"
Variância amostral = 0°00`00,06027" unid.^2
Desvio padrão amostral = 0°00`14,72979"
Coef. de variação = 1,13661051481461E-5
Momento de assimetria = 0,457227398714617 (distribuição positivamente assimétrica - alongada à direita)

Estatística com distribuição de Frequências
Número de classe = 4
Valor inferior = 359°58`44,00000"
Valor superior = 359°59`22,00000"
Amplitude total = 0°00`38,00000"
Amplitude de classe = 0°00`09,50000"

Amostra 1 ordenada

Observações	Resíduos
359,9775	-0,0052
359,978055555556	-0,0046
359,9825	-0,0002

359,983888888889 0,0012
359,986388888889 0,0037
359,987777777778 0,0051
Sequência do cálculo Shapiro-Wilk
x(n-i+1) x(i) a(n-i+1)*[x(n-i+1)-x(i))]
359,987777777778 359,9775 0,00660963888903179
359,986388888889 359,978055555556 0,0023383333332398
359,983888888889 359,9825 0,000121527777787499

Média = 359,9827
Variância = 0,0000
D.Padrão = 0,0042
b = 0,0091
SQE = 0,0001
W_calc = 0,9195
W = 0,7130
Conclusão do teste de normalidade de Shapiro-Wilk.
Hipótese H0: não é rejeitada.
As observações são provenientes de uma distribuição normal ao nível de significância de 1%.

Amostra 2 ordenada
Observações Resíduos
359,982222222222 -0,0015
359,982777777778 -0,0009
359,982777777778 -0,0009
359,982777777778 -0,0009
359,985555555556 0,0019
359,986111111111 0,0024
Sequência do cálculo Shapiro-Wilk
x(n-i+1) x(i) a(n-i+1)*[x(n-i+1)-x(i))]
359,986111111111 359,982222222222 0,00250094444451589
359,985555555556 359,982777777778 0,000779444444506802
359,982777777778 359,982777777778 0

Média = 359,9837
Variância = 0,0000
D.Padrão = 0,0017
b = 0,0033
SQE = 0,0000
W_calc = 0,7691
W = 0,7130
Conclusão do teste de normalidade de Shapiro-Wilk.
Hipótese H0: não é rejeitada.
As observações são provenientes de uma distribuição normal ao nível de significância de 1%.

Amostra 3 ordenada
Observações Resíduos
359,978888888889 -0,0044
359,981111111111 -0,0022
359,981388888889 -0,0019
359,981666666667 -0,0016
359,987222222222 0,0039
359,989444444444 0,0062
Sequência do cálculo Shapiro-Wilk
x(n-i+1) x(i) a(n-i+1)*[x(n-i+1)-x(i))]
359,989444444444 359,978888888889 0,00678827777742051
359,987222222222 359,981111111111 0,0017147777777466
359,981666666667 359,981388888889 2,43055555750004E-5

Média = 359,9833

Variância = 0,0000
D.Padrão = 0,0041
b = 0,0085
SQE = 0,0001
W_calc = 0,8687
W = 0,7130
Conclusão do teste de normalidade de Shapiro-Wilk.
Hipótese H0: não é rejeitada.
As observações são provenientes de uma distribuição normal ao nível de significância de 1%.

TESTE T: ANáLISE DE MéDIAS DE AMOSTRAS EM PAR
Amostra1
Número de elementos 6
Média = 359°58`57,7"
Var = 0°00`00,06441"

Amostra2
Número de elementos 6
Média = 359°59`01,3"
Var = 0°00`00,01007"

Discrepâncias
d1 :-0,000277777777999977
d2 :0,00166666666699999
d3 :0,00361111111100001
d4 :0,005
d5 :-0,00861111111099999
d6 :-0,00750000000000001
Média = -0°00`03,7"
D.Pad = 0°00`20,68494"

ANÁLISE AMOSTRA1 X AMOSTRA2
Teste de hipótese
Hipótese -> H0: médias populacionais iguais
Hipótese -> H1: médias populacionais diferentes
Nível de significância do teste = 1%
Graus de Liberdade = 5
Estatística do teste t = 0,4342
Probabilidade resultante = 65,9%
t_Crítico bi-caudal = 4,032
CONCLUSÃO :
Teste bi-caudal: t<=t_crítico, então
as médias das amostras: Amostra1 e Amostra2 são iguais ao nível de significância de 1%

TESTE T: ANáLISE DE MéDIAS DE AMOSTRAS EM PAR
Amostra1
Número de elementos 6
Média = 359°58`57,7"
Var = 0°00`00,06441"

Amostra3
Número de elementos 6
Média = 359°58`59,8"
Var = 0°00`00,06027"

Discrepâncias
d1 :0,000833333333000008
d2 :0,00277777777800001
d3 :-0,000833333333000008
d4 :-0,00166666666600002

d5 :-0,00388888888899999
d6 :-0,000833333333000008
Média = -0°00`02,2"
D.Pad = 0°00`08,13429"

ANÁLISE AMOSTRA1 X AMOSTRA3
Teste de hipótese
Hipótese -> H0: médias populacionais iguais
Hipótese -> H1: médias populacionais diferentes
Nível de significância do teste = 1%
Graus de Liberdade = 5
Estatística do teste t = 0,6525
Probabilidade resultante = 72,9%
t_Crítico bi-caudal = 4,032
CONCLUSÃO :
Teste bi-caudal: t<=t_crítico, então
as médias das amostras: Amostra1 e Amostra3 são iguais ao nível de significância de 1%

TESTE T: ANáLISE DE MéDIAS DE AMOSTRAS EM PAR
Amostra2
Número de elementos 6
Média = 359°59`01,3"
Var = 0°00`00,01007"

Amostra3
Número de elementos 6
Média = 359°58`59,8"
Var = 0°00`00,06027"

Discrepâncias
d1 :0,00111111111099998
d2 :0,00111111111100001
d3 :-0,00444444444400002
d4 :-0,00666666666600002
d5 :0,004722222222
d6 :0,006666666667
Média = 0°00`01,5"
D.Pad = 0°00`18,52296"

ANÁLISE AMOSTRA2 X AMOSTRA3
Teste de hipótese
Hipótese -> H0: médias populacionais iguais
Hipótese -> H1: médias populacionais diferentes
Nível de significância do teste = 1%
Graus de Liberdade = 5
Estatística do teste t = 0,1984
Probabilidade resultante = 57,5%
t_Crítico bi-caudal = 4,032
CONCLUSÃO :
Teste bi-caudal: t<=t_crítico, então
as médias das amostras: Amostra2 e Amostra3 são iguais ao nível de significância de 1%

RESUMO DA ANÁLISE PELO TESTE T

GRUPOS	Estatística t	t-crítico	CONCLUSÃO
AMOSTRA1 X AMOSTRA2	0,4342	4,032	Não diferem
AMOSTRA1 X AMOSTRA3	0,6525	4,032	Não diferem
AMOSTRA2 X AMOSTRA3	0,1984	4,032	Não diferem

PILAR 2 (Article 2)

Amostra1 = prisma 360°
Amostra2 = prisma circular
Amostra3 = folha refletiva

ESTATíSTICA DESCRITIVA
Amostra1
Número de elementos =6
Média aritmética = 179°59`26,3"
Variância amostral = 0°00`00,01741" unid.^2
Desvio padrão amostral = 0°00`07,91623"
Coef. de variação = 1,22170360570419E-5
Momento de assimetria = 0,270265066788952 (distribuição positivamente assimétrica - alongada à direita)

Estatística com distribuição de Frequências
Número de classe = 4
Valor inferior = 179°59`18,00000"
Valor superior = 179°59`38,00000"
Amplitude total = 0°00`20,00000"
Amplitude de classe = 0°00`05,00000"

Amostra2
Número de elementos =6
Média aritmética = 179°59`35,2"
Variância amostral = 0°00`00,00305" unid.^2
Desvio padrão amostral = 0°00`03,31160"
Coef. de variação = 5,11068318454951E-6
Momento de assimetria = 0,677161643649897 (distribuição positivamente assimétrica - alongada à direita)

Estatística com distribuição de Frequências
Número de classe = 4
Valor inferior = 179°59`32,00000"
Valor superior = 179°59`41,00000"
Amplitude total = 0°00`09,00000"
Amplitude de classe = 0°00`02,25000"

Amostra3
Número de elementos =6
Média aritmética = 179°59`33,2"
Variância amostral = 0°00`00,02638" unid.^2
Desvio padrão amostral = 0°00`09,74508"
Coef. de variação = 1,50393330032874E-5
Momento de assimetria = -0,306234703881555 (distribuição negativamente assimétrica - alongada à esquerda)

Estatística com distribuição de Frequências
Número de classe = 4
Valor inferior = 179°59`19,00000"
Valor superior = 179°59`42,00000"
Amplitude total = 0°00`23,00000"
Amplitude de classe = 0°00`05,75000"

Amostra 1 ordenada

Observações	Resíduos
179,988333333333	-0,0023
179,988888888889	-0,0018
179,989166666667	-0,0015

179,991388888889 0,0007
179,992222222222 0,0016
179,993888888889 0,0032
Sequência do cálculo Shapiro-Wilk

x(n-i+1)	x(i)	a(n-i+1)*[x(n-i+1)-x(i))]
179,993888888889	179,988333333333	0,0035727777780636
179,992222222222	179,988888888889	0,000935333333239799
179,991388888889	179,989166666667	0,000194444444425

Média = 179,9906
Variância = 0,0000
D.Padrão = 0,0022
b = 0,0047
SQE = 0,0000
W_calc = 0,9147
W = 0,7130
Conclusão do teste de normalidade de Shapiro-Wilk.
Hipótese H0: não é rejeitada.
As observações são provenientes de uma distribuição normal ao nível de significância de 1%.

Amostra 2 ordenada

Observações	Resíduos
179,992222222222	-0,0009
179,9925	-0,0006
179,9925	-0,0006
179,993333333333	0,0002
179,993333333333	0,0002
179,994722222222	0,0016

Sequência do cálculo Shapiro-Wilk

x(n-i+1)	x(i)	a(n-i+1)*[x(n-i+1)-x(i))]
179,994722222222	179,992222222222	0,00160775
179,993333333333	179,9925	0,000233833333239802
179,993333333333	179,9925	7,29166666375007E-5

Média = 179,9931
Variância = 0,0000
D.Padrão = 0,0009
b = 0,0019
SQE = 0,0000
W_calc = 0,8663
W = 0,7130
Conclusão do teste de normalidade de Shapiro-Wilk.
Hipótese H0: não é rejeitada.
As observações são provenientes de uma distribuição normal ao nível de significância de 1%.

Amostra 3 ordenada

Observações	Resíduos
179,988611111111	-0,0039
179,990277777778	-0,0023
179,991944444444	-0,0006
179,994444444444	0,0019
179,995	0,0025
179,995	0,0025

Sequência do cálculo Shapiro-Wilk

x(n-i+1)	x(i)	a(n-i+1)*[x(n-i+1)-x(i))]
179,995	179,988611111111	0,0041086944445159
179,995	179,990277777778	0,0013250555554932
179,994444444444	179,991944444444	0,00021875

Média = 179,9925

Variância = 0,0000
D.Padrão = 0,0027
b = 0,0057
SQE = 0,0000
W_calc = 0,8721
W = 0,7130
Conclusão do teste de normalidade de Shapiro-Wilk.
Hipótese H0: não é rejeitada.
As observações são provenientes de uma distribuição normal ao nível de significância de 1%.

TESTE T: ANáLISE DE MéDIAS DE AMOSTRAS EM PAR
Amostra1
Número de elementos 6
Média = 179°59`26,3"
Var = 0°00`00,01741"

Amostra2
Número de elementos 6
Média = 179°59`35,2"
Var = 0°00`00,00305"

Discrepâncias
d1 :-0,005
d2 :-0,00555555555500001
d3 :-0,000277777777999991
d4 :0,001388888889
d5 :-0,003333333333
d6 :-0,00194444444400001
Média = -0°00`08,8"
D.Pad = 0°00`09,74508"

ANÁLISE AMOSTRA1 X AMOSTRA2
Teste de hipótese
Hipótese -> H0: médias populacionais iguais
Hipótese -> H1: médias populacionais diferentes
Nível de significância do teste = 1%
Graus de Liberdade = 5
Estatística do teste t = 2,2203
Probabilidade resultante = 96,1%
t_Crítico bi-caudal = 4,032
CONCLUSÃO :
Teste bi-caudal: t<=t_crítico, então
as médias das amostras: Amostra1 e Amostra2 são iguais ao nível de significância de 1%

TESTE T: ANáLISE DE MéDIAS DE AMOSTRAS EM PAR
Amostra1
Número de elementos 6
Média = 179°59`26,3"
Var = 0°00`00,01741"

Amostra3
Número de elementos 6
Média = 179°59`33,2"
Var = 0°00`00,02638"

Discrepâncias
d1 :-0,006666666667
d2 :-0,005833333333
d3 :0,000277777778000005
d4 :-0,000555555555000004

d5 :0,000277777778000005
d6 :0,001111111111
Média = -0°00`06,8"
D.Pad = 0°00`12,31936"

ANÁLISE AMOSTRA1 X AMOSTRA3
Teste de hipótese
Hipótese -> H0: médias populacionais iguais
Hipótese -> H1: médias populacionais diferentes
Nível de significância do teste = 1%
Graus de Liberdade = 5
Estatística do teste t = 1,3587
Probabilidade resultante = 88,4%
t_Crítico bi-caudal = 4,032
CONCLUSÃO :
Teste bi-caudal: t<=t_crítico, então
as médias das amostras: Amostra1 e Amostra3 são iguais ao nível de significância de 1%

TESTE T: ANáLISE DE MéDIAS DE AMOSTRAS EM PAR
Amostra2
Número de elementos 6
Média = 179°59`35,2"
Var = 0°00`00,00305"

Amostra3
Número de elementos 6
Média = 179°59`33,2"
Var = 0°00`00,02638"

Discrepâncias
d1 :-0,00166666666699999
d2 :-0,000277777777999991
d3 :0,000555555555999995
d4 :-0,00194444444400001
d5 :0,003611111111
d6 :0,00305555555500001
Média = 0°00`02,0"
D.Pad = 0°00`08,43801"

ANÁLISE AMOSTRA2 X AMOSTRA3
Teste de hipótese
Hipótese -> H0: médias populacionais iguais
Hipótese -> H1: médias populacionais diferentes
Nível de significância do teste = 1%
Graus de Liberdade = 5
Estatística do teste t = 0,5806
Probabilidade resultante = 70,7%
t_Crítico bi-caudal = 4,032
CONCLUSÃO :
Teste bi-caudal: t<=t_crítico, então
as médias das amostras: Amostra2 e Amostra3 são iguais ao nível de significância de 1%

RESUMO DA ANÁLISE PELO TESTE T

GRUPOS	Estatística t	t-crítico	CONCLUSÃO
AMOSTRA1 X AMOSTRA2	2,2203	4,032	Não diferem
AMOSTRA1 X AMOSTRA3	1,3587	4,032	Não diferem
AMOSTRA2 X AMOSTRA3	0,5806	4,032	Não diferem

PILAR 3 (Article 2)

Amostra1 = prisma 360°
Amostra2 = prisma circular
Amostra3 = folha refletiva

ESTATíSTICA DESCRITIVA
Amostra1
Número de elementos =6
Média aritmética = 179°59`36,5"
Variância amostral = 0°00`00,07997" unid.^2
Desvio padrão amostral = 0°00`16,96762"
Coef. de variação = 2,61855425542558E-5
Momento de assimetria = 0,55486446753185 (distribuição positivamente assimétrica - alongada à direita)

Estatística com distribuição de Frequências
Número de classe = 4
Valor inferior = 179°59`22,00000"
Valor superior = 180°00`02,00000"
Amplitude total = 0°00`40,00000"
Amplitude de classe = 0°00`10,00000"

Amostra2
Número de elementos =6
Média aritmética = 179°59`36,7"
Variância amostral = 0°00`00,00019" unid.^2
Desvio padrão amostral = 0°00`00,81650"
Coef. de variação = 1,26007096178503E-6
Momento de assimetria = 0,476289671946513 (distribuição positivamente assimétrica - alongada à direita)

Estatística com distribuição de Frequências
Número de classe = 4
Valor inferior = 179°59`36,00000"
Valor superior = 179°59`38,00000"
Amplitude total = 0°00`02,00000"
Amplitude de classe = 0°00`00,50000"

Amostra3
Número de elementos =6
Média aritmética = 179°59`31,8"
Variância amostral = 0°00`00,01082" unid.^2
Desvio padrão amostral = 0°00`06,24233"
Coef. de variação = 9,63364193291136E-6
Momento de assimetria = 0,411416491095784 (distribuição positivamente assimétrica - alongada à direita)

Estatística com distribuição de Frequências
Número de classe = 4
Valor inferior = 179°59`25,00000"
Valor superior = 179°59`41,00000"
Amplitude total = 0°00`16,00000"
Amplitude de classe = 0°00`04,00000"

Amostra 1 ordenada

Observações	Resíduos
179,989444444444	-0,0040
179,990555555556	-0,0029
179,990833333333	-0,0026

179,991111111111 -0,0024
179,998333333333 0,0049
180,000555555556 0,0071
Sequência do cálculo Shapiro-Wilk

x(n-i+1)	x(i)	a(n-i+1)*[x(n-i+1)-x(i))]
180,000555555556	179,989444444444	0,0071455555561272
179,998333333333	179,990555555556	0,0021824444442262
179,991111111111	179,990833333333	2,43055555750004E-5

Média = 179,9935
Variância = 0,0000
D.Padrão = 0,0047
b = 0,0094
SQE = 0,0001
W_calc = 0,7875
W = 0,7130
Conclusão do teste de normalidade de Shapiro-Wilk.
Hipótese H0: não é rejeitada.
As observações são provenientes de uma distribuição normal ao nível de significância de 1%.

Amostra 2 ordenada

Observações	Resíduos
179,993333333333	-0,0002
179,993333333333	-0,0002
179,993333333333	-0,0002
179,993611111111	0,0001
179,993611111111	0,0001
179,993888888889	0,0004

Sequência do cálculo Shapiro-Wilk

x(n-i+1)	x(i)	a(n-i+1)*[x(n-i+1)-x(i))]
179,993888888889	179,993333333333	0,000357277778063597
179,993611111111	179,993333333333	7,79444445068013E-5
179,993611111111	179,993333333333	2,43055555750004E-5

Média = 179,9935
Variância = 0,0000
D.Padrão = 0,0002
b = 0,0005
SQE = 0,0000
W_calc = 0,8210
W = 0,7130
Conclusão do teste de normalidade de Shapiro-Wilk.
Hipótese H0: não é rejeitada.
As observações são provenientes de uma distribuição normal ao nível de significância de 1%.

Amostra 3 ordenada

Observações	Resíduos
179,990277777778	-0,0019
179,991111111111	-0,0011
179,991388888889	-0,0008
179,991666666667	-0,0005
179,993888888889	0,0017
179,994722222222	0,0025

Sequência do cálculo Shapiro-Wilk

x(n-i+1)	x(i)	a(n-i+1)*[x(n-i+1)-x(i))]
179,994722222222	179,990277777778	0,00285822222193641
179,993888888889	179,991111111111	0,000779444444506798
179,991666666667	179,991388888889	2,43055555750004E-5

Média = 179,9922

Variância = 0,0000
D.Padrão = 0,0017
b = 0,0037
SQE = 0,0000
W_calc = 0,8920
W = 0,7130
Conclusão do teste de normalidade de Shapiro-Wilk.
Hipótese H0: não é rejeitada.
As observações são provenientes de uma distribuição normal ao nível de significância de 1%.

TESTE T: ANáLISE DE MéDIAS DE AMOSTRAS EM PAR
Amostra1
Número de elementos 6
Média = 179°59`36,5"
Var = 0°00`00,07997"

Amostra2
Número de elementos 6
Média = 179°59`36,7"
Var = 0°00`00,00019"

Discrepâncias
d1 :0,005
d2 :0,00694444444499999
d3 :-0,0025
d4 :-0,0025
d5 :-0,003333333333
d6 :-0,00388888888900001
Média = -0°00`00,2"
D.Pad = 0°00`17,03428"

ANÁLISE AMOSTRA1 X AMOSTRA2
Teste de hipótese
Hipótese -> H0: médias populacionais iguais
Hipótese -> H1: médias populacionais diferentes
Nível de significância do teste = 1%
Graus de Liberdade = 5
Estatística do teste t = 0,0240
Probabilidade resultante = 50,9%
t_Crítico bi-caudal = 4,032
CONCLUSÃO :
Teste bi-caudal: t<=t_crítico, então
as médias das amostras: Amostra1 e Amostra2 são iguais ao nível de significância de 1%

TESTE T: ANáLISE DE MéDIAS DE AMOSTRAS EM PAR
Amostra1
Número de elementos 6
Média = 179°59`36,5"
Var = 0°00`00,07997"

Amostra3
Número de elementos 6
Média = 179°59`31,8"
Var = 0°00`00,01082"

Discrepâncias
d1 :0,003611111111
d2 :0,006666666667
d3 :0
d4 :-0,000555555555999995

d5 :-0,001111111111
d6 :-0,000833333334
Média = 0°00`04,7"
D.Pad = 0°00`11,34313"

ANÁLISE AMOSTRA1 X AMOSTRA3
Teste de hipótese
Hipótese -> H0: médias populacionais iguais
Hipótese -> H1: médias populacionais diferentes
Nível de significância do teste = 1%
Graus de Liberdade = 5
Estatística do teste t = 1,0077
Probabilidade resultante = 82,0%
t_Crítico bi-caudal = 4,032
CONCLUSÃO :
Teste bi-caudal: t<=t_crítico, então
as médias das amostras: Amostra1 e Amostra3 são iguais ao nível de significância de 1%

TESTE T: ANáLISE DE MéDIAS DE AMOSTRAS EM PAR
Amostra2
Número de elementos 6
Média = 179°59`36,7"
Var = 0°00`00,00019"

Amostra3
Número de elementos 6
Média = 179°59`31,8"
Var = 0°00`00,01082"

Discrepâncias
d1 :-0,001388888889
d2 :-0,000277777777999991
d3 :0,0025
d4 :0,00194444444400001
d5 :0,002222222222
d6 :0,00305555555500001
Média = 0°00`04,8"
D.Pad = 0°00`06,33772"

ANÁLISE AMOSTRA2 X AMOSTRA3
Teste de hipótese
Hipótese -> H0: médias populacionais iguais
Hipótese -> H1: médias populacionais diferentes
Nível de significância do teste = 1%
Graus de Liberdade = 5
Estatística do teste t = 1,8681
Probabilidade resultante = 94,0%
t_Crítico bi-caudal = 4,032
CONCLUSÃO :
Teste bi-caudal: t<=t_crítico, então
as médias das amostras: Amostra2 e Amostra3 são iguais ao nível de significância de 1%

RESUMO DA ANÁLISE PELO TESTE T

GRUPOS	Estatística t	t-crítico	CONCLUSÃO
AMOSTRA1 X AMOSTRA2	0,0240	4,032	Não diferem
AMOSTRA1 X AMOSTRA3	1,0077	4,032	Não diferem
AMOSTRA2 X AMOSTRA3	1,8681	4,032	Não diferem

PILAR 4 (Article 2)

Amostra1 = prisma 360°
Amostra2 = prisma circular
Amostra3 = folha refletiva

ESTATíSTICA DESCRITIVA
Amostra1
Número de elementos =6
Média aritmética = 180°01`11,3"
Variância amostral = 0°00`00,00874" unid.^2
Desvio padrão amostral = 0°00`05,60952"
Coef. de variação = 8,65570722891402E-6
Momento de assimetria = -0,537785059493621 (distribuição negativamente assimétrica - alongada à esquerda)

Estatística com distribuição de Frequências
Número de classe = 4
Valor inferior = 180°01`02,00000"
Valor superior = 180°01`17,00000"
Amplitude total = 0°00`15,00000"
Amplitude de classe = 0°00`03,75000"

Amostra2
Número de elementos =6
Média aritmética = 180°01`12,2"
Variância amostral = 0°00`00,00071" unid.^2
Desvio padrão amostral = 0°00`01,60208"
Coef. de variação = 2,47207342398553E-6
Momento de assimetria = 0,0225175968495795 (distribuição positivamente assimétrica - alongada à direita)

Estatística com distribuição de Frequências
Número de classe = 4
Valor inferior = 180°01`10,00000"
Valor superior = 180°01`14,00000"
Amplitude total = 0°00`04,00000"
Amplitude de classe = 0°00`01,00000"

Amostra3
Número de elementos =6
Média aritmética = 180°01`09,3"
Variância amostral = 0°00`00,01207" unid.^2
Desvio padrão amostral = 0°00`06,59293"
Coef. de variação = 1,01731792605431E-5
Momento de assimetria = 0,035153667177386 (distribuição positivamente assimétrica - alongada à direita)

Estatística com distribuição de Frequências
Número de classe = 4
Valor inferior = 180°01`00,00000"
Valor superior = 180°01`17,00000"
Amplitude total = 0°00`17,00000"
Amplitude de classe = 0°00`04,25000"

Amostra 1 ordenada

Observações	Resíduos
180,017222222222	-0,0026
180,018888888889	-0,0009
180,019722222222	-0,0001

180,020833333333 0,0010
180,020833333333 0,0010
180,021388888889 0,0016
Sequência do cálculo Shapiro-Wilk
x(n-i+1) x(i) a(n-i+1)*[x(n-i+1)-x(i))]
180,021388888889 180,017222222222 0,0026795833335477
180,020833333333 180,018888888889 0,000545611110986398
180,020833333333 180,019722222222 9,72222222124999E-5

Média = 180,0198
Variância = 0,0000
D.Padrão = 0,0016
b = 0,0033
SQE = 0,0000
W_calc = 0,9093
W = 0,7130
Conclusão do teste de normalidade de Shapiro-Wilk.
Hipótese H0: não é rejeitada.
As observações são provenientes de uma distribuição normal ao nível de significância de 1%.

Amostra 2 ordenada
Observações Resíduos
180,019444444444 -0,0006
180,019722222222 -0,0003
180,02 0,0000
180,02 0,0000
180,020555555556 0,0005
180,020555555556 0,0005
Sequência do cálculo Shapiro-Wilk
x(n-i+1) x(i) a(n-i+1)*[x(n-i+1)-x(i))]
180,020555555556 180,019444444444 0,000714555556127203
180,020555555556 180,019722222222 0,0002338333335204
180,02 180,02 0

Média = 180,0200
Variância = 0,0000
D.Padrão = 0,0004
b = 0,0009
SQE = 0,0000
W_calc = 0,9083
W = 0,7130
Conclusão do teste de normalidade de Shapiro-Wilk.
Hipótese H0: não é rejeitada.
As observações são provenientes de uma distribuição normal ao nível de significância de 1%.

Amostra 3 ordenada
Observações Resíduos
180,016666666667 -0,0026
180,018611111111 -0,0006
180,018611111111 -0,0006
180,018888888889 -0,0004
180,021388888889 0,0021
180,021388888889 0,0021
Sequência do cálculo Shapiro-Wilk
x(n-i+1) x(i) a(n-i+1)*[x(n-i+1)-x(i))]
180,021388888889 180,016666666667 0,0030368611109682
180,021388888889 180,018611111111 0,000779444444506798
180,018888888889 180,018611111111 2,43055555750004E-5

Média = 180,0193

Variância = 0,0000
D.Padrão = 0,0018
b = 0,0038
SQE = 0,0000
W_calc = 0,8796
W = 0,7130
Conclusão do teste de normalidade de Shapiro-Wilk.
Hipótese H0: não é rejeitada.
As observações são provenientes de uma distribuição normal ao nível de significância de 1%.

TESTE T: ANáLISE DE MéDIAS DE AMOSTRAS EM PAR
Amostra1
Número de elementos 6
Média = 180°01`11,3"
Var = 0°00`00,00874"

Amostra2
Número de elementos 6
Média = 180°01`12,2"
Var = 0°00`00,00071"

Discrepâncias
d1 :-0,000277777778000005
d2 :0,001388888889
d3 :-0,0025
d4 :-0,00166666666699999
d5 :0,000277777776999999
d6 :0,00138888888899999
Média = -0°00`00,8"
D.Pad = 0°00`05,74166"

ANÁLISE AMOSTRA1 X AMOSTRA2
Teste de hipótese
Hipótese -> H0: médias populacionais iguais
Hipótese -> H1: médias populacionais diferentes
Nível de significância do teste = 1%
Graus de Liberdade = 5
Estatística do teste t = 0,3555
Probabilidade resultante = 63,2%
t_Crítico bi-caudal = 4,032
CONCLUSÃO :
Teste bi-caudal: t<=t_crítico, então
as médias das amostras: Amostra1 e Amostra2 são iguais ao nível de significância de 1%

TESTE T: ANáLISE DE MéDIAS DE AMOSTRAS EM PAR
Amostra1
Número de elementos 6
Média = 180°01`11,3"
Var = 0°00`00,00874"

Amostra3
Número de elementos 6
Média = 180°01`09,3"
Var = 0°00`00,01207"

Discrepâncias
d1 :0,001111111111
d2 :0,00194444444399999
d3 :0,000555555555000004
d4 :0,000277777778000005

d5 :-0,000555555555999995
d6 :0
Média = 0°00`02,0"
D.Pad = 0°00`03,16228"

ANÁLISE AMOSTRA1 X AMOSTRA3
Teste de hipótese
Hipótese -> H0: médias populacionais iguais
Hipótese -> H1: médias populacionais diferentes
Nível de significância do teste = 1%
Graus de Liberdade = 5
Estatística do teste t = 1,5492
Probabilidade resultante = 90,9%
t_Crítico bi-caudal = 4,032
CONCLUSÃO :
Teste bi-caudal: t<=t_crítico, então
as médias das amostras: Amostra1 e Amostra3 são iguais ao nível de significância de 1%

TESTE T: ANáLISE DE MéDIAS DE AMOSTRAS EM PAR
Amostra2
Número de elementos 6
Média = 180°01`12,2"
Var = 0°00`00,00071"

Amostra3
Número de elementos 6
Média = 180°01`09,3"
Var = 0°00`00,01207"

Discrepâncias
d1 :0,001388888889
d2 :0,00055555555499999
d3 :0,00305555555500001
d4 :0,001944444445
d5 :-0,000833333332999994
d6 :-0,00138888888899999
Média = 0°00`02,8"
D.Pad = 0°00`06,08002"

ANÁLISE AMOSTRA2 X AMOSTRA3
Teste de hipótese
Hipótese -> H0: médias populacionais iguais
Hipótese -> H1: médias populacionais diferentes
Nível de significância do teste = 1%
Graus de Liberdade = 5
Estatística do teste t = 1,1415
Probabilidade resultante = 84,7%
t_Crítico bi-caudal = 4,032
CONCLUSÃO :
Teste bi-caudal: t<=t_crítico, então
as médias das amostras: Amostra2 e Amostra3 são iguais ao nível de significância de 1%

RESUMO DA ANÁLISE PELO TESTE T

GRUPOS	Estatística t	t-crítico	CONCLUSÃO
AMOSTRA1 X AMOSTRA2	0,3555	4,032	Não diferem
AMOSTRA1 X AMOSTRA3	1,5492	4,032	Não diferem
AMOSTRA2 X AMOSTRA3	1,1415	4,032	Não diferem

PILAR 5 (Article 2)

Amostra1 = prisma 360°
Amostra2 = prisma circular
Amostra3 = folha refletiva

ESTATíSTICA DESCRITIVA
Amostra1
Número de elementos =6
Média aritmética = 180°02`13,0"
Variância amostral = 0°00`00,01711" unid.^2
Desvio padrão amostral = 0°00`07,84857"
Coef. de variação = 1,2109500285508E-5
Momento de assimetria = -0,620512002640811 (distribuição negativamente assimétrica - alongada à esquerda)

Estatística com distribuição de Frequências
Número de classe = 4
Valor inferior = 180°02`00,00000"
Valor superior = 180°02`20,00000"
Amplitude total = 0°00`20,00000"
Amplitude de classe = 0°00`05,00000"

Amostra2
Número de elementos =6
Média aritmética = 180°02`19,2"
Variância amostral = 0°00`00,00427" unid.^2
Desvio padrão amostral = 0°00`03,92003"
Coef. de variação = 6,04813628748536E-6
Momento de assimetria = 0,44422662158108 (distribuição positivamente assimétrica - alongada à direita)

Estatística com distribuição de Frequências
Número de classe = 4
Valor inferior = 180°02`15,00000"
Valor superior = 180°02`25,00000"
Amplitude total = 0°00`10,00000"
Amplitude de classe = 0°00`02,50000"

Amostra3
Número de elementos =6
Média aritmética = 180°02`12,0"
Variância amostral = 0°00`00,01822" unid.^2
Desvio padrão amostral = 0°00`08,09938"
Coef. de variação = 1,24965017823961E-5
Momento de assimetria = -0,242791764404881 (distribuição negativamente assimétrica - alongada à esquerda)

Estatística com distribuição de Frequências
Número de classe = 4
Valor inferior = 180°02`01,00000"
Valor superior = 180°02`21,00000"
Amplitude total = 0°00`20,00000"
Amplitude de classe = 0°00`05,00000"

Amostra 1 ordenada

Observações	Resíduos
180,033333333333	-0,0036
180,035277777778	-0,0017
180,037777777778	0,0008

180,037777777778 0,0008
180,038611111111 0,0017
180,038888888889 0,0019
Sequência do cálculo Shapiro-Wilk
x(n-i+1) x(i) a(n-i+1)*[x(n-i+1)-x(i))]
180,038888888889 180,033333333333 0,0035727777780636
180,038611111111 180,035277777778 0,000935333333239803
180,037777777778 180,037777777778 0

Média = 180,0369
Variância = 0,0000
D.Padrão = 0,0022
b = 0,0045
SQE = 0,0000
W_calc = 0,8552
W = 0,7130
Conclusão do teste de normalidade de Shapiro-Wilk.
Hipótese H0: não é rejeitada.
As observações são provenientes de uma distribuição normal ao nível de significância de 1%.

Amostra 2 ordenada
Observações Resíduos
180,0375 -0,0012
180,038055555556 -0,0006
180,038055555556 -0,0006
180,038333333333 -0,0003
180,039722222222 0,0011
180,040277777778 0,0016
Sequência do cálculo Shapiro-Wilk
x(n-i+1) x(i) a(n-i+1)*[x(n-i+1)-x(i))]
180,040277777778 180,0375 0,0017863888890318
180,039722222222 180,038055555556 0,000467666666479601
180,038333333333 180,038055555556 2,43055554874999E-5

Média = 180,0387
Variância = 0,0000
D.Padrão = 0,0011
b = 0,0023
SQE = 0,0000
W_calc = 0,8756
W = 0,7130
Conclusão do teste de normalidade de Shapiro-Wilk.
Hipótese H0: não é rejeitada.
As observações são provenientes de uma distribuição normal ao nível de significância de 1%.

Amostra 3 ordenada
Observações Resíduos
180,033611111111 -0,0031
180,034444444444 -0,0022
180,036388888889 -0,0003
180,038055555556 0,0014
180,038333333333 0,0017
180,039166666667 0,0025
Sequência do cálculo Shapiro-Wilk
x(n-i+1) x(i) a(n-i+1)*[x(n-i+1)-x(i))]
180,039166666667 180,033611111111 0,0035727777780636
180,038333333333 180,034444444444 0,0010912222222534
180,038055555556 180,036388888889 0,000145833333362499

Média = 180,0367

Variância = 0,0000
D.Padrão = 0,0022
b = 0,0048
SQE = 0,0000
W_calc = 0,9141
W = 0,7130
Conclusão do teste de normalidade de Shapiro-Wilk.
Hipótese H0: não é rejeitada.
As observações são provenientes de uma distribuição normal ao nível de significância de 1%.

TESTE T: ANáLISE DE MéDIAS DE AMOSTRAS EM PAR
Amostra1
Número de elementos 6
Média = 180°02`13,0"
Var = 0°00`00,01711"

Amostra2
Número de elementos 6
Média = 180°02`19,2"
Var = 0°00`00,00427"

Discrepâncias
d1 :-0,000277777778000005
d2 :0,000277777777999991
d3 :-0,00472222222300001
d4 :-0,00305555555500001
d5 :-0,00166666666699999
d6 :-0,000833333333000008
Média = -0°00`06,2"
D.Pad = 0°00`06,76511"

ANÁLISE AMOSTRA1 X AMOSTRA2
Teste de hipótese
Hipótese -> H0: médias populacionais iguais
Hipótese -> H1: médias populacionais diferentes
Nível de significância do teste = 1%
Graus de Liberdade = 5
Estatística do teste t = 2,2328
Probabilidade resultante = 96,2%
t_Crítico bi-caudal = 4,032
CONCLUSÃO :
Teste bi-caudal: t<=t_crítico, então
as médias das amostras: Amostra1 e Amostra2 são iguais ao nível de significância de 1%

TESTE T: ANáLISE DE MéDIAS DE AMOSTRAS EM PAR
Amostra1
Número de elementos 6
Média = 180°02`13,0"
Var = 0°00`00,01711"

Amostra3
Número de elementos 6
Média = 180°02`12,0"
Var = 0°00`00,01822"

Discrepâncias
d1 :0,00138888888899999
d2 :-0,000277777778000005
d3 :-0,000277777778000005
d4 :0,000833333334

d5 :0,000277777778000005
d6 :-0,000277777778000005
Média = 0°00`01,0"
D.Pad = 0°00`02,52982"

ANÁLISE AMOSTRA1 X AMOSTRA3
Teste de hipótese
Hipótese -> H0: médias populacionais iguais
Hipótese -> H1: médias populacionais diferentes
Nível de significância do teste = 1%
Graus de Liberdade = 5
Estatística do teste t = 0,9682
Probabilidade resultante = 81,1%
t_Crítico bi-caudal = 4,032
CONCLUSÃO :
Teste bi-caudal: t<=t_crítico, então
as médias das amostras: Amostra1 e Amostra3 são iguais ao nível de significância de 1%

TESTE T: ANáLISE DE MéDIAS DE AMOSTRAS EM PAR
Amostra2
Número de elementos 6
Média = 180°02`19,2"
Var = 0°00`00,00427"

Amostra3
Número de elementos 6
Média = 180°02`12,0"
Var = 0°00`00,01822"

Discrepâncias
d1 :0,00166666666699999
d2 :-0,000555555555999995
d3 :0,004444444445
d4 :0,00388888888900001
d5 :0,001944444445
d6 :0,000555555555000004
Média = 0°00`07,2"
D.Pad = 0°00`06,88234"

ANÁLISE AMOSTRA2 X AMOSTRA3
Teste de hipótese
Hipótese -> H0: médias populacionais iguais
Hipótese -> H1: médias populacionais diferentes
Nível de significância do teste = 1%
Graus de Liberdade = 5
Estatística do teste t = 2,5507
Probabilidade resultante = 97,4%
t_Crítico bi-caudal = 4,032
CONCLUSÃO :
Teste bi-caudal: t<=t_crítico, então
as médias das amostras: Amostra2 e Amostra3 são iguais ao nível de significância de 1%

RESUMO DA ANÁLISE PELO TESTE T

GRUPOS	Estatística t	t-crítico	CONCLUSÃO
AMOSTRA1 X AMOSTRA2	2,2328	4,032	Não diferem
AMOSTRA1 X AMOSTRA3	0,9682	4,032	Não diferem
AMOSTRA2 X AMOSTRA3	2,5507	4,032	Não diferem

PILAR 6 (Article 2)

Amostra1 = prisma 360°
Amostra2 = prisma circular
Amostra3 = folha refletiva

ESTATíSTICA DESCRITIVA
Amostra1
Número de elementos =6
Média aritmética = 179°59`46,2"
Variância amostral = 0°00`00,00260" unid.^2
Desvio padrão amostral = 0°00`03,06050"
Coef. de variação = 4,72309627162881E-6
Momento de assimetria = 0,392764494932728 (distribuição positivamente assimétrica - alongada à direita)

Estatística com distribuição de Frequências
Número de classe = 4
Valor inferior = 179°59`43,00000"
Valor superior = 179°59`51,00000"
Amplitude total = 0°00`08,00000"
Amplitude de classe = 0°00`02,00000"

Amostra2
Número de elementos =6
Média aritmética = 179°59`56,5"
Variância amostral = 0°00`00,00775" unid.^2
Desvio padrão amostral = 0°00`05,28205"
Coef. de variação = 8,15134813027873E-6
Momento de assimetria = -0,166249282902712 (distribuição negativamente assimétrica - alongada à esquerda)

Estatística com distribuição de Frequências
Número de classe = 4
Valor inferior = 179°59`49,00000"
Valor superior = 180°00`03,00000"
Amplitude total = 0°00`14,00000"
Amplitude de classe = 0°00`03,50000"

Amostra3
Número de elementos =6
Média aritmética = 179°59`47,8"
Variância amostral = 0°00`00,00494" unid.^2
Desvio padrão amostral = 0°00`04,21505"
Coef. de variação = 6,5048326151358E-6
Momento de assimetria = -0,42409332068345 (distribuição negativamente assimétrica - alongada à esquerda)

Estatística com distribuição de Frequências
Número de classe = 4
Valor inferior = 179°59`41,00000"
Valor superior = 179°59`53,00000"
Amplitude total = 0°00`12,00000"
Amplitude de classe = 0°00`03,00000"

Amostra 1 ordenada

Observações	Resíduos
179,995277777778	-0,0009
179,995555555556	-0,0006
179,995555555556	-0,0006

179,996388888889 0,0002
179,996666666667 0,0005
179,9975 0,0013
Sequência do cálculo Shapiro-Wilk
x(n-i+1) x(i) a(n-i+1)*[x(n-i+1)-x(i))]
179,9975 179,995277777778 0,0014291111109682
179,996666666667 179,995555555556 0,0003117777777466
179,996388888889 179,995555555556 7,29166666374995E-5

Média = 179,9962
Variância = 0,0000
D.Padrão = 0,0009
b = 0,0018
SQE = 0,0000
W_calc = 0,9104
W = 0,7130
Conclusão do teste de normalidade de Shapiro-Wilk.
Hipótese H0: não é rejeitada.
As observações são provenientes de uma distribuição normal ao nível de significância de 1%.

Amostra 2 ordenada
Observações Resíduos
179,996944444444 -0,0021
179,997777777778 -0,0012
179,999166666667 0,0001
179,999166666667 0,0001
180,000277777778 0,0013
180,000833333333 0,0018
Sequência do cálculo Shapiro-Wilk
x(n-i+1) x(i) a(n-i+1)*[x(n-i+1)-x(i))]
180,000833333333 179,996944444444 0,00250094444451589
180,000277777778 179,997777777778 0,000701500000000001
179,999166666667 179,999166666667 0

Média = 179,9990
Variância = 0,0000
D.Padrão = 0,0015
b = 0,0032
SQE = 0,0000
W_calc = 0,9528
W = 0,7130
Conclusão do teste de normalidade de Shapiro-Wilk.
Hipótese H0: não é rejeitada.
As observações são provenientes de uma distribuição normal ao nível de significância de 1%.

Amostra 3 ordenada
Observações Resíduos
179,994722222222 -0,0019
179,995833333333 -0,0008
179,996944444444 0,0003
179,996944444444 0,0003
179,997222222222 0,0006
179,998055555556 0,0014
Sequência do cálculo Shapiro-Wilk
x(n-i+1) x(i) a(n-i+1)*[x(n-i+1)-x(i))]
179,998055555556 179,994722222222 0,00214366666709539
179,997222222222 179,995833333333 0,000389722222253397
179,996944444444 179,996944444444 0

Média = 179,9966

Variância = 0,0000
D.Padrão = 0,0012
b = 0,0025
SQE = 0,0000
W_calc = 0,9363
W = 0,7130
Conclusão do teste de normalidade de Shapiro-Wilk.
Hipótese H0: não é rejeitada.
As observações são provenientes de uma distribuição normal ao nível de significância de 1%.

TESTE T: ANáLISE DE MéDIAS DE AMOSTRAS EM PAR
Amostra1
Número de elementos 6
Média = 179°59`46,2"
Var = 0°00`00,00260"

Amostra2
Número de elementos 6
Média = 179°59`56,5"
Var = 0°00`00,00775"

Discrepâncias
d1 :-0,004722222222
d2 :-0,00527777777699999
d3 :-0,001388888889
d4 :-0,00166666666700001
d5 :-0,000277777776999999
d6 :-0,00388888888900001
Média = -0°00`10,3"
D.Pad = 0°00`07,31209"

ANÁLISE AMOSTRA1 X AMOSTRA2
Teste de hipótese
Hipótese -> H0: médias populacionais iguais
Hipótese -> H1: médias populacionais diferentes
Nível de significância do teste = 1%
Graus de Liberdade = 5
Estatística do teste t = 3,4616
Probabilidade resultante = 99,1%
t_Crítico bi-caudal = 4,032
CONCLUSÃO :
Teste bi-caudal: t<=t_crítico, então
as médias das amostras: Amostra1 e Amostra2 são iguais ao nível de significância de 1%

TESTE T: ANáLISE DE MéDIAS DE AMOSTRAS EM PAR
Amostra1
Número de elementos 6
Média = 179°59`46,2"
Var = 0°00`00,00260"

Amostra3
Número de elementos 6
Média = 179°59`47,8"
Var = 0°00`00,00494"

Discrepâncias
d1 :-0,00249999999999999
d2 :-0,000277777776999999
d3 :-0,000555555555000004
d4 :0,000277777778000005

d5 :-0,000277777776999999
d6 :0,000555555555999995
Média = -0°00`01,7"
D.Pad = 0°00`03,88158"

ANÁLISE AMOSTRA1 X AMOSTRA3
Teste de hipótese
Hipótese -> H0: médias populacionais iguais
Hipótese -> H1: médias populacionais diferentes
Nível de significância do teste = 1%
Graus de Liberdade = 5
Estatística do teste t = 1,0518
Probabilidade resultante = 82,9%
t_Crítico bi-caudal = 4,032
CONCLUSÃO :
Teste bi-caudal: t<=t_crítico, então
as médias das amostras: Amostra1 e Amostra3 são iguais ao nível de significância de 1%

TESTE T: ANáLISE DE MéDIAS DE AMOSTRAS EM PAR
Amostra2
Número de elementos 6
Média = 179°59`56,5"
Var = 0°00`00,00775"

Amostra3
Número de elementos 6
Média = 179°59`47,8"
Var = 0°00`00,00494"

Discrepâncias
d1 :0,00222222222200001
d2 :0,00499999999999999
d3 :0,000833333334
d4 :0,00194444444500001
d5 :0
d6 :0,004444444445
Média = 0°00`08,7"
D.Pad = 0°00`07,08990"

ANÁLISE AMOSTRA2 X AMOSTRA3
Teste de hipótese
Hipótese -> H0: médias populacionais iguais
Hipótese -> H1: médias populacionais diferentes
Nível de significância do teste = 1%
Graus de Liberdade = 5
Estatística do teste t = 2,9942
Probabilidade resultante = 98,5%
t_Crítico bi-caudal = 4,032
CONCLUSÃO :
Teste bi-caudal: t<=t_crítico, então
as médias das amostras: Amostra2 e Amostra3 são iguais ao nível de significância de 1%

RESUMO DA ANÁLISE PELO TESTE T

GRUPOS	Estatística t	t-crítico	CONCLUSÃO
AMOSTRA1 X AMOSTRA2	3,4616	4,032	Não diferem
AMOSTRA1 X AMOSTRA3	1,0518	4,032	Não diferem
AMOSTRA2 X AMOSTRA3	2,9942	4,032	Não diferem

PILAR 7 (Article 2)

Amostra1 = prisma 360°
Amostra2 = prisma circular
Amostra3 = folha refletiva

ESTATíSTICA DESCRITIVA
Amostra1
Número de elementos =6
Média aritmética = 359°58`36,0"
Variância amostral = 0°00`00,00433" unid.^2
Desvio padrão amostral = 0°00`03,94968"
Coef. de variação = 3,04779285936758E-6
Momento de assimetria = -0,5680429143319 (distribuição negativamente assimétrica - alongada à esquerda)

Estatística com distribuição de Frequências
Número de classe = 4
Valor inferior = 359°58`30,00000"
Valor superior = 359°58`39,00000"
Amplitude total = 0°00`09,00000"
Amplitude de classe = 0°00`02,25000"

Amostra2
Número de elementos =6
Média aritmética = 359°58`32,7"
Variância amostral = 0°00`00,00152" unid.^2
Desvio padrão amostral = 0°00`02,33809"
Coef. de variação = 1,80420366978651E-6
Momento de assimetria = -0,136191562866063 (distribuição negativamente assimétrica - alongada à esquerda)

Estatística com distribuição de Frequências
Número de classe = 4
Valor inferior = 359°58`30,00000"
Valor superior = 359°58`35,00000"
Amplitude total = 0°00`05,00000"
Amplitude de classe = 0°00`01,25000"

Amostra3
Número de elementos =6
Média aritmética = 359°58`32,8"
Variância amostral = 0°00`00,00582" unid.^2
Desvio padrão amostral = 0°00`04,57894"
Coef. de variação = 3,53336826988055E-6
Momento de assimetria = 0,370543772462618 (distribuição positivamente assimétrica - alongada à direita)

Estatística com distribuição de Frequências
Número de classe = 4
Valor inferior = 359°58`28,00000"
Valor superior = 359°58`39,00000"
Amplitude total = 0°00`11,00000"
Amplitude de classe = 0°00`02,75000"

Amostra 1 ordenada

Observações	Resíduos
359,975	-0,0017
359,975555555556	-0,0011
359,977222222222	0,0006

359,977222222222 0,0006
359,9775 0,0008
359,9775 0,0008
Sequência do cálculo Shapiro-Wilk

x(n-i+1)	x(i)	a(n-i+1)*[x(n-i+1)-x(i))]
359,9775	359,975	0,00160775
359,9775	359,975555555556	0,000545611110986406
359,977222222222	359,977222222222	0

Média = 359,9767
Variância = 0,0000
D.Padrão = 0,0011
b = 0,0022
SQE = 0,0000
W_calc = 0,7704
W = 0,7130
Conclusão do teste de normalidade de Shapiro-Wilk.
Hipótese H0: não é rejeitada.
As observações são provenientes de uma distribuição normal ao nível de significância de 1%.

Amostra 2 ordenada

Observações	Resíduos
359,975	-0,0007
359,975	-0,0007
359,975555555556	-0,0002
359,976111111111	0,0004
359,976388888889	0,0006
359,976388888889	0,0006

Sequência do cálculo Shapiro-Wilk

x(n-i+1)	x(i)	a(n-i+1)*[x(n-i+1)-x(i))]
359,976388888889	359,975	0,000893194444515893
359,976388888889	359,975	0,000389722222253397
359,976111111111	359,975555555556	4,86111110625003E-5

Média = 359,9757
Variância = 0,0000
D.Padrão = 0,0006
b = 0,0013
SQE = 0,0000
W_calc = 0,8406
W = 0,7130
Conclusão do teste de normalidade de Shapiro-Wilk.
Hipótese H0: não é rejeitada.
As observações são provenientes de uma distribuição normal ao nível de significância de 1%.

Amostra 3 ordenada

Observações	Resíduos
359,974444444444	-0,0013
359,975	-0,0008
359,975	-0,0008
359,975555555556	-0,0002
359,977222222222	0,0014
359,9775	0,0017

Sequência do cálculo Shapiro-Wilk

x(n-i+1)	x(i)	a(n-i+1)*[x(n-i+1)-x(i))]
359,9775	359,974444444444	0,00196502777806361
359,977222222222	359,975	0,000623555555493199
359,975555555556	359,975	4,86111111499984E-5

Média = 359,9758

Variância = 0,0000
D.Padrão = 0,0013
b = 0,0026
SQE = 0,0000
W_calc = 0,8598
W = 0,7130
Conclusão do teste de normalidade de Shapiro-Wilk.
Hipótese H0: não é rejeitada.
As observações são provenientes de uma distribuição normal ao nível de significância de 1%.

TESTE T: ANáLISE DE MéDIAS DE AMOSTRAS EM PAR
Amostra1
Número de elementos 6
Média = 359°58`36,0"
Var = 0°00`00,00433"

Amostra2
Número de elementos 6
Média = 359°58`32,7"
Var = 0°00`00,00152"

Discrepâncias
d1 :0,000833333333000008
d2 :0,00138888888900002
d3 :0,0025
d4 :0,002222222222
d5 :-0,000555555555999981
d6 :-0,000833333333000008
Média = 0°00`03,3"
D.Pad = 0°00`05,00666"

ANÁLISE AMOSTRA1 X AMOSTRA2
Teste de hipótese
Hipótese -> H0: médias populacionais iguais
Hipótese -> H1: médias populacionais diferentes
Nível de significância do teste = 1%
Graus de Liberdade = 5
Estatística do teste t = 1,6308
Probabilidade resultante = 91,8%
t_Crítico bi-caudal = 4,032
CONCLUSÃO :
Teste bi-caudal: t<=t_crítico, então
as médias das amostras: Amostra1 e Amostra2 são iguais ao nível de significância de 1%

TESTE T: ANáLISE DE MéDIAS DE AMOSTRAS EM PAR
Amostra1
Número de elementos 6
Média = 359°58`36,0"
Var = 0°00`00,00433"

Amostra3
Número de elementos 6
Média = 359°58`32,8"
Var = 0°00`00,00582"

Discrepâncias
d1 :0,002222222222
d2 :0,00305555555600001
d3 :0
d4 :0

d5 :0
d6 :0
Média = 0°00`03,2"
D.Pad = 0°00`04,99667"

ANÁLISE AMOSTRA1 X AMOSTRA3
Teste de hipótese
Hipótese -> H0: médias populacionais iguais
Hipótese -> H1: médias populacionais diferentes
Nível de significância do teste = 1%
Graus de Liberdade = 5
Estatística do teste t = 1,5524
Probabilidade resultante = 90,9%
t_Crítico bi-caudal = 4,032
CONCLUSÃO :
Teste bi-caudal: t<=t_crítico, então
as médias das amostras: Amostra1 e Amostra3 são iguais ao nível de significância de 1%

TESTE T: ANáLISE DE MéDIAS DE AMOSTRAS EM PAR
Amostra2
Número de elementos 6
Média = 359°58`32,7"
Var = 0°00`00,00152"

Amostra3
Número de elementos 6
Média = 359°58`32,8"
Var = 0°00`00,00582"

Discrepâncias
d1 :0,00138888888899999
d2 :0,00166666666699999
d3 :-0,0025
d4 :-0,002222222222
d5 :0,00055555555599981
d6 :0,00083333333000008
Média = -0°00`00,2"
D.Pad = 0°00`06,61564"

ANÁLISE AMOSTRA2 X AMOSTRA3
Teste de hipótese
Hipótese -> H0: médias populacionais iguais
Hipótese -> H1: médias populacionais diferentes
Nível de significância do teste = 1%
Graus de Liberdade = 5
Estatística do teste t = 0,0617
Probabilidade resultante = 52,3%
t_Crítico bi-caudal = 4,032
CONCLUSÃO :
Teste bi-caudal: t<=t_crítico, então
as médias das amostras: Amostra2 e Amostra3 são iguais ao nível de significância de 1%

RESUMO DA ANÁLISE PELO TESTE T

GRUPOS	Estatística t	t-crítico	CONCLUSÃO
AMOSTRA1 X AMOSTRA2	1,6308	4,032	Não diferem
AMOSTRA1 X AMOSTRA3	1,5524	4,032	Não diferem
AMOSTRA2 X AMOSTRA3	0,0617	4,032	Não diferem

APPENDIX D - AstGeoTop TRAVERSES COMPUTATIONS REPORTS

REPORTS FOR TRAVERSE COMPUTATIONS - 360° PRISM (Article 2)

AstGeoTop - Lev.Planimétrico©Versão 2012.11.11
AJUSTAMENTO PELO MÉTODO TRADICIONAL
DADOS CLASSIFICATÓRIOS DA POLIGONAL NBR 13.133(94)
Classe de Poligonal :Poligonal definida pelo usuário
Goniômetro - Classe 3: precisão alta
Precisão Angular : 05 "
MED - Classe 3: precisão alta
Precisão Linear : (2mm + 2ppm x D)

PLANILHA TOPOGRÁFICA DE CÁLCULO ANALÍTICO

Est.	P.Vis.	Ângulo	Distância	Âng.Compens.	Azimute	Coordenadas Parciais X	Coordenadas Parciais Y	Coord. Parciais Comp. X	Coord. Parciais Comp. Y	Coord. Totais X	Coord. Totais Y
P1	P3	359°58`57,7"	12,739	359°59`00,7"	0°00`00,0"	0,0000	12,7390	0,0000	12,7389	1000,0000	1000,0000
P3	P4	179°59`36,5"	33,125	179°59`39,5"	359°59`39,5"	-0,0033	33,1250	-0,0032	33,1249	1000,0000	1012,7389
P4	P7	180°01`11,3"	121,629	180°01`11,7"	0°00`51,2"	0,0302	121,6290	0,0305	121,6285	999,9968	1045,8638
P7	P6	359°58`36,0"	32,258	359°58`36,9"	179°59`28,1"	0,0050	-32,2580	0,0051	-32,2581	1000,0273	1167,4923
P6	P5	179°59`46,2"	39,480	179°59`48,7"	179°59`16,7"	0,0083	-39,4800	0,0084	-39,4802	1000,0324	1135,2342
P5	P2	180°02`13,0"	87,453	180°02`14,4"	180°01`31,1"	-0,0386	-87,4530	-0,0384	-87,4534	1000,0408	1095,7540
P2	P1	179°59`26,3"	8,301	179°59`28,2"	180°00`59,3"	-0,0024	-8,3006	-0,0024	-8,3006	1000,0024	1008,3006

S.ang = 1620°00`00,0" Ex=-0,0009 Ey=0,0014 Ex=0,0000 Ey=0,0000

Perímetro = 334,985 m
Área = 2,894 m2
Área = 0,0002894 ha
Área = 0,0001196 Alq.SP

VALORES MÁXIMOS ACEITÁVEIS APÓS O AJUSTAMENTO

Tolerância do fechamento angular = 0°00`39,7"
Erro médio máximo aceitável em azimute = 0°00`15,0"

Tolerância do erro de fechamento linear = 0,0579 m
Erro relativo linear máximo aceitável = 1/5787,7854
Erro médio relativo máximo aceitável entre duas estações poligonais = 1/2362,8535

Erro médio máximo aceitável em coordenadas (posição) = 0,0236 m
---

VALORES OBTIDOS APÓS O AJUSTAMENTO

Erro de fechamento angular = -0°00`13,0"
Erro médio em azimute = 0°00`02,5"

Erro de fechamento linear = 0,0017 m
Erro relativo linear = 1/202953,0757
Erro médio relativo entre duas estações poligonais

P1	P3	1/202952,2237
P3	P4	1/202952,2236
P4	P7	1/202952,2238
P7	P6	1/202953,9277
P6	P5	1/202953,9277
P5	P2	1/202953,9274
P2	P1	1/202953,9275

Erro médio em coordenadas (posição) dos vértices = 0,0182 m

CONCLUSÃO APÓS O AJUSTAMENTO - POLIGONAL Poligonal definida pelo usuário
Fechamento angular : dentro da especificação
Erro médio em Azimute : dentro da especificação
Erro de fechamento linear : dentro da especificação
Erro relativo linear : dentro da especificação
Erro relativo entre duas estações poligonais : dentro da especificação
Erro médio em posição : dentro da especificação

PLANILHA COM ELEMENTOS DA POLIGONAL AJUSTADOS

Est.	P.Vis.	Ângulo	Distância	Azimute	Coord. Totais X	Coord. Totais Y
P1	P3	359°59`01,8"	12,739	0°00`00,0"	1000,0000	1000,0000
P3	P4	179°59`39,5"	33,125	359°59`39,5"	1000,0000	1012,7389
P4	P7	180°01`11,7"	121,628	0°00`51,2"	999,9967	1045,8638
P7	P6	359°58`35,8"	32,258	179°59`27,0"	1000,0269	1167,4923
P6	P5	179°59`48,7"	39,480	179°59`15,7"	1000,0321	1135,2342
P5	P2	180°02`14,4"	87,453	180°01`30,1"	1000,0405	1095,7540
P2	P1	179°59`28,2"	8,301	180°00`58,2"	1000,0023	1008,3006

Perímetro = 334,984 m
Área = 2,885 m2
Área = 0,0002885 ha
Área = 0,0001192 Alq.SP

AstGeoTop - Lev.Planimétrico©Versão 2012.11.11
AJUSTAMENTO PELO MÉTODO DOS MÍNIMOS QUADRADOS
MODELO PARAMÉTRICO (Variação de Coordenadas)

DADOS CLASSIFICATÓRIOS DA POLIGONAL NBR 13.133(94)
Classe de Poligonal :Poligonal definida pelo usuário
Goniômetro - Classe 3: precisão alta
Precisão Angular : 05 "
MED - Classe 3: precisão alta
Precisão Linear : (2mm + 2ppm x D)

VETOR DOS RESÍDUOS DO AJUSTAMENTO (V=AX-L)

Est.	P.Vis.	Ângulo	Distância
P1	P3	4,0285"	-0,0002
P3	P4	3,9342"	-0,0002
P4	P7	0,0711"	-0,0002
P7	P6	0,2963"	0,0002
P6	P5	2,3547"	0,0002
P5	P2	0,7853"	0,0002
P2	P1	1,5299"	0,0002

PARÂMETROS AJUSTADOS Xa, Desvios-padrão e Erro Posicional(1*sigma)

Est.	X(m)	SigmaX(m)	Y(m)	SigmaY(m)	P.Posição(m)
P1	1000,0000	0,0000	1000,0000	0,0000	0,0000
P3	1000,0000	0,0000	1012,7388	0,0025	0,0025
P4	999,9969	0,0005	1045,8636	0,0033	0,0033
P7	1000,0274	0,0024	1167,4924	0,0036	0,0044
P6	1000,0324	0,0019	1135,2342	0,0036	0,0041
P5	1000,0407	0,0014	1095,7540	0,0033	0,0036
P2	1000,0023	0,0001	1008,3008	0,0025	0,0025

OBSERVACOES AJUSTADAS La e Desvios-padrão (1*sigma)

Est.	P.Vis.	Ângulo	Sigma Âng."	Distância(m)	Sig.Dist.(m)
P1	P3	359°59`02,8"	3,0232	12,739	0,0025
P3	P4	179°59`40,7"	3,2445	33,125	0,0025
P4	P7	180°01`11,0"	0,5591	121,629	0,0026
P7	P6	359°58`36,3"	1,1253	32,258	0,0025
P6	P5	179°59`48,6"	1,7532	39,480	0,0025
P5	P2	180°02`13,9"	1,7934	87,453	0,0026
P2	P1	179°59`26,6"	2,3458	8,301	0,0025

CONTROLE DE QUALIDADE DO AJUSTAMENTO

Variância da Unidade Peso Estimada a Posteriori = 1,884
******** Teste de Hipótese Qui-quadrado ***********
Estatística do teste vTPV = 5,653
Percentil inferior da distribuição Qui-quadrado = 0,22
Percentil superior da distribuição Qui-quadrado = 9,35
Conclusão
Ao nível de significância de 5%:
NÃO É REJEITADA a hipótese de que as observações ponderadas sejam provenientes de uma distribuição normal

PLANILHA COM ELEMENTOS DA POLIGONAL AJUSTADOS POR MMQ

Est.	P.Vis.	Ângulo	Distância	Azimute	Coord. Totais	
					X	Y
P1	P3	359°59`02,8"	12,739	0°00`00,0"	1000,0000	1000,0000
P3	P4	179°59`40,7"	33,125	359°59`40,7"	1000,0000	1012,7388
P4	P7	180°01`11,0"	121,629	0°00`51,7"	999,9969	1045,8636
P7	P6	359°58`36,3"	32,258	179°59`28,0"	1000,0274	1167,4924
P6	P5	179°59`48,6"	39,480	179°59`16,6"	1000,0324	1135,2342
P5	P2	180°02`13,9"	87,453	180°01`30,6"	1000,0407	1095,7540
P2	P1	179°59`26,6"	8,301	180°00`57,2"	1000,0023	1008,3008

Perímetro = 334,985 m
Área = 2,871 m2
Área = 0,0002871 ha
Área = 0,0001186 Alq.SP

****

PLANILHA COM ELEMENTOS DA POLIGONAL AJUSTADOS PELO MÉTODO TRADICIONAL

Est.	P.Vis.	Ângulo	Distância	Azimute	Coord. Totais	
					X	Y
P1	P3	359°59`01,8"	12,739	0°00`00,0"	1000,0000	1000,0000
P3	P4	179°59`39,5"	33,125	359°59`39,5"	1000,0000	1012,7389
P4	P7	180°01`11,7"	121,628	0°00`51,2"	999,9967	1045,8638
P7	P6	359°58`35,8"	32,258	179°59`27,0"	1000,0269	1167,4923
P6	P5	179°59`48,7"	39,480	179°59`15,7"	1000,0321	1135,2342
P5	P2	180°02`14,4"	87,453	180°01`30,1"	1000,0405	1095,7540
P2	P1	179°59`28,2"	8,301	180°00`58,2"	1000,0023	1008,3006

Perímetro = 334,985 m
Área = 2,885 m2

PLANILHA DE DISCREPÂNCIAS DOS AJUSTAMENTOS (MMQ - MÉTODO TRADICIONAL)

Est.	P.Vis.	Ângulo	Distância	Azimute	Coord. Totais X	Y
P1	P3	0°00`01,1"	0,000	0°00`00,0"	0,0000	0,0000
P3	P4	0°00`01,2"	0,000	0°00`01,2"	0,0000	-0,0001
P4	P7	-0°00`00,7"	0,000	0°00`00,5"	0,0002	-0,0002
P7	P6	0°00`00,5"	0,000	0°00`01,0"	0,0005	0,0001
P6	P5	-0°00`00,1"	0,000	0°00`01,0"	0,0003	0,0000
P5	P2	-0°00`00,5"	0,000	0°00`00,5"	0,0002	0,0000
P2	P1	-0°00`01,6"	0,000	-0°00`01,1"	0,0000	0,0002

Perímetro = 0,000 m
Área = -0,014 m2

REPORTS FOR TRAVERSE COMPUTATIONS - CIRCULAR PRISM (Article 2)

AstGeoTop - Lev.Planimétrico©Versão 2012.11.11
AJUSTAMENTO PELO MÉTODO TRADICIONAL

DADOS CLASSIFICATÓRIOS DA POLIGONAL NBR 13.133(94)
Classe de Poligonal :Poligonal definida pelo usuário
Goniômetro - Classe 3: precisão alta
Precisão Angular : 05 "
MED - Classe 3: precisão alta
Precisão Linear : (2mm + 2ppm x D)

PLANILHA TOPOGRÁFICA DE CÁLCULO ANALÍTICO

Est.	P.Vis.	Ângulo	Distância	Âng.Compens.	Azimute	Coordenadas Parciais X	Coordenadas Parciais Y	Coord. Parciais Comp. X	Coord. Parciais Comp. Y	Coord. Totais X	Coord. Totais Y
P1	P3	359°59`01,3"	12,739	359°58`58,1"	0°00`00,0"	0,0000	12,7390	0,0001	12,7390	1000,0000	1000,0000
P3	P4	179°59`36,7"	33,126	179°59`33,5"	359°59`33,5"	-0,0043	33,1260	-0,0041	33,1259	1000,0001	1012,7390
P4	P7	180°01`12,2"	121,630	180°01`11,8"	0°00`45,3"	0,0267	121,6300	0,0273	121,6296	999,9960	1045,8649
P7	P6	359°58`32,7"	32,259	359°58`31,8"	179°59`17,1"	0,0067	-32,2590	0,0069	-32,2591	1000,0232	1167,4945
P6	P5	179°59`56,5"	39,480	179°59`53,9"	179°59`10,9"	0,0094	-39,4800	0,0096	-39,4801	1000,0301	1135,2354
P5	P2	180°02`19,2"	87,454	180°02`17,7"	180°01`28,7"	-0,0376	-87,4540	-0,0372	-87,4543	1000,0396	1095,7553
P2	P1	179°59`35,2"	8,301	179°59`33,2"	180°01`01,9"	-0,0025	-8,3010	-0,0025	-8,3010	1000,0025	1008,3010

S.ang = 1620°00`00,0" Ex=-0,0015 Ey=0,0010 Ex=0,0000 Ey=0,0000

Perímetro = 334,989 m
Área = 2,983 m2
Área = 0,0002983 ha
Área = 0,0001233 Alq.SP

VALORES MÁXIMOS ACEITÁVEIS APÓS O AJUSTAMENTO

Tolerância do fechamento angular = 0°00`39,7"
Erro médio máximo aceitável em azimute = 0°00`15,0"

Tolerância do erro de fechamento linear = 0,0579 m
Erro relativo linear máximo aceitável = 1/5787,8234
Erro médio relativo máximo aceitável entre duas estações poligonais = 1/2362,8690

Erro médio máximo aceitável em coordenadas (posição) = 0,0236 m
---

VALORES OBTIDOS APÓS O AJUSTAMENTO

Erro de fechamento angular = 0°00`13,8"
Erro médio em azimute = 0°00`02,3"

Erro de fechamento linear = 0,0018 m
Erro relativo linear = 1/184206,1027
Erro médio relativo entre duas estações poligonais
P1 P3 1/184205,5489
P3 P4 1/184205,5488
P4 P7 1/184205,5491
P7 P6 1/184206,6567
P6 P5 1/184206,6567
P5 P2 1/184206,6561
P2 P1 1/184206,6562

Erro médio em coordenadas (posição) dos vértices = 0,0191 m

CONCLUSÃO APÓS O AJUSTAMENTO - POLIGONAL Poligonal definida pelo usuário
Fechamento angular : dentro da especificação
Erro médio em Azimute : dentro da especificação
Erro de fechamento linear : dentro da especificação
Erro relativo linear : dentro da especificação

Erro relativo entre duas estações poligonais : dentro da especificação
Erro médio em posição : dentro da especificação

PLANILHA COM ELEMENTOS DA POLIGONAL AJUSTADOS

Est.	P.Vis.	Ângulo	Distância	Azimute	Coord. Totais X	Y
P1	P3	359°59`00,0"	12,739	0°00`00,0"	1000,0000	1000,0000
P3	P4	179°59`33,5"	33,126	359°59`33,5"	1000,0000	1012,7390
P4	P7	180°01`11,8"	121,630	0°00`45,3"	999,9957	1045,8649
P7	P6	359°58`29,9"	32,259	179°59`15,2"	1000,0225	1167,4945
P6	P5	179°59`53,9"	39,480	179°59`09,1"	1000,0295	1135,2354
P5	P2	180°02`17,7"	87,454	180°01`26,8"	1000,0392	1095,7553
P2	P1	179°59`33,2"	8,301	180°01`00,0"	1000,0024	1008,3010

Perímetro = 334,989 m
Área = 2,988 m2
Área = 0,0002988 ha
Área = 0,0001235 Alq.SP

AstGeoTop - Lev.Planimétrico©Versão 2012.11.11
AJUSTAMENTO PELO MÉTODO DOS MÍNIMOS QUADRADOS
MODELO PARAMÉTRICO (Variação de Coordenadas)

DADOS CLASSIFICATÓRIOS DA POLIGONAL NBR 13.133(94)
Classe de Poligonal :Poligonal definida pelo usuário
Goniômetro - Classe 3: precisão alta
Precisão Angular : 05 "
MED - Classe 3: precisão alta
Precisão Linear : (2mm + 2ppm x D)

VETOR DOS RESÍDUOS DO AJUSTAMENTO (V=AX-L)

Est.	P.Vis.	Ângulo	Distância
P1	P3	-2,3222"	-0,0001
P3	P4	-2,8238"	-0,0001
P4	P7	-0,0784"	-0,0001
P7	P6	-0,8201"	0,0001
P6	P5	-5,3726"	0,0001
P5	P2	-1,3608"	0,0001
P2	P1	-1,0221"	0,0001

PARÂMETROS AJUSTADOS Xa, Desvios-padrão e Erro Posicional(1*sigma)

Est.	X(m)	SigmaX(m)	Y(m)	SigmaY(m)	P.Posição(m)
P1	1000,0000	0,0000	1000,0000	0,0000	0,0000
P3	1000,0000	0,0000	1012,7389	0,0029	0,0029
P4	999,9958	0,0006	1045,8647	0,0038	0,0038
P7	1000,0229	0,0030	1167,4946	0,0041	0,0051
P6	1000,0295	0,0024	1135,2354	0,0041	0,0048
P5	1000,0393	0,0017	1095,7553	0,0038	0,0041
P2	1000,0025	0,0001	1008,3011	0,0029	0,0029

OBSERVACOES AJUSTADAS La e Desvios-padrão (1*sigma)

Est.	P.Vis.	Ângulo	Sigma Âng."	Distância(m)	Sig.Dist.(m)
P1	P3	359°58`57,9"	3,6915	12,739	0,0029
P3	P4	179°59`33,8"	3,9619	33,126	0,0029
P4	P7	180°01`12,1"	0,6827	121,630	0,0029
P7	P6	359°58`31,8"	1,3741	32,259	0,0029
P6	P5	179°59`51,0"	2,1408	39,480	0,0029
P5	P2	180°02`18,0"	2,1898	87,454	0,0029
P2	P1	179°59`35,3"	2,8644	8,301	0,0029

CONTROLE DE QUALIDADE DO AJUSTAMENTO

Variância da Unidade Peso Estimada a Posteriori = 2,495
******** Teste de Hipótese Qui-quadrado **********
Estatística do teste vTPV = 7,486
Percentil inferior da distribuição Qui-quadrado = 0,22
Percentil superior da distribuição Qui-quadrado = 9,35
Conclusão
Ao nível de significância de 5%:
NÃO É REJEITADA a hipótese de que as observações ponderadas sejam provenientes de uma distribuição normal

PLANILHA COM ELEMENTOS DA POLIGONAL AJUSTADOS POR MMQ

Est.	P.Vis.	Ângulo	Distância	Azimute	Coord. Totais	
					X	Y
P1	P3	359°58`57,9"	12,739	0°00`00,0"	1000,0000	1000,0000
P3	P4	179°59`33,8"	33,126	359°59`33,8"	1000,0000	1012,7389
P4	P7	180°01`12,1"	121,630	0°00`46,0"	999,9958	1045,8647
P7	P6	359°58`31,8"	32,259	179°59`17,8"	1000,0229	1167,4946
P6	P5	179°59`51,0"	39,480	179°59`08,8"	1000,0295	1135,2354
P5	P2	180°02`18,0"	87,454	180°01`26,8"	1000,0393	1095,7553
P2	P1	179°59`35,3"	8,301	180°01`02,1"	1000,0025	1008,3011

Perímetro = 334,989 m
Área = 2,974 m2
Área = 0,0002974 ha
Área = 0,0001229 Alq.SP

****

PLANILHA COM ELEMENTOS DA POLIGONAL AJUSTADOS PELO MÉTODO TRADICIONAL

Est.	P.Vis.	Ângulo	Distância	Azimute	Coord. Totais	
					X	Y
P1	P3	359°59`00,0"	12,739	0°00`00,0"	1000,0000	1000,0000
P3	P4	179°59`33,5"	33,126	359°59`33,5"	1000,0000	1012,7390
P4	P7	180°01`11,8"	121,630	0°00`45,3"	999,9957	1045,8649
P7	P6	359°58`29,9"	32,259	179°59`15,2"	1000,0225	1167,4945
P6	P5	179°59`53,9"	39,480	179°59`09,1"	1000,0295	1135,2354
P5	P2	180°02`17,7"	87,454	180°01`26,8"	1000,0392	1095,7553
P2	P1	179°59`33,2"	8,301	180°01`00,0"	1000,0024	1008,3010

Perímetro = 334,989 m
Área = 2,988 m2

PLANILHA DE DISCREPÂNCIAS DOS AJUSTAMENTOS (MMQ - MÉTODO TRADICIONAL)

Est.	P.Vis.	Ângulo	Distância	Azimute	Coord. Totais	
					X	Y
P1	P3	-0°00`02,1"	0,000	0°00`00,0"	0,0000	0,0000
P3	P4	0°00`00,3"	0,000	0°00`00,3"	0,0000	-0,0001
P4	P7	0°00`00,3"	0,000	0°00`00,7"	0,0001	-0,0002
P7	P6	0°00`02,0"	0,000	0°00`02,6"	0,0004	0,0001
P6	P5	-0°00`02,9"	0,000	-0°00`00,3"	0,0000	0,0000
P5	P2	0°00`00,3"	0,000	-0°00`00,0"	0,0001	0,0000
P2	P1	0°00`02,1"	0,000	0°00`02,1"	0,0001	0,0001

Perímetro = 0,000 m
Área = -0,014 m2

REPORTS FOR TRAVERSE COMPUTATIONS - REFLECTIVE SHEET (Article 2)

DADOS CLASSIFICATÓRIOS DA POLIGONAL NBR 13.133(94)
Classe de Poligonal :Poligonal definida pelo usuário
Goniômetro - Classe 3: precisão alta
Precisão Angular : 05 "
MED - Classe 3: precisão alta
Precisão Linear : (2mm + 2ppm x D)

PLANILHA TOPOGRÁFICA DE CÁLCULO ANALÍTICO

Est.	P.Vis.	Ângulo	Distância	Âng.Compens.	Azimute	Coordenadas Parciais X	Coordenadas Parciais Y	Coord. Parciais Comp. X	Coord. Parciais Comp. Y	Coord. Totais X	Coord. Totais Y
P1	P3	359°58`59,8"	12,739	359°59`02,9"	0°00`00,0"	0,0000	12,7390	-0,0001	12,7391	1000,0000	1000,0000
P3	P4	179°59`31,8"	33,126	179°59`34,9"	359°59`34,9"	-0,0040	33,1260	-0,0042	33,1263	999,9999	1012,7391
P4	P7	180°01`09,3"	121,629	180°01`09,7"	0°00`44,6"	0,0263	121,6290	0,0257	121,6302	999,9958	1045,8655
P7	P6	359°58`32,8"	32,261	359°58`33,7"	179°59`18,3"	0,0065	-32,2610	0,0064	-32,2607	1000,0215	1167,4956
P6	P5	179°59`47,8"	39,478	179°59`50,3"	179°59`08,6"	0,0098	-39,4780	0,0097	-39,4776	1000,0279	1135,2350
P5	P2	180°02`12,0"	87,455	180°02`13,4"	180°01`22,0"	-0,0348	-87,4550	-0,0352	-87,4541	1000,0375	1095,7574
P2	P1	179°59`33,2"	8,303	179°59`35,1"	180°00`57,1"	-0,0023	-8,3033	-0,0023	-8,3032	1000,0023	1008,3032

S.ang = 1620°00`00,0" Ex=0,0015 Ey=-0,0033 Ex=0,0000 Ey=0,0000

Perímetro = 334,991 m
Área = 2,857 m2
Área = 0,0002857 ha
Área = 0,0001181 Alq.SP

VALORES MÁXIMOS ACEITÁVEIS APÓS O AJUSTAMENTO

Tolerância do fechamento angular = 0°00`39,7"
Erro médio máximo aceitável em azimute = 0°00`15,0"

Tolerância do erro de fechamento linear = 0,0579 m
Erro relativo linear máximo aceitável = 1/5787,8433
Erro médio relativo máximo aceitável entre duas estações poligonais = 1/2362,8771

Erro médio máximo aceitável em coordenadas (posição) = 0,0236 m
---

VALORES OBTIDOS APÓS O AJUSTAMENTO

Erro de fechamento angular = -0°00`13,3"
Erro médio em azimute = 0°00`02,3"

Erro de fechamento linear = 0,0036 m
Erro relativo linear = 1/92252,7313
Erro médio relativo entre duas estações poligonais
P1 P3 1/92253,6384
P3 P4 1/92253,6384
P4 P7 1/92253,6383
P7 P6 1/92251,8241
P6 P5 1/92251,8241
P5 P2 1/92251,8243
P2 P1 1/92251,8243

Erro médio em coordenadas (posição) dos vértices = 0,0269 m

CONCLUSÃO APÓS O AJUSTAMENTO - POLIGONAL Poligonal definida pelo usuário
Fechamento angular : dentro da especificação
Erro médio em Azimute : dentro da especificação
Erro de fechamento linear : dentro da especificação

Erro relativo linear : dentro da especificação
Erro relativo entre duas estações poligonais : dentro da especificação
Erro médio em posição : fora da especificação

PLANILHA COM ELEMENTOS DA POLIGONAL AJUSTADOS

Est.	P.Vis.	Ângulo	Distância	Azimute	Coord. Totais X	Coord. Totais Y
P1	P3	359°59`01,0"	12,739	0°00`00,0"	1000,0000	1000,0000
P3	P4	179°59`34,9"	33,126	359°59`34,9"	1000,0000	1012,7391
P4	P7	180°01`09,7"	121,630	0°00`44,6"	999,9960	1045,8655
P7	P6	359°58`35,6"	32,261	179°59`20,2"	1000,0222	1167,4956
P6	P5	179°59`50,3"	39,478	179°59`10,5"	1000,0285	1135,2350
P5	P2	180°02`13,4"	87,454	180°01`23,9"	1000,0380	1095,7574
P2	P1	179°59`35,1"	8,303	180°00`59,0"	1000,0024	1008,3032

Perímetro = 334,991 m
Área = 2,866 m2
Área = 0,0002866 ha
Área = 0,0001184 Alq.SP

AstGeoTop - Lev.Planimétrico©Versão 2012.11.11
AJUSTAMENTO PELO MÉTODO DOS MÍNIMOS QUADRADOS
MODELO PARAMÉTRICO (Variação de Coordenadas)

DADOS CLASSIFICATÓRIOS DA POLIGONAL NBR 13.133(94)
Classe de Poligonal :Poligonal definida pelo usuário
Goniômetro - Classe 3: precisão alta
Precisão Angular : 05 "
MED - Classe 3: precisão alta
Precisão Linear : (2mm + 2ppm x D)

VETOR DOS RESÍDUOS DO AJUSTAMENTO (V=AX-L)

Est.	P.Vis.	Ângulo	Distância
P1	P3	2,1825"	0,0005
P3	P4	2,6831"	0,0005
P4	P7	0,0757"	0,0005
P7	P6	0,8047"	-0,0005
P6	P5	5,2594"	-0,0005
P5	P2	1,3265"	-0,0005
P2	P1	0,9681"	-0,0005

PARÂMETROS AJUSTADOS Xa, Desvios-padrão e Erro Posicional(1*sigma)

Est.	X(m)	SigmaX(m)	Y(m)	SigmaY(m)	P.Posição(m)
P1	1000,0000	0,0000	1000,0000	0,0000	0,0000
P3	1000,0000	0,0000	1012,7395	0,0030	0,0030
P4	999,9959	0,0006	1045,8659	0,0039	0,0039
P7	1000,0218	0,0030	1167,4954	0,0043	0,0052
P6	1000,0284	0,0023	1135,2349	0,0043	0,0049
P5	1000,0379	0,0017	1095,7574	0,0039	0,0042
P2	1000,0023	0,0001	1008,3028	0,0030	0,0030

OBSERVACOES AJUSTADAS La e Desvios-padrão (1*sigma)

Est.	P.Vis.	Ângulo	Sigma Âng."	Distância(m)	Sig.Dist.(m)
P1	P3	359°59`02,9"	3,6686	12,740	0,0030
P3	P4	179°59`34,5"	3,9373	33,126	0,0030
P4	P7	180°01`09,5"	0,6785	121,630	0,0030
P7	P6	359°58`33,9"	1,3656	32,261	0,0030
P6	P5	179°59`52,6"	2,1276	39,478	0,0030
P5	P2	180°02`13,6"	2,1762	87,455	0,0030
P2	P1	179°59`33,2"	2,8467	8,303	0,0030

CONTROLE DE QUALIDADE DO AJUSTAMENTO

Variância da Unidade Peso Estimada a Posteriori = 2,653
******** Teste de Hipótese Qui-quadrado **********
Estatística do teste vTPV = 7,960
Percentil inferior da distribuição Qui-quadrado = 0,22
Percentil superior da distribuição Qui-quadrado = 9,35
Conclusão
Ao nível de significância de 5%:
NÃO É REJEITADA a hipótese de que as observações ponderadas sejam provenientes de uma distribuição normal

PLANILHA COM ELEMENTOS DA POLIGONAL AJUSTADOS POR MMQ

Est.	P.Vis.	Ângulo	Distância	Azimute	Coord. Totais	
					X	Y
P1	P3	359°59`02,9"	12,740	0°00`00,0"	1000,0000	1000,0000
P3	P4	179°59`34,5"	33,126	359°59`34,5"	1000,0000	1012,7395
P4	P7	180°01`09,5"	121,630	0°00`43,9"	999,9959	1045,8659
P7	P6	359°58`33,9"	32,261	179°59`17,8"	1000,0218	1167,4954
P6	P5	179°59`52,6"	39,478	179°59`10,4"	1000,0284	1135,2349
P5	P2	180°02`13,6"	87,455	180°01`24,0"	1000,0379	1095,7574
P2	P1	179°59`33,2"	8,303	180°00`57,1"	1000,0023	1008,3028

Perímetro = 334,993 m
Área = 2,877 m2
Área = 0,0002877 ha
Área = 0,0001189 Alq.SP

****

PLANILHA COM ELEMENTOS DA POLIGONAL AJUSTADOS PELO MÉTODO TRADICIONAL

Est.	P.Vis.	Ângulo	Distância	Azimute	Coord. Totais X	Coord. Totais Y
P1	P3	359°59`01,0"	12,739	0°00`00,0"	1000,0000	1000,0000
P3	P4	179°59`34,9"	33,126	359°59`34,9"	1000,0000	1012,7391
P4	P7	180°01`09,7"	121,630	0°00`44,6"	999,9960	1045,8655
P7	P6	359°58`35,6"	32,261	179°59`20,2"	1000,0222	1167,4956
P6	P5	179°59`50,3"	39,478	179°59`10,5"	1000,0285	1135,2350
P5	P2	180°02`13,4"	87,454	180°01`23,9"	1000,0380	1095,7574
P2	P1	179°59`35,1"	8,303	180°00`59,0"	1000,0024	1008,3032

Perímetro = 334,991 m
Área = 2,866 m2

PLANILHA DE DISCREPÂNCIAS DOS AJUSTAMENTOS (MMQ - MÉTODO TRADICIONAL)

Est.	P.Vis.	Ângulo	Distância	Azimute	Coord. Totais X	Coord. Totais Y
P1	P3	0°00`01,9"	0,000	0°00`00,0"	0,0000	0,0000
P3	P4	-0°00`00,4"	0,000	-0°00`00,4"	0,0000	0,0004
P4	P7	-0°00`00,3"	-0,001	-0°00`00,6"	-0,0001	0,0004
P7	P6	-0°00`01,7"	0,000	-0°00`02,4"	-0,0004	-0,0002
P6	P5	0°00`02,2"	0,000	-0°00`00,1"	-0,0001	-0,0001
P5	P2	0°00`00,2"	0,000	0°00`00,1"	-0,0001	0,0000
P2	P1	-0°00`01,9"	0,000	-0°00`01,9"	-0,0001	-0,0004

Perímetro = 0,002 m
Área = 0,011 m2

APPENDIX E - PYTHON SCRIPTS

Article 1 Script

```
import pandas as pd
import math
df1 = pd.read_csv('FILE_NAME.txt', sep=",", header = None)
df2 = df1[[6,0,2,4]]
df3 = df2.rename(columns={6: 'Station', 0: 'Point',2: 'H Direction', 4: 'H Distance'})
raw_data = df3.loc[df3['Station'].isin(['P1','P7'])]
all_raw_directions = raw_data['H Direction']
all_directions_PD = all_raw_directions[::2]
all_directions_PI = all_raw_directions[1::2]
media_PD_PI_directions = []
def grau (β):
  grau = int(β)
  return grau
def minuto (β):
  minuto = int((β - int(β))*100)
  return minuto
def segundo (β):
  segundo = ((((β - int(β))*100) - int((β - int(β))*100)))*100
  return segundo
def ang_dec (β):
  ang_dec = grau(β) + minuto(β)/60 + segundo(β)/3600
  return ang_dec
def grau_ (β):
  grau_ = int (β)
  return grau_
def minuto_ (β):
  minuto_ = (int((β - int(β))*60))/100
  return minuto_
def segundo_ (β):
  segundo_ = ((((((β - int(β))*60)) - (int((β - int(β))*60)))*60))/10000
  return segundo_
def ang_GMS (β):
  ang_GMS = (grau_(β) + minuto_(β) + segundo_(β))
  return (ang_GMS)
def mediaPDPIsimples (apd,api):
  mediaPDPIsimples = int(apd)+((apd-int(apd))+(api-int(api)))/2
  return mediaPDPIsimples
def mediac (apd,api):
  if api-int(api)==0:
  mediac = abs(-(((1-(api-int(api)))+(apd-int(apd)))/2)+apd+1)
  else:
  mediac = abs(-(((1-(api-int(api)))+(apd-int(apd)))/2)+apd)
  return mediac
for i,j in zip(all_directions_PD,all_directions_PI):
  if abs((i-int(i))-(j-int(j)))<0.1:
  mediaspdpi_ = mediaPDPIsimples(i,j)
  else:
  mediaspdpi_ = mediac(i,j)
  media_PD_PI_directions.append(mediaspdpi_)
all_raw_distances = raw_data['H Distance']
all_distances_PD = all_raw_distances[::2] # all distances in PD
all_distances_PI = all_raw_distances[1::2] # all distances in PI
media_PD_PI_distances = [] # media for PD and PI distances
for i,j in zip(all_distances_PD,all_distances_PI):
  Media_PD_PI_distances = (i+j)/2
  media_PD_PI_distances.append(Media_PD_PI_distances)
media_PD_PI_directions_P1 = media_PD_PI_directions[0:6]
media_PD_PI_directions_P7 = media_PD_PI_directions[6:12]
media_PD_PI_distances_P1 = media_PD_PI_distances[0:6]
media_PD_PI_distances_P7 = media_PD_PI_distances[6:12]
station_P1 = ['P1','P1','P1','P1','P1','P1']
point_P1 = ['P2','P3','P4','P5','P6','P7']
angular_reduction_P1 = 360-media_PD_PI_directions_P1[5]
angular_reduction_P7 = -media_PD_PI_directions_P7[0]
red_directions_P1 = []
```

```
for i in media_PD_PI_directions_P1:
  Red = i+angular_reduction_P1
  if int(Red)==360:
  Red_=Red-360
  else:
  Red_=Red
  red_directions_P1.append(Red_)
red_directions_P7 = []
for i in media_PD_PI_directions_P7:
  ReD = i+angular_reduction_P7
  if int(ReD)==360:
  ReD_=ReD-360
  else:
  ReD_=ReD
  red_directions_P7.append(ReD_)
backsight_P1 = ['P7','P7','P7','P7','P7','P7']
raw_data_angles_GMS = []
red_directions_P1_GMS = []
red_directions_P7_GMS = []
for i in red_directions_P7:
  red_directions_P7_GMS_ = ang_GMS(i)
  red_directions_P7_GMS.append(red_directions_P7_GMS_)
for i in red_directions_P1:
  red_directions_P1_GMS_ = ang_GMS(i)
  red_directions_P1_GMS.append(red_directions_P1_GMS_)
for i in raw_data ['H Direction']:
  Raw_data_GMS = ang_GMS(i)
  raw_data_angles_GMS.append(Raw_data_GMS)
raw_data_GMS = list(zip(raw_data['Station'],raw_data['Point'],raw_data_angles_GMS,raw_data['H Distance']))
df_raw_data_GMS = pd.DataFrame(raw_data_GMS, columns = ['Station','Point','H Direction','H Distance'])
directions_and_distances_P1 =
list(zip(backsight_P1,station_P1,point_P1,red_directions_P1_GMS,media_PD_PI_distances_P1))
df_distances_and_directions_P1 = pd.DataFrame(directions_and_distances_P1, columns =
['Backsight','Station','Foresight','Angle', 'Distances'])
station_P7 = ['P7','P7','P7','P7','P7','P7']
point_P7 = ['P1','P2','P3','P4','P5','P6']
backsight_P7 = ['P1','P1','P1','P1','P1','P1']
directions_and_distances_P7 =
list(zip(backsight_P7,station_P7,point_P7,red_directions_P7_GMS,media_PD_PI_distances_P7))
df_distances_and_directions_P7 = pd.DataFrame(directions_and_distances_P7, columns =
['Backsight','Station','Foresight','Angle', 'Distances'])
delta_P1 = []
for i,j in zip(red_directions_P1,media_PD_PI_distances_P1):
  Delta_P1 = j*math.sin((math.pi/180)*i)
  delta_P1.append(Delta_P1)
delta_P7 = []
for i,j in zip(red_directions_P7,media_PD_PI_distances_P7):
  Delta_P7 = -j*math.sin((math.pi/180)*i)
  delta_P7.append(Delta_P7)
diferenca_deltas =
[delta_P7[1]-delta_P1[0],delta_P7[2]-delta_P1[1],delta_P7[3]-delta_P1[2],delta_P7[4]-delta_P1[3],delta_P7[5]-delt
a_P1[4]]
media_deltas =
[(delta_P7[1]+delta_P1[0])/2,(delta_P7[2]+delta_P1[1])/2,(delta_P7[3]+delta_P1[2])/2,(delta_P7[4]+delta_P1[3])/2,
(delta_P7[5]+delta_P1[4])/2]
delta_P7_final =
[round(delta_P7[1],5),round(delta_P7[2],5),round(delta_P7[3],5),round(delta_P7[4],5),round(delta_P7[5],5)]
delta_P1_final =
[round(delta_P1[0],5),round(delta_P1[1],5),round(delta_P1[2],5),round(delta_P1[3],5),round(delta_P1[4],5)]
dif_deltas_finais = []
for i,j in zip(delta_P1_final,delta_P7_final):
  Dif_deltas_finais = i-j
  dif_deltas_finais.append(Dif_deltas_finais)
deltas_medios_finais = []
for i,j in zip(delta_P7_final,delta_P1_final):
  Deltas_medios_finais = round((i+j)/2,5)
  deltas_medios_finais.append(Deltas_medios_finais)
```

```
def sd (angulos, distanciamedia):
  sd =
math.sqrt((math.sin(math.pi/180*angulos)*0.002)**2+(distanciamedia*math.cos(math.pi/180*angulos)*0.0000242
406840587)**2)
  return sd
angulos_para_sd_P1 = []
for i in red_directions_P1_GMS:
  Angulos_para_sd_P1 = ang_dec(i)
  angulos_para_sd_P1.append(Angulos_para_sd_P1)
angulos_para_sd_P7 = []
for i in red_directions_P7_GMS:
  Angulos_para_sd_P7 = ang_dec(i)
  angulos_para_sd_P7.append(Angulos_para_sd_P7)
sd_P1 = []
for i,j in zip(angulos_para_sd_P1,media_PD_PI_distances_P1):
  SD_P1 = sd(i,j)
  sd_P1.append(SD_P1)
sd_P7 = []
for i,j in zip(angulos_para_sd_P7,media_PD_PI_distances_P7):
  SD_P7 = sd(i,j)
  sd_P7.append(SD_P7)
sd_P1_final = [sd_P1[0],sd_P1[1],sd_P1[2],sd_P1[3],sd_P1[4]]
sd_P7_final = [sd_P1[1],sd_P1[2],sd_P1[3],sd_P1[4],sd_P1[5]]
media_sd = []
for i,j in zip(sd_P1_final,sd_P7_final):
  Media_sd = (i+j)/2
  media_sd.append(Media_sd)
```

Article 2 Script

```
import pandas as pd
import numpy as np
import math
df = pd.read_csv('FILE_NAME.txt', sep=",", header = None)
df2 = df[df[1].notna()]
df3 = df2.drop(0)
df4 = df3.drop(columns=[10])
df5 = df4.rename(columns={
  0: "Base Point",
  1: "Target Point",
  2: "Horizontal Distance(m)",
  3: "Slope Distance",
  4: "Horizontal Direction",
  5: "Zenith Angle",
  6: "HI/Base Ant. Ht",
  7: "HR/Ant Ht",
  8: "Code",
  9: "Vertical Distance"
})
df6 = df5['Target Point'].str.startswith('P')
df7 = df5[df6]
df10 = df7.drop(columns=['Code','Vertical Distance','Slope Distance','Zenith Angle','HI/Base Ant. Ht','HR/Ant Ht'])
def grau (β):
  grau = int(β)
  return grau
def minuto (β):
  minuto = int((β - int(β))*100)
  return minuto
def segundo (β):
  segundo = ((((β - int(β))*100) - int((β - int(β))*100)))*100
  return segundo
def ang_dec (β):
  ang_dec = grau(β) + minuto(β)/60 + segundo(β)/3600
  return ang_dec
def grau_ (β):
```

```
  grau_ = int (β)
  return grau_
def minuto_ (β):
  minuto_ = (int((β - int(β))*60))/100
  return minuto_
def segundo_ (β):
  segundo_ = ((((((β - int(β))*60)) - (int((β - int(β))*60)))*60))/10000
  return segundo_
def ang_GMS (β):
  ang_GMS = (grau_(β) + minuto_(β) + segundo_(β))
  return (ang_GMS)
def media_de_tres_em_tres(β):
  medias__ = []
  for i in range(0, len(β), 3):
      subgrupo = β[i:i+3]
      media__ = sum(subgrupo) / len(subgrupo)
      medias__.append(media__)
  return medias__
def alternar_com_zeros(β):
  resultado__ = []
  for elemento in β:
      resultado__.append(elemento)
      resultado__.extend([0] * 5)
  return resultado__
opH = pd.DataFrame(df10, columns=['Base Point','Target Point', 'Horizontal Direction'])
oph = opH.reset_index()
brutos = oph.dropna()
filtro  = brutos['Horizontal Direction'] != 0
oph = brutos[filtro]
Estacao = oph['Base Point']
Ponto_Visado = oph['Target Point']
Direcoes_Horizontais_brutas = oph['Horizontal Direction']
test_list_H_brutas = Direcoes_Horizontais_brutas.values.tolist()
test_list_H_brutas_float = []
for i in test_list_H_brutas:
  test_list_H_brutas_ = float(i)
  test_list_H_brutas_float.append(test_list_H_brutas_)
decgmsh = []
for i in test_list_H_brutas_float:
  virgulah = i-int(i)
  decgmsh.append(virgulah)
maximo = max(decgmsh)
test_list_H_ = []
Direcoes_Horizontais = []
if maximo >= 0.6:
  test_list_H_ = test_list_H_brutas_float
else:
  for i in test_list_H_brutas_float:
  Dir_Horiz_ = ang_dec(i)
  Direcoes_Horizontais.append(Dir_Horiz_)
  test_list_H_ = Direcoes_Horizontais
res = test_list_H_[::2] + test_list_H_[1::2]
direcoes_H_PD_ = res[0:42]
direcoes_H_PI_ = res[42:84]
test_list_E = Estacao.values.tolist()
res__ = test_list_E[::2] + test_list_E[1::2]
test_list_PV = Ponto_Visado.values.tolist()
res___ = test_list_PV[::2] + test_list_PV[1::2]
estacoes_H_PD = res__[0:42]
estacoes_H_PI = res__[42:84]
angularmean = []
for i,j in zip(direcoes_H_PD_,direcoes_H_PI_):
  if abs((i-int(i))-(j-int(j)))<0.02:
  pdpimedia = int(i)+((i-int(i))+(j-int(j)))/2
  else:
  if (i-int(i))-(j-int(j))>0:
    pdpimedia = int(i)+((i-int(i))+(1-(j-int(j))))/2
```

```
  else:
    pdpimedia = int(i)+((i-int(i))+(-1+(j-int(j))))/2
  angularmean.append(pdpimedia)
medias_linhas_pares = angularmean[::2]
medias_linhas_impares = angularmean[1::2]
reduzidas = []
for i,j in zip(medias_linhas_pares,medias_linhas_impares):
  if (-i+j)>=0:
  Reduzidas = -i+j
  else:
  Reduzidas = (-i+j)+360
  reduzidas.append(Reduzidas)
reduzidas_zero = []
for i in medias_linhas_pares:
  Reduzidas_zero = i-i
  reduzidas_zero.append(Reduzidas_zero)
reduzidas_alternadas = [item for pair in zip(reduzidas_zero, reduzidas) for item in pair]
medias_finais = media_de_tres_em_tres(reduzidas)
medias_finais_alternadas = alternar_com_zeros(medias_finais)
reduzidas_alternadas_GMS = []
for i in medias_finais_alternadas:
  reduzidas_alternadas_gms = ang_GMS(i)
  reduzidas_alternadas_GMS.append(reduzidas_alternadas_gms)
targets = df5['Target Point']
targets_pares = targets[::2]
Table = list(zip(estacoes_H_PD,targets_pares,direcoes_H_PD_,direcoes_H_PI_,angularmean,
reduzidas_alternadas, reduzidas_alternadas_GMS))
dfTable = pd.DataFrame(Table, columns = ['Station','Target', 'Direct_(dec)', 'Reverse_(dec)',
'Mean_(dec)','Reduced_Mean_(dec)', 'Final_Directions_(DMS)'])
dfTable # Table of Prussian Method
```